DOI:10.14753/SE.2015.1738

NOVEL BARRIERS TO THROMBOLYSIS: THE ROLE OF MECHANICAL STRESS AND NEUTROPHIL EXTRACELLULAR TRAPS

PhD Thesis

Imre Varjú

Doctoral School of Molecular Medicine
Semmelweis University

Supervisor: Krasimir Kolev, DSc

Official reviewers: Jolán Hársfalvi, DSc
Béla Nagy Jr, PhD

Chairman of the final examination committee: Zoltán Benyó, DSc

Members of the final examination committee: Imre Bodó, PhD
Nándor Müllner, PhD

Budapest
2014

DOI:10.14753/SE.2015.1738

DOI:10.14753/SE.2015.1738

ABBREVIATIONS

2S, 3S: 2 and 3-times stretched fibrin

α2-AP: α2-plasmin inhibitor

α2-MG: α2-macroglobulin

A340, A405: absorbance measured at 340 and 405 nm

ADAMTS-13: a disintegrin and metalloproteinase with a thrombospondin type 1 motif, member 13

Ag: antigen

Akt: protein kinase B

apo(a): apoprotein (a)

aPC: activated protein C

Arg: arginine

AT: antithrombin

C5a: complement 5a

CD: cluster of differentiation

CXCL: CXC chemokine ligand

DMSO: dimethyl-sulphoxide

DNA: desoxy-ribonucleic-acid

DVT: deep vein thrombosis

EDTA: ethylenediamine tetraacetic acid

EGF: epidermal growth factor

EGTA: ethyleneglycol-bis-(β-aminoethylether)-*N*,*N*,*N′*,*N′*-tetraacetic acid

ER: endoplasmic reticulum

ERK: extracellular signal-regulated kinase

ET: extracellular trap

FV/FVIII/FIX: factor V/VIII/IX

FIXa/FXa/FXIIa/FXIIIa: activated factor IX/X/XII/XIII

FcR: Fc receptor

FDP: fibrin degradation product

Fg: fibrinogen

fMLP: formyl-Methionyl-Leucyl-Phenylalanine

FpA, FpB: fibrinopeptide A and B

GAG: glucoseaminoglycan

GFP: green fluorescent protein

Glu: glutamate

GM-CSF: granulocyte-monocyte colony stimulating factor

GpIbα: glycoprotein Ibα

HEPES: 4-(2-hydroxiehyl)-1- piperazin-ethane-sulphonic acid

HIF1α: Hypoxia inducible factor 1α

HIV-1: Human immunodeficiency virus 1

IFN: interferon

IL: interleukine

Ile: isoleucine

K1-K5: kringle domains 1-5

Kd: dissociation constant

Km: Michaelis-Menten constant

Ks: permeability constant

Lp(a): lipoprotein a

LPS: lipopolysaccharide

LRP1: LDL-receptor related protein 1

Lys: lysine

Mac-1: macrophage-1 antigen

MAPK: Mitogen activated protein kinase

Mcl-1: myeloid cell leukemia-1

MEK: MAPK/ERK kinase

MMP: matrix metalloproteinase

MPO: myeloperoxidase

mTOR: mammalian target of rapamycin

NADPH: Nicotinamide Adenine Dinucleotide Phosphate Hydrogen

NE: neutrophil elastase

NET: neutrophil extracellular trap

NFκB: nuclear factor kappa B

NS: non-stretched fibrin

PAD4: peptidyl-arginin-deiminase 4

PAI-1/-2: plasminogen-activator inhibitor-1/-2

PAR1: protease-activated receptor 1

PBS: Phosphate buffered saline

PC: protein C

PF4: platelet factor 4

PHOX: phagocyte-oxidase

PI3K: Phosphatidyl-inositol-3-kinase

PKB: protein-kinase B (also known as Akt)

PKC: protein-kinase C

Plg: plasminogen (Glu, Lys)

PMA: phorbol 12-myristate 13-acetate

PMN: polymorphonuclear cell

Pn: plasmin

proTh: prothrombin

Rac2: ras-related C3 botulinum toxin substrate 2

Raf: rat fibrosarcoma

Ras: rat sarcoma

RBC: red blood cell

RCL: reactive chain loop

ROS: reactive oxygen species

SAK: staphylokinase

SAK-Pn: staphylokinase-plasmin complex

sctPA: single chain tPA

scuPA: single chain uPA

SD: standard deviation

SDS-PAGE: sodium-dodecyl-sulphate polyacrylamide gel-electrophoresis

SEM: scanning electron microscope

Ser: serine

Serpin: serine protease inhibitor

SK: streptokinase

SK-Pn: streptokinase-plasmin complex

SOD: superoxide-dismutase

SPPL: SPectrozyme-PL, Spectrozyme-plasmin: H-D-norleucyl-hexahydrotyrosyl-lysine-p-nitroanilide

Src: eukaryotic sarcoma tyrosine- kinase

TAFI: thrombin activatable fibrinolysis inhibitor

TAFIa: active form of TAFI

TBS: TRIS buffered saline

tctPA: two-chained tPA

TF: tissue factor

TFPI: tissue factor pathway inhibitor

Th: thrombin

TLR: toll like receptor

TM: thrombomodulin

TNFα: tumor necrosis factor α

tPA: tissue type plasminogen activator

tPA-GFP: GFP-tagged tPA

tPA-YFP:YFP-tagged tPA

TRIS: Tris(Hydroxymethyl)aminomethane

uPA: urokinase type plasminogen activator

uPAR: uPA-receptor

Val: valine

vWF: von Willebrand factor

YFP: yellow fluorescent protein

DOI:10.14753/SE.2015.1738

1. INTRODUCTION

Cardio- and cerebrovascular diseases represent the major causes of death (35.8%) in the world according to recent data of World Health Organisation (1). The underlying cause in these cases is the formation of intravascular thrombi (composed of blood cells and plasma components embedded in a fibrin network), blocking the supply of oxygen and nutrients, therefore leading to the damage of the respective tissue. Statistics of mortality have shown improvement in developed countries within the last two decades, which can be partially accounted for the development of efficient tools regarding the prevention of thrombus formation (e.g. anticoagulants like warfarin and antiaggregants such as aspirin (2) and the therapeutic degradation of already formed clots by thrombolytic agents (e.g. tPA). Despite this tendency, thrombolytic therapy often proves to be inefficient in the long term, and is accompanied by a serious risk for bleedings as a side effect (3,4). Taken together, these facts point out the importance of the improvement of current thrombolytic therapeutic protocols, which requires determination of the factors influencing the efficiency of the respective enzymes in the dissolution of thrombi.

This thesis focuses on two of the numerous factors: *mechanical stress* to which fibrin formed in the circulation is exposed; and a recently recognized fundamental scaffold of venous and arterial thrombi: *neutrophil extracellular traps* (5) representing a web-like meshwork composed of DNA, histones and granular components released from granulocytes.

Since degradation of the fibrin scaffold itself is sufficient for the dissolution of thrombi, this introductory chapter gives a detailed description of fibrin structure and the factors influencing it. This is followed by the assessment of elements and regulation of fibrinolysis, the process of enzymatic degradation of the fibrin network. Finally, the chapter describes formation, structure and haemostatic effects of neutrophil extracellular traps.

DOI:10.14753/SE.2015.1738

1.1. The fibrin net

1.1.1. Precursor and product– fibrinogen and fibrin

Fibrinogen, the soluble, 340 kDa precursor of fibrin is a 45 nm long glycoprotein which consists of two peripheral 'D' domains and a middle region (E domain) connected to each other by coiled-coil domains ((6), Fig. 1). The molecule is a heterohexamer containing 3 pairs of polypeptide chains (Aα, Bß, γ) linked together by disulphide-bridges (7-11).

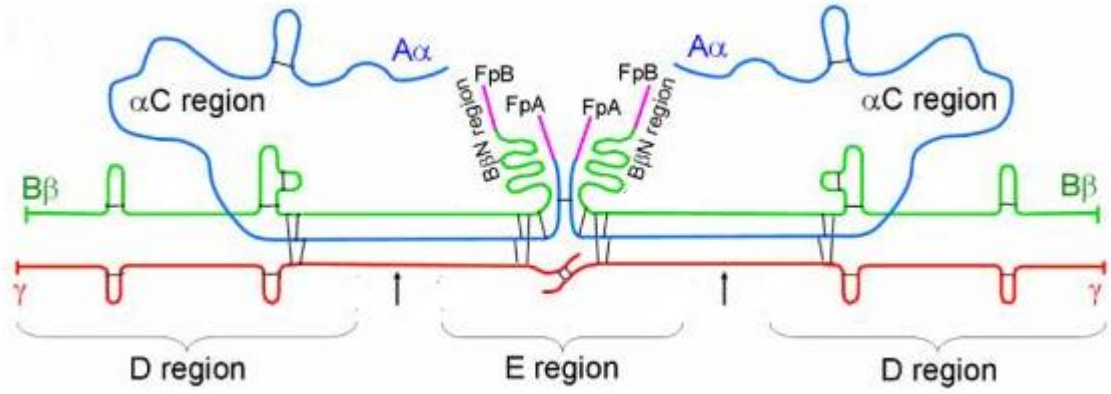

Figure 1. Schematic structure of fibrinogen. *The N-terminal regions of chains are found in the E region, while C-terminal sequences are localized in the peripheral regions, except for those of Aα chains. Black lines represent disulphide bridges, arrows point to sites of plasmin-mediated cleavage. For more detailed description, see text. Modified from (12).*

Proteolytic action of thrombin results in the cleavage of the N-terminals of Aα chains, releasing two fibrinopeptide A (FpA) molecules per fibrinogen, and leaving 'desA fibrin' behind (13-15). This leads to the exposure of two "A-knob" sequences, which are able to interact with C terminal "knobhole" regions found in γ chains of two other fibrin monomers. Aggregation of molecules in such a manner (head-to-head interactions stabilized by head-to-side linkages) results in a double-chained, half-staggered alignment of monomers with a longitudinal periodicity of 22.5 nm, and a lateral periodicity of ~5-10 nm (16), called a protofibril ((17-22), Fig. 2). Following this initial step, thrombin cleaves a further sequence (fibrinopeptide B (FpB)) from the N-terminals of Bß-chains, leading to the formation of 'des AB fibrin'. The B-knobs exposed in these

molecules are partially responsible for the lateral aggregation of protofibrils and the branching of fibrin fibres (Fig. 2, (23)). Furthermore, following cleavage of FpB, αC-

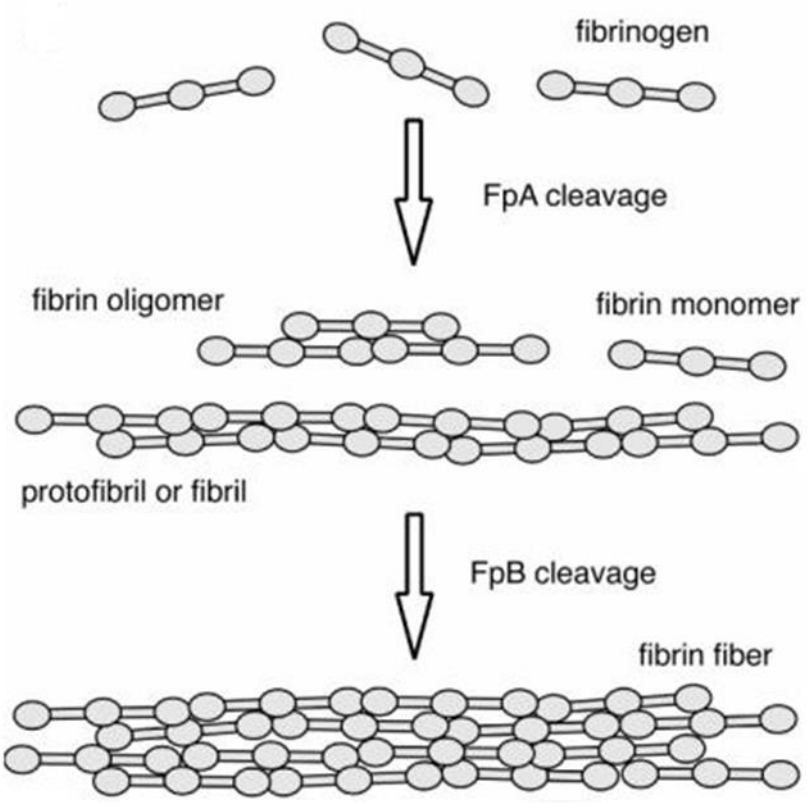

Figure 2. Schematic assembly of the fibrin network. *Fibrin(ogen) monomers are symbolized by rods with three (two peripheral and a central) nodules representing D and E domains. Further description in text. Modified from (12).*

domains dissociate from E domains which makes them available for homophylic interactions, thereby promoting lateral fibril associations and assembly of an extensive fibre network (24,25). Fibre diameter values are typically in the 100-200 nm range, the structure of the fibres, however, is inhomogeneous. 70-80% of the fibre cross section is occupied by channels (26-28) that function like capillaries allowing the axial but not the radial diffusion of typically 50-90 kDa (diameter in the range of 10 nm in hydrated form (29)) proteins participating in fibrinolysis. The meshwork encloses pores with diameters in the range of 0.1 – 5 μm (30), which enable diffusion of bigger proteins up to 470 kDa (31).

1.1.2. Catalyst of formation- thrombin

Formation of thrombin from its zymogen (prothrombin) catalysed by FXa is a two-step process that takes place in the final stage of the coagulation cascade ((32-34), Fig. 3). Hydrolysis of the first peptide bond mostly results in the formation of meizothrombin, which can be further converted to thrombin during the second cleavage causing the

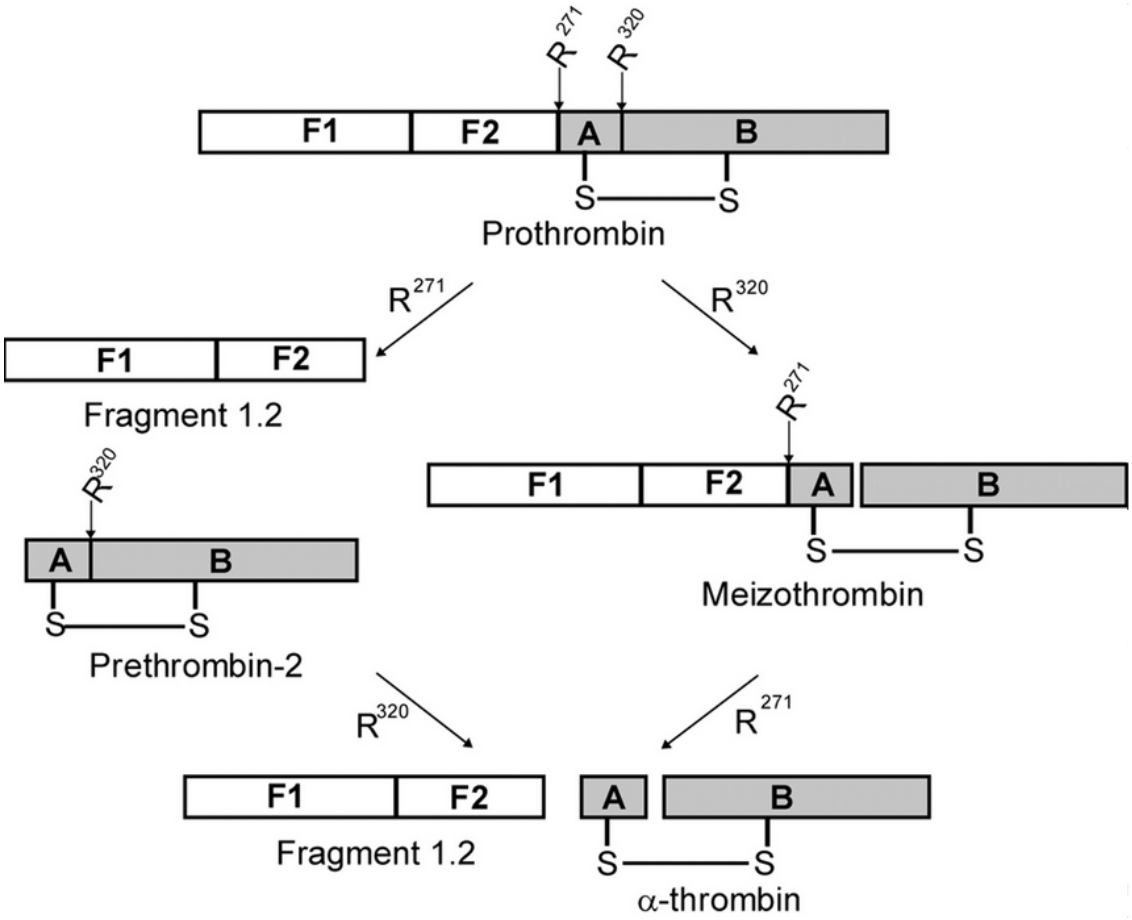

Figure 3. Scheme of prothrombin activation. *Human prothrombin consists of fragment 1 (F1), fragment 2 (F2), and the A and B chains of α-thrombin. Prothrombin is activated to α-thrombin by cleavage at Arg271 (R^{271}) and Arg320 (R^{320}).Regardless of the order of cleavages, α-thrombin and fragment 1.2 are generated. Modified from (35).*

release of F1.2 zymogenic fragment (36). The formed two-chain serine protease, thrombin possesses an active site rich in negative charges allowing interaction with Arg-rich amino acid sequences (37), and two allosteric exosites (I and II). Exosite I is essential for binding to fibrinogen (38) and thrombomodulin (39), and takes part in the

direct (PAR1 (40), FV (41), FVIII (42,43)) and indirect (protein C (44), FXIII (45)) recognition of other substrates of thrombin. Exosite II is responsible for binding to heparin; and GpIbα found on the surface of platelets (46-48). Furthermore, in concert with exosite I, exosite II plays a role in the interaction with FV and FVIII (49,50). The primary endogenous inhibitors of thrombin (heparin cofactor II (51), protein C inhibitor (52), protease nexin 1 (53), and antithrombin (54)) belong to the serpin (serine protease inhibitor) family (55-57) (see also: 1.2.2.2.). The inhibition of thrombin exerted by serpins can be enhanced by GAGs like heparan sulphate and heparin, which are able to bind both serpins and exosite II (37).

1.1.3. Influence of blood components on structural parameters: fibre thickness and pore size

Concentrations of enzyme and substrate (thrombin and fibrinogen) are major determinants of fibre thickness: fibre diameter values show positive correlation with thrombin concentrations up to 10 nM, while above this value fibre thickness decreases (58) (Fig. 4.). In vivo fibrinogen concentrations vary in a narrower range (5-20 μM) than thrombin concentrations, nevertheless this variation is also able to influence clot structure (29). However, in a plasma environment rich in macromolecules, the physicochemical behaviour of fibrinogen differs from the in vitro situation (59). As a consequence of the ‘space occupying’ effect by plasma proteins (e.g. albumin and immunoglobulins), participation of fibrinogen in chemical reactions (e.g. hydrolysis by thrombin) and binding interactions (e.g. with platelets) corresponds to that of its 10-times concentrated ideal solution. Another consequence is the self-association of molecules: according to sedimentation equilibrium studies, fibrinogen is dominantly present in a dimer form in the presence of 40 g/l albumin (60).

In addition, plasma components are also able to directly influence structural parameters of clots. FXIIIa, a calcium-dependent transglutaminase activated by thrombin, alters the molecular structure of fibrin by introducing covalent γ-glutamil-ε-amino-lysine isopeptide bonds between γ- (and, to a smaller extent, Aα-) chains of adjacent fibrin monomers, which also has severe consequences regarding mechanical and lytic resistance of the network (see 1.1.4.). Presence of immunoglobulins decreases the mass/length ratio of fibrin (thinner fibres are formed) (61,62), which can be partially

elucidated by direct inhibition of fibrin-polymerization (63,64). Activated protein C (65) and arginine (66) also contribute to the decrease of fibre diameters, while appearance of vessel wall components in the circulation causes thickening of the fibrin bundles (67).

The cellular components present in the bloodstream have further complex influence on clot structure. In vitro, red blood cells at cell counts near the physiological haematocrit values increase the average pore size approximately two-fold (68). Platelets in vivo form aggregates in the interior of clots. Fibrin strands originating from these zones (attached to glycoprotein IIb/IIIa receptors on the surface of platelets) are thinner and have a higher density (58). Contraction of platelets leading to retraction of thrombi (69) further modifies the structural and lytic parameters of clots (see 1.2.3.). Interaction of fibrin with phospholipids secreted upon thrombocyte activation (70) limits its availability for thrombin- (and plasmin-) mediated cleavage (71,72).

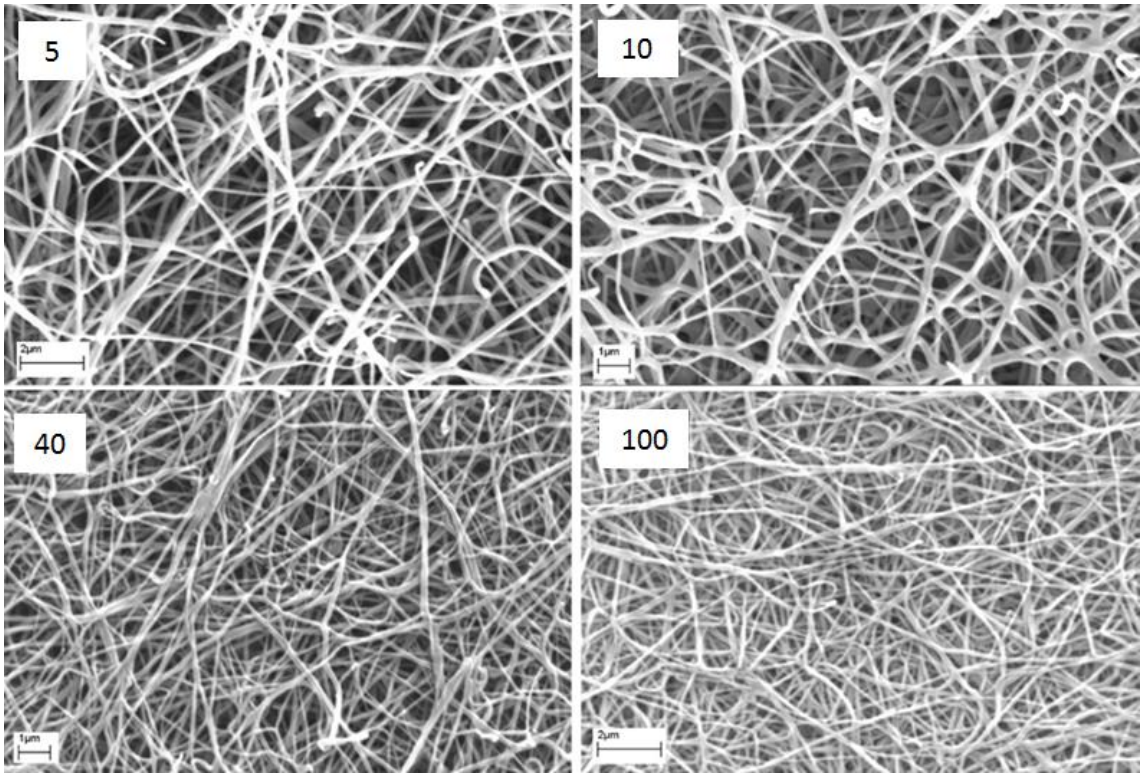

Figure 4. SEM images of pure fibrin clots. *Clots contain 6 μM fibrinogen clotted with the indicated thrombin concentrations (in nM). Samples were prepared as described in 3.3.1.*

Release of certain platelet-derived proteins also influences structural parameters, e.g. actin contributes to the appearance of thinner fibres (73). Furthermore, besides providing a surface not only for the assembly of coagulation complexes but also FXIIIa, platelets contribute to the covalent modification of the meshwork by the secretion of their own transglutaminases.

1.1.4. Influence of mechanical stress on structural parameters

To maintain integrity of haemostasis, and to minimalize and localize the effects of clot formation, fibrin fulfils multiple criteria: it possesses not only firmness and plasticity at the same time (74), but also adequate permeability to allow the diffusion of fibrinolytic enzymes (75). FXIIIa-catalysed crosslinking profoundly alters viscoelastic properties of fibrin: both the elastic limit (the maximal extent of stretching, after the cessation of which the original structure can be regenerated) and the extensibility (extent of stretching that causes rupture of the polymer) of fibre strands show increase (76). In plasma clots, cross-linked structures bear 8.5-times higher elastic moduli compared to control. Following rupture, broken ends of fibres shrink nearly to their original size, which shows that stretching is largely accompanied by elastic alterations. The aforementioned effect of crosslinking is unique among biopolymers: as a comparison, introduction of crosslinks to collagen or keratin increases the stiffness and decreases the extensibility of these structures (77). The increased extensibility in the case of fibrin might be a consequence of axial alignment of crosslinks. Extensibility of whole fibrin nets is however 50-60% lower than that of individual fibres. This finding raises the assumption that disassembly of clots is not primarily due to rupture of single fibres, but more likely to dissociation at branching points of the fibrin network.

In vivo, stenosis of a blood vessel profoundly changes the rheological conditions around the obstruction. In addition to a several-fold increase of shear rate (78), the mechanical forces (radial, axial and circumferential) acting on the vessel wall show a heterogeneous pattern of relative strength at different locations of the stenotic region (stenosis throat, pre- and post-stenotic shoulder), but in all cases the axial force is two- to three-fold stronger than the radial force (79). Thus, if thrombi are formed at stenotic sites of blood vessels, the fibrin fibres on their surface will be exposed to enhanced

shear stress with well-defined directionality, which leads to the prediction of longitudinal alignment of these fibres.

In vitro, stretching results in the decrease of clot volume (Fig. 5), which is a consequence of water expulsion (protein concentration of a 3-times stretched clot is 10 times higher compared to its non-stretched counterpart). SEM images show that fibrin

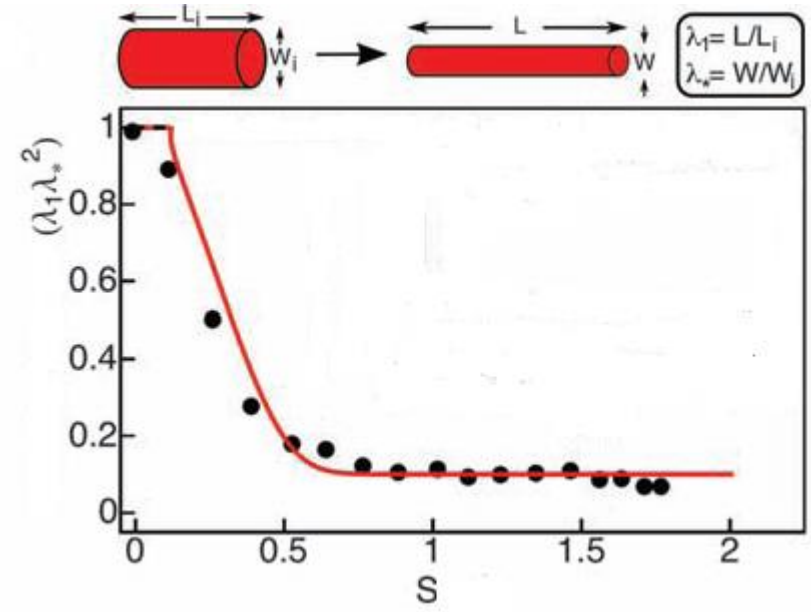

Figure 5. Effect of stretching on relative clot volume. *S represents extent of stretching defined as* $S=(L/L_i)-1$*, where* L_i *is the initial and L is the stretched clot length.* W_i *and W stand for initial and final diameter of cross section. Relative clot volume* $(\lambda_1\lambda_*^2)$ *is defined as* $(L/L_i)*(W/W_i)^2$*. Modified from (80).*

arrangement in non-stretched clots is essentially random, and stretching renders it ordered (80,81). The microscopic changes are accompanied by alterations on a molecular scale: upon stretching, tertiary structure of fibrin monomers changes, certain (possibly coiled-coiled (82)) domains unfold, which leads to exposure of hydrophobic amino acid residues. The latter form hydrophobic interactions which lead to tighter packing of protofibrils and the consequential expulsion of water (80,81).

DOI:10.14753/SE.2015.1738

1.2. The lysis of fibrin nets

Shortly after the formation of intravascular fibrin clots, fibrinolysis begins. This process can be divided into two steps (Fig. 6.): 1. activation of plasminogen (Plg) to plasmin 2. proteolytic breakdown of the fibrin network (72). Plasmin, a serine protease formed by activators (e.g. tissue-type plasminogen activator (tPA), urokinase-type plasminogen activator (uPA)) from its zymogenic precursor plasminogen, plays a central role in the process. After its activation taking place on fibrin strands, cell surfaces, or in the circulation, plasmin digests fibrin releasing soluble fibrin degradation products (FDPs). The most important end products are E and D fragments (central and peripheral domains of fibrin monomers, respectively, see before) (83), and D-dimers: two adjacent D domains ligated by FXIIIa activity, released from the covalently cross-linked fibrin. Proteolysis of 25% of the total D-E connections is sufficient for complete lysis of the clot (84).

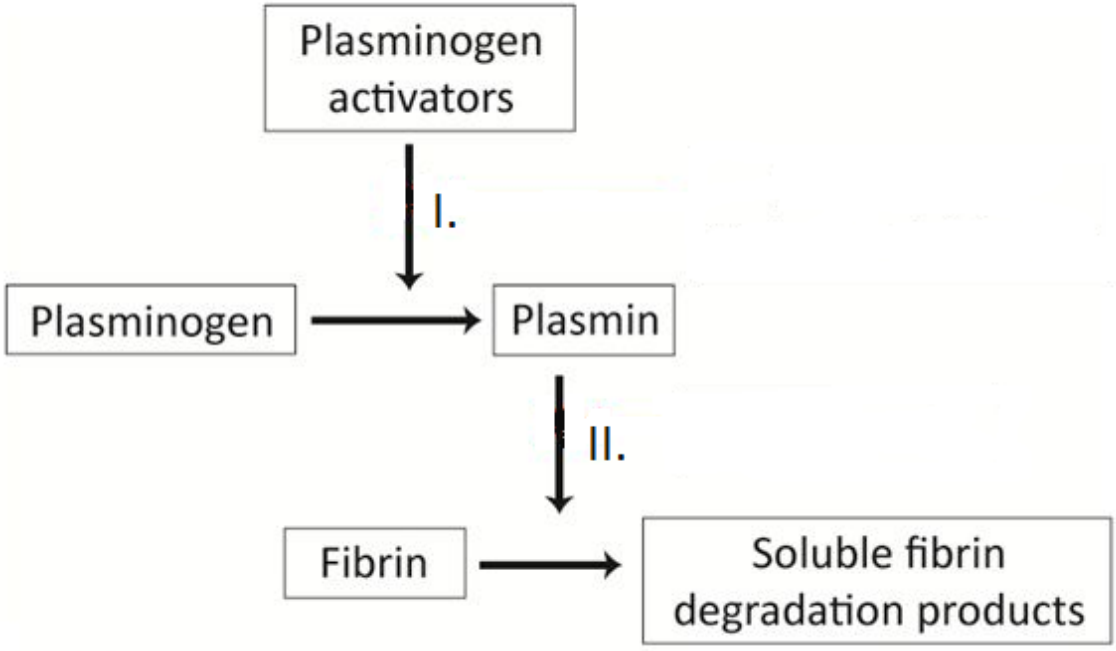

Figure 6. The two-step process of fibrinolysis. *For description, see text.*

The process of fibrinolysis is carried out by a multi-component system regulated by a set of interdependent biochemical reactions, the constituents of which will be described in detail within this section.

DOI:10.14753/SE.2015.1738

1.2.1. Mechanism and morphology of fibrinolysis

1.2.1.1. Microscopic observations

Confocal microscopic studies of fibrinolysis using labelled fibrinogen, Plg and Plg-activators revealed two phases of the process: a pre-lytic phase with accumulation of Plg on fibrin surface without any movement of the lysis front; and a final lytic phase with continuous thinning and eventual disappearance of fibres (85). The lytic zone is 5-8 μm wide in the case of tPA (with uPA, it is thicker), but the pre-lytic zone penetrates deeper. Concentration of Plg in the latter zone can be up to 30-fold higher compared to its plasma concentrations. tPA shows similar accumulation, while uPA is only weakly bound to digested fibrin. These observations can be elucidated by binding data showing that plasminogen as well as tPA bind to fibrin with a dissociation constant of 10^{-8} - 10^{-6} M (86-88), whereas clots contain binding sites in the micromolar range (at least one per fibrin monomer). As a consequence, when fibrinolytic enzymes enter this adhesive environment, their diffusion slows down remarkably, which may lead to accumulation in a thin (pre)lytic layer. Activation of plasminogen leads to plasmin-induced exposure of additional C-terminal lysines resulting in the migration of lysine-binding fibrinolytic enzymes along concentration micro-gradients (89).

Further morphological information is gained by the help of scanning electron microscopy (SEM) using purified components: plasmin, Plg, tPA, fibrinogen and thrombin (90). SEM images of fibrin being digested show free, 'cut' fibre ends (appearing to have been transversely rather than longitudinally digested) and lack of fibrin strand continuity. More pronounced digestion results in lateral assembly of strands forming thick bundles and the increase of average pore size of fibrin clots (Fig. 7.). These studies were carried out according to an 'external lysis' model, where Plg was applied on clot surface. In vivo, however, clotting and lysis may occur at the same time, and lysis might proceed without the appearance of a distinct lytic front ('internal lysis'). The latter model can be studied in a system where fibrin formation occurs in the presence of Plg and tPA (91). During this type of lysis, strands also appear to be preferentially digested transversely, and thinner individual fibres are digested faster than thicker ones. Frayed fibres form lateral interactions, and similarly to the findings of the former lysis model, average fibre diameter and pore size show transitional increase (91).

DOI:10.14753/SE.2015.1738

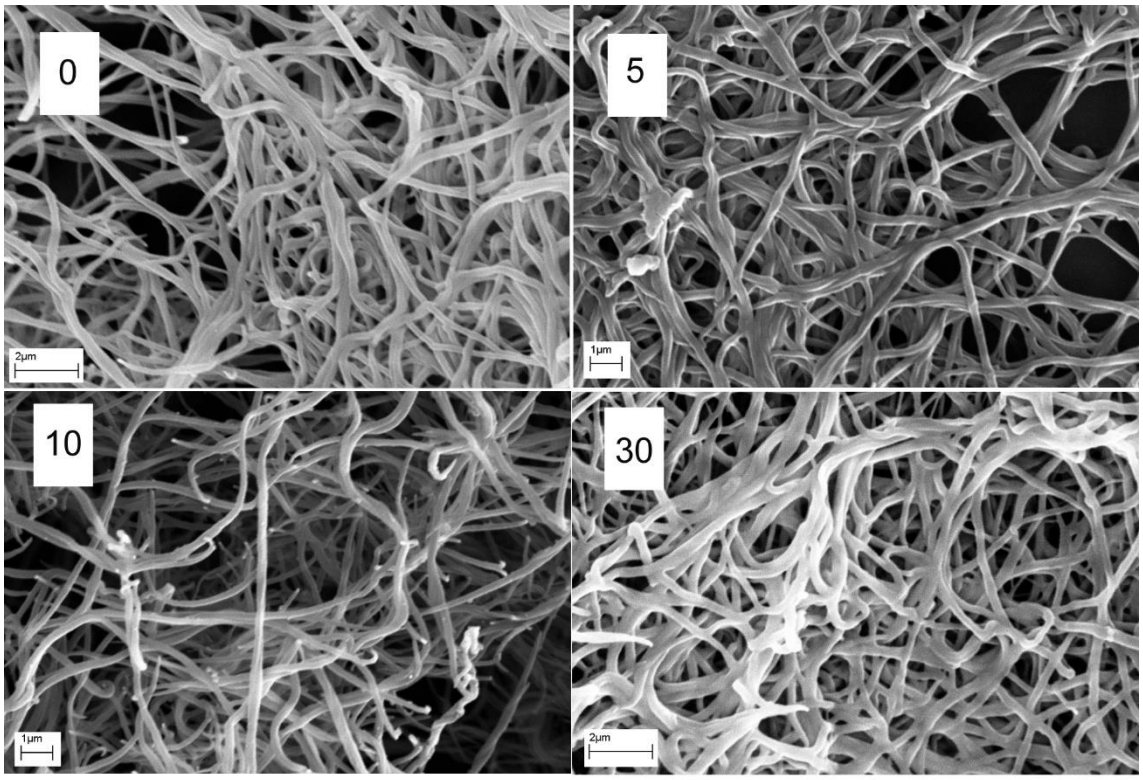

Figure 7. Effect of fibrinolysis on the macroscopic appearance of clot surfaces visualized by SEM. *Clots were prepared from 6 µM fibrinogen and 0.2 µM plasminogen clotted with 3.5 nM thrombin. Lysis was initiated with 0.55µM tPA added to the surface. Numbers indicate minutes elapsed after the beginning of lysis. As lysis proceeds, cut-end fibres appear (10), and lateral aggregation of digested fibrin strands causes thickening of fibres (30). Preparation of samples is described in 3.3.1.*

This is accompanied by increased turbidity, but not rigidity of the clots (92). In the late phase, decrease of absorbance and disassembly of the system into large fragments is seen.

1.2.1.2. Molecular model of fibrinolysis

Despite the fact that individual thin fibres lyse more quickly than thick fibres, in the case of whole fibrin clots, speed of lysis is mostly directly proportional to average fibre diameter (93). This phenomenon taken together with the aforementioned microscopic findings, supports the view that plasmin preferentially digests fibrin fibres in the transverse direction: under these circumstances plasmin might be more efficient in

DOI:10.14753/SE.2015.1738

digesting fibrin nets composed of thicker fibres, where the number of fibres in a given area is less than in a meshwork of fine fibres.

Plasmin binds near the end-to-end junction of two adjacent fibrin monomers, and, given its flexibility, is able to access cleavage sites on both of them. Hydrolysis of the susceptible peptide bonds generates C-terminal lysines which provide binding sites for additional plasmin (and also plasminogen, tPA) molecules. Since average distances between cleavage sites are shorter in the transverse than in the longitudinal direction (5-10 nm and 22.5 nm, respectively) plasmin movement proceeds in the former direction, which eventually leads to the complete bisection of the fibre (16) (Fig. 8.).

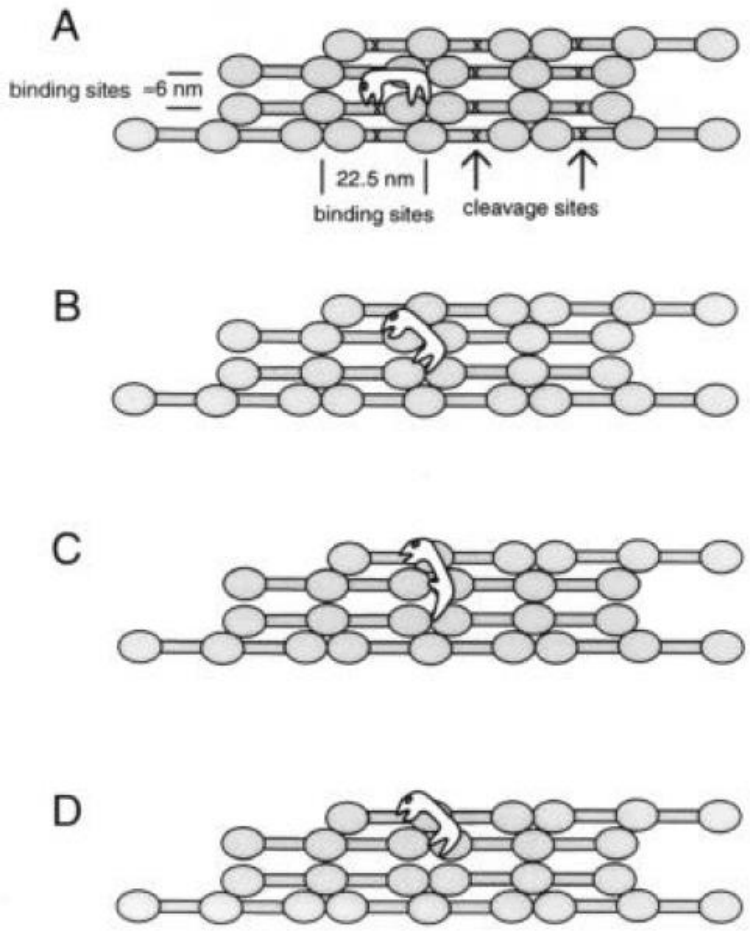

Figure 8. 'Crawling' model of plasmin. *Rods with three (two peripheral and a central) nodules represent monomers of fibrin containing two D domains and an E domain, respectively. Plasmin is symbolized by a creature with a head (catalytic domain) and limbs (lysine binding Kringle domains). Conformational changes of plasmin allow the processive mechanism of action: A) Binding sites for plasmin are localized 22.5 nm away from each other longitudinally in fibrin fibres, but only 6 nm*

away from each other in the fibre cross section. B) Plasmin rotates around a binding site. C) The induced conformational change allows binding of plasmin to another site. D) Another conformational change restores initial state of plasmin, which enables cleavage of another monomer in the same cross section. Modified from (16).

Although not proved, this 'crawling' model of plasmin (16) is in good agreement with the multiple lysine binding sites and conformational changes of plasmin. According to the model, while 'crawling', a plasmin(ogen) molecule is able to form a bridge between lysines located in two neighbouring protofibrils. This notion is supported by experimental data showing that Plg causes precipitation of FDP-s (94), and that Plg added to polymerizing fibrin results in increased fibre diameter (95,96).

1.2.2. Soluble components of the fibrinolytic system

1.2.2.1. Plasminogen and its activators

Human *plasminogen* is a 92 kDa, single-chain glycoprotein synthesized and secreted by the liver. Plasma concentration of the protein is approximately 2 μM (97), and it can also be found in certain body fluids and tissues. The mature protein, Glu-plasminogen, named after its N-terminal amino acid, glutamate, consists of an N-terminal pre-activation peptide, 5 homologous Kringle-domains, and the catalytic serine protease domain (Fig. 9) (98). Cleavage (leading to formation of Lys-plasminogen) or non-proteolytic displacement of the pre-activation peptide has functional consequences: susceptibility for certain activators and the affinity to fibrin increase. Kringle domains consisting of a polypeptide chain of around 80 amino acids stabilized by 3 disulphide bridges (99) are not unique to plasminogen, but can be found in other molecules influencing haemostasis (urokinase- and tissue type plasminogen activators (uPA and tPA), FXII, lipoprotein-a Lp(a), hepatocyte growth factors (100)). Kringle domains are responsible for binding plasminogen to small substances like Cl^-, α,ω-diamino-acids, or ε-aminocaproic acid, and also to lysine residues of fibrinogen, fibrin, and certain proteins of the extracellular matrix (101-103). Kringle 5 bears the highest affinity towards lysines located within the native peptide chain of fibrin (104,105), while Kringles1 and 4 preferentially bind to C-terminal lysines exposed in the course of fibrin

DOI:10.14753/SE.2015.1738

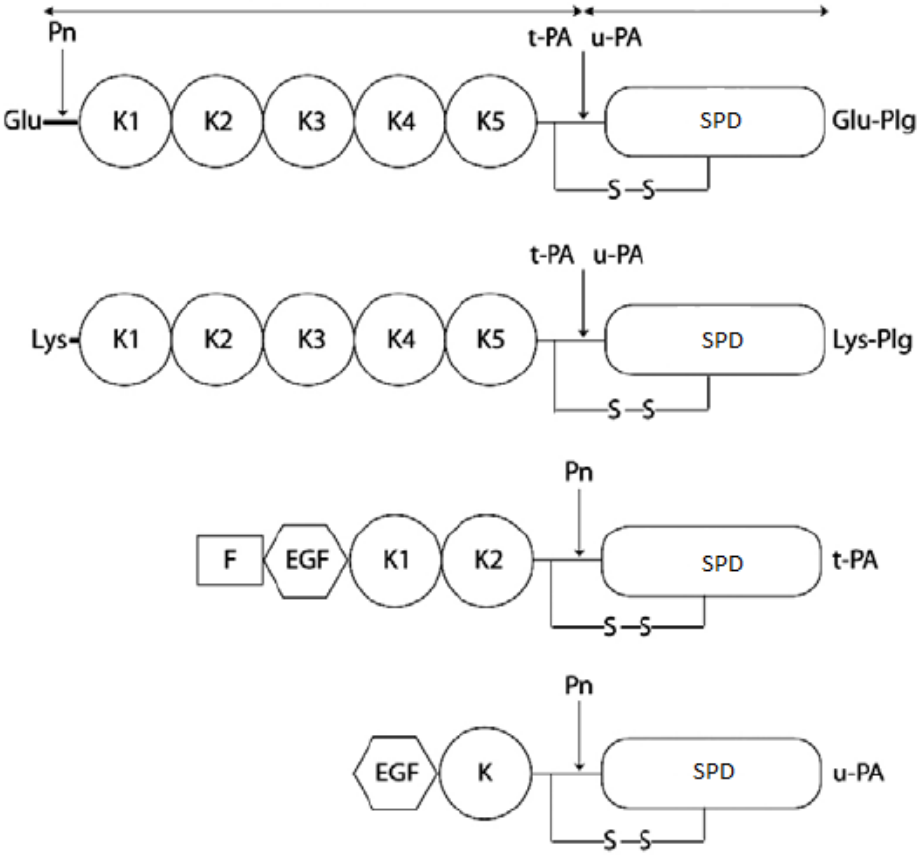

Figure 9. Plasminogen and its activators. *Sites of cleavage for different proteases are shown. K1-5:Kringle 1-5; F: finger-domain; EGF: epidermal growth factor-like domain; SPD: serine protease-like catalytic domain. Long and short arrows at the top of the figure represent heavy and light chains, respectively. Modified from (97).*

digestion (98). Interaction with lysine induces a profound conformational change in plasminogen: length of the molecule increases from 15 to 24 nm (106). Plasminogen in this ‘open’ conformation has similar characteristics to Lys-plasminogen formed by e.g. plasmin-catalysed proteolytic cleavage of the pre-activation peptide (72).

The trypsin-like catalytic domain becomes active in the two-chain form of the molecule. This requires activation of plasminogen to plasmin by tPA or uPA mediated cleavage of the peptide bond Arg561-Val562 near Kringle 5 (107).

Tissue-type plasminogen activator (tPA) mainly synthesised by vascular endothelial cells, is a 70 kDa, single chain glycoprotein (108,109) that reaches a plasma concentration of 60-70 pM (110,111). However, only 20% of this quantity is found in free form, the rest is bound to its primary inhibitor, plasminogen activator inhibitor-1 (PAI-1). tPA consists of an N-terminal finger-domain, an epidermal growth factor

(EGF)-like domain, two Kringles, and a serine protease-type catalytic domain (Fig. 9). Unlike most zymogens, this single-chain form of tPA (sctPA) possesses remarkable activity (about 10% of the two-chain from, tctPA formed following plasmin-mediated cleavage), however, in the absence of fibrin, its efficiency as a plasminogen-activator is low (112), which makes it a so-called fibrin-specific activator. tPA binds to low (lysine-independent (113)) and high (lysine-dependent (88)) affinity binding sites exposed in fibrin but not fibrinogen through its Kringle 2- and finger domains (114,115). Binding induces a conformational change similar to that of plasminogen, resulting in a 100-fold increase in the speed of plasminogen activation (116,117). Since binding sites for Plg and tPA in fibrin partially overlap, the two molecules come to close proximity, which increases the efficiency of plasmin generation. These mechanisms localized on fibrin surface ensure that formation of plasmin is conferred to fibrin deposits, this way sparing circulating fibrinogen from digestion (118).

Endothelial, epithelial, vascular smooth muscle cells, macrophages and granulocytes synthesize another type of plasminogen activators, *uPA* (*urokinase-type*, named after the fact that it appears in the urine (119)), the plasma concentration of which is approximately 2 ng/ml (120), but may vary under certain pathophysiological circumstances (121-123). It is secreted as a 55 kDa, single chain molecule (scuPA) consisting of an N-terminal EGF-like domain, a Kringle, and a catalytic domain homologous to that of tPA (Fig. 9). scuPA, possessing 1% of the final uPA activity, can be converted to its active two-chain form (tcuPA) by proteolytic action of kallikrein, FXIIa, trypsin, cathepsins (124,125), and plasmin. tcuPA is a fibrin-non-selective activator able to activate both fibrin-bound and free forms of Plg (126). The Kringle found in uPA domain is unable to bind lysine, but forms interactions with PAI-1 (127) and heparin (128). The EGF-like domain binds to receptors found on the surface of certain cells (uPAR), inducing cell migration and tissue remodelling (129), while the trypsin-like catalytic domain contributes to these processes by the cleavage of certain growth factors and metalloproteases (MMP-s) (97).

Streptokinase (SK) is a 47 kDa protein synthesized by the bacterium *Streptococcus haemolyticus*. Despite its name, SK possesses no enzymatic activity, however, it is able to form a 1:1 equimolar complex with Plg that functions as a Plg-activator (130,131). The formed plasmin cleaves SK, releasing an N-terminal peptide

that forms non-covalent interactions with the central fragment, thus inhibiting the binding of the SK-plasmin(ogen) complex to fibrin. This makes SK a fibrin non-selective activator, similarly to uPA (132).

Staphylokinase (SAK) is a 15.5 kDa protein synthesized by *Staphylococcus aureus*. Similarly to SK, SAK is not an enzyme, but is able to form a 1:1 complex with fibrin-bound plasmin. This interaction leads to a conformational change of the active centre which makes it similar to that of plasminogen activators, enabling the SAK-plasmin complex to convert Plg to plasmin (133). In the absence of fibrin, the complex formed between SAK and trace amounts of plasmin found in the plasma is quickly inhibited by alpha2-plasmin inhibitor (α2-antiplasmin, α2-AP), therefore SAK is regarded as a fibrin-selective activator.

1.2.2.2. Inhibitors of fibrinolysis

TAFI (*thrombin-activatable fibrinolysis inhibitor*, other names: plasma procarboxypeptidase B, R, U (134,135)), a member of the metalloprotease family synthesized and secreted by the liver as a 60 kDa, extensively glycosylated (136) single-chain propeptide (134), reaches a plasma concentration of 220-270 nM (135,137). TAFI eliminates the C-terminal lysine residues exposed during plasmin-catalysed digestion of fibrin (138), which leads to reduction of the number of plasmin(ogen) binding sites. Since plasmin bound to C-terminal lysines is known to be protected against α2-AP-mediated inhibition, TAFI also decreases the half-life of plasmin (139). Furthermore, TAFI slows down the conversion of Glu-Plg to Lys-Plg, which leads to hindered activation of plasminogen (140). Finally, higher concentrations of TAFI directly inhibit plasmin (141).

In order to gain its peptidase activity, TAFI needs to be proteolitically converted to its active form TAFIa (135,142). Thrombin is a weak activator, however, in the presence of thrombomodulin and calcium (138,143), the reaction speed increases more than 1000-fold (144). In comparison with thrombin alone, plasmin is 8-times more efficient, and the speed of activation increases in the presence of heparin, however, it is still far from that of the thrombin-thrombomodulin complex.

Heat-sensitivity of TAFI is remarkable: half-life of the molecule at 37°C is not more than a few minutes (145-148). Conformational change afterwards causes exposure

of peptide regions with high affinity towards α2-macroglobulin, which mediates the clearance of the molecule (147-149). FXIIIa plays an important role in the stabilization of TAFIa activity by covalently binding the molecule to fibrin (150).

PAI-1 (plasminogen activator inhibitor-1), the primary inhibitor of uPA and tPA, belongs to the family of serpins (serine protease inhibitors) (151). The molecule is a 50 kDa single chain glycoprotein synthesised by platelets (152), endothelial-, liver- and other, mainly perivascular cells (153,154). Basal plasma concentration of PAI-1 is generally low (0.4 nM), but reaches high local values in platelet-rich thrombi (155) and at sites of vessel injury (due to its high affinity towards vitronectin present in the extracellular matrix (156,157)). These local mechanisms presumably prevent premature lysis of thrombi.

PAI-1 forms a 1:1 complex with both uPA and tPA (158,159), however, fibrin-bound plasminogen activators are relatively protected from inhibition (151). The tertiary structure of PAI-1 contains a reactive centre loop (RCL) characteristic for serpins, which behaves as a 'bait-substrate' for the respective protease. Upon protease action, an Arg-Met peptide bond in the RCL is hydrolysed, and a consequential conformational change of the RCL N-terminal displaces the protease to the opposite side of the serpin (160). This leads to the disintegration of the serine protease active centre and the inhibition of dissociation of the complex (161-163). Upon cleavage of the RCL, the serpin forms a dead-end product, and the complex is eliminated from the circulation (164-166). In addition to the inhibition of plasminogen activators, PAI-1 exerts direct inhibitory effect on plasmin (167).

Similarly to TAFI, PAI-1 is fairly unstable (168), and binding to vitronectin (either in the plasma or in the extracellular matrix) prolongs its lifetime (169,170). This interaction induces a conformational change in the molecule that enables binding to integrins, making PAI-1 a modulator of cellular adhesion and motility (171-173).

Another member of the serpin family, *PAI-2* is a 10-50-fold slower inhibitor of uPA and tctPA (in vitro) than PAI-1 (174-177) synthesised primarily by monocytes (178) and placental trophoblasts (179,180). The majority of PAI-2 molecules are found in the form of a 43 kDa non-glycosylated intracellular protein (179)), however, upon

stimulation by thrombin, it is secreted in the circulation as a 60-70 kDa glycoprotein (181-183). The polypeptide chain contains a glutamine-rich sequence which makes the molecule a good substrate for FXIIIa and other transglutaminases enabling covalent crosslinking of PAI-2 onto fibrin surface (184).

Besides its role in haemostasis, a growing amount of evidence supports the view that PAI-2 is also a regulator of intracellular proteolysis (185).

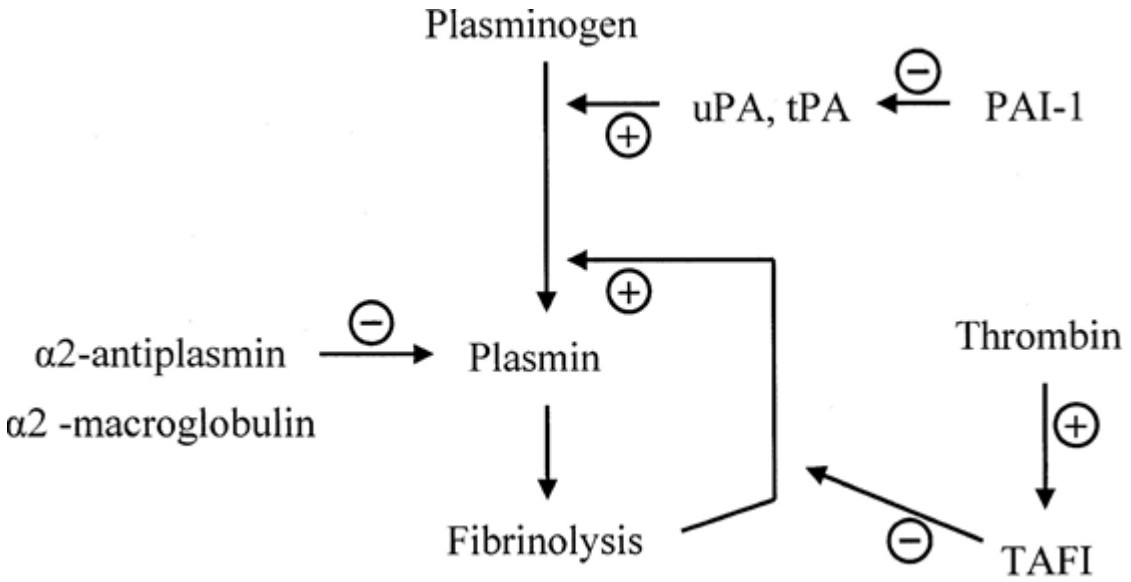

Figure 10. Regulation of fibrinolysis. *A variety of negative and positive regulations is shown. For detailed description, see text.*

α2-AP (α2-plasmin inhibitor/α2-antiplasmin), another serpin, is the primary plasmin inhibitor in humans. α2-AP is expressed as a 70 kDa, single chain glycoprotein in hepatocytes. The molecule reaches a concentration of 1 μM in plasma, where its half-life is approximately 3 days (186,187).

α2-AP exerts its anti-fibrinolytic activity through different mechanisms. 1) It forms a stable complex with plasmin (188). 2) Similarly to PAI-2 or TAFI, the molecule can be linked to Aα chains of fibrin by FXIIIa, which increases the lytic resistance of fibrin (189). 3) Lysine residues on the surface of α2-AP show high affinity towards Kringles found in plasmin(ogen) (188), and competitively inhibit the interaction between plasminogen and fibrin.

Lp(a) (lipoprotein a) is a plasma protein, which, similarly to LDL, contains an apolar lipid core and a surrounding phospholipid monolayer with embedded glycoproteins. LDL contains apo B100, a 500 kDa glycoprotein, while in Lp(a), apolipoprotein(a) (apo(a)) is linked to apo B100 by disulphide bridges (190).

apo(a) bears structural homology with Plg: it has many isoforms containing Kringle 4-like (KIV, lysine-binding) (191) and Kringle 5-like (KV) structures, and an inactive serine protease-like region homologous to that of Plg (192). Instead of the Arg561-Val562 bond at the site of proteolytic cleavage in Plg, a Ser-Ile pair is found, which probably prevents recognition by proteases (193).

This structural homology between apo(a) and Plg results in competition regarding binding to lysine residues in fibrin (194-197), interactions with receptors on the surface of endothelial cells (198), platelets (199), and monocytes (200). apo(a) is also able to bind to the tertiary complex of Plg-tPA-fibrin, which prevents activation of Plg (201).Taken together, high levels of plasma Lp(a) are potentially anti-fibrinolytic, however, affinity of different Lp(a) isoforms towards fibrin depends on the number of Kringles: shorter isoforms show higher affinity, and therefore exert stronger inhibition on Plg activation (202).

α2-macroglobulin (α2-MG) is a 725 kDa homotetramer synthesised in the liver and found in the plasma in a concentration of approximately 3 μM. The molecule is able to bind to various enzymes, and also enzyme-substrate complexes (203). Plasmin and their activators are also able to bind to α2-MG, which results in a relatively slow inhibition of their activity (204) (Fig. 10). Cell surface- or fibrin bound plasmin molecules are protected from this type of inhibition (205). α2-MG possesses scavenger functions: complexes containing α2-MG are internalized by LDL-receptor related protein 1 (LRP1), and are degraded in liver cells (206).

1.2.3. Cellular modulation of fibrinolysis

Intravascular thrombi are heterogeneous systems composed of fibrin scaffold and various soluble and cellular factors. To gain detailed information on fibrino- and thrombolysis in vivo, in addition to fibrin structure, the multidirectional interactions of

platelets, cells, extra- and intracellular proteins and lipids need to be taken into consideration.

In the course of formation of arterial thrombi, the *platelet* content of 10 ml of whole blood is compacted in a volume of 400 μl, whereas the fibrinogen concentration of the same thrombi correspond to that in plasma (207), and Plg and α2-AP concentrations are substantially lower (110).

Presence of platelets leads to decreased velocity and hampered efficiency of fibrinolysis (208,209). This is partially due to release of *PAI-1* (see 1.2.2.2.): high local concentrations of PAI-1 originate primarily from within platelets. During therapeutic fibrinolysis, however, their effect is 'overcome' by the applied concentrations of tPA (72).

Platelet-mediated *retraction* of thrombi (see 1.1.3.) leads to decreased mechanical (210) and lytic (208) susceptibility of clots, probably due to decrease of the fluid phase leading to limited diffusion of fibrinolytic enzymes. Furthermore, the fibres in platelet-rich areas of thrombi are more tightly packed and thinner than the ones in other clot regions, serving as a worse substrate for plasmin (58).

Histochemistry applied on arterial thrombi suggests that *phospholipid* concentrations (originating primarily from activated platelets (70)) exceed that of fibrin (207,211). Besides triggering the formation of coagulation complexes (e. g. tenase, prothrombinase (212)) phospholipids exert anti-fibrinolytic effects by limiting the diffusion of fibrinolytic enzymes (210) and directly inhibiting tPA- and plasmin-dependent fibrinolysis (211,72).

Platelet filopodia surrounding fibrin strands contain thick bundles of *myosin* (213), and high amounts of this protein are present in arterial thrombi (214). According to SEM studies, after 2 hours of initiation of thrombus formation, platelets start exhibiting morphological signs of necrosis (207). This leads to exposure of intracellular components, and allows interaction of fibrin and platelet-borne proteins (70). Myosin exerts multiple effects on fibrinolysis: hinders tPA-/uPA/plasmin-mediated lysis by serving as a source of 'false' binding sites for these proteins (214), while it weakens the interaction between the digested clot and the released FDPs, and (in higher concentrations) functions as a cofactor for tPA-induced plasminogen activation (215).

DOI:10.14753/SE.2015.1738

Red blood cells are no longer considered as passively trapped inert elements of thrombi, given their eptifibatide-sensitive interactions with fibrin(ogen) (216) resulting in altered fibrin structure (see 1.1.3.) and hindered fibrinolysis: red blood cells inhibit tPA induced plasmin generation on fibrin surface and tPA induced lysis of clots (217).

Neutrophil granulocytes (polymorphonuclear PMN cells) are present in thrombi in a smaller number than platelets, nevertheless, they play an important role in the formation and the elimination of thrombi. The role of neutrophil extracellular traps and other PMN-borne factors on fibrinolysis is discussed in the detail in the next section (1.3.).

DOI:10.14753/SE.2015.1738

1.3. The role of neutrophils and neutrophil extracellular traps in haemostasis

As a response to inflammatory stimuli, polymorphonuclear (PMN, neutrophil) cells are able to expel a mixture of their nuclear and granular elements. These web-like composite structures are called neutrophil extracellular traps (NETs) that are able to entrap invading pathogens. NETs are composed of DNA, histones, granular enzymes and proteins (such as cathepsin G or elastase), and seem to be a universal tool of defence: humans, animals and even plants (218) are capable of extracellular trap formation, indicating that these webs provide an evolutionarily conserved protective mechanism.

Besides their protective function, a role for NETs is emerging in the pathogenesis of many diseases (219,220), and may be of interest regarding the pathogenesis of thrombosis. Stimulation of coagulation by NETs can result in unwanted thrombosis (221) and infection is a common event in the development of deep vein thrombosis (222,223). Targeting the release of nucleosomes, development of NETs and the availability of circulating histones could be a strategy for prevention or therapeutic intervention in venous thromboembolism, sepsis and other diseases involving cell death and lysis.

This chapter describes the formation and structure of NETs and discusses the possible connections and interrelations between this newly recognized form of innate immunity and components of the haemostatic system.

1.3.1. Triggers of NET formation

NETs can be formed in response to all major types of microbes (bacteria, fungi, protozoa, viruses) and their products, as well as inflammatory mediators, ROS, cell-cell interactions, and certain non-infectious or non-physiological stimuli. Table 1. shows a set of examples for various triggers.

Table 1. Triggers of NET formation. *Several microbial and chemical stimuli have been identified. A summary based on (224-227).*

Microbial stimuli	**Chemical stimuli**
Bacteria	**Microbial toxins and components**
Enterococcus faecalis	*δ-Toxin from Staphylococcus epidermidis*
Escherichia coli	*fMLP (+rapamycin)*
Haemophilus influenzae	*Glucose oxidase*
Helicobacter pylori	*M1 protein-fibrinogen complex*
Klebsiella pneumoniae	*Lipophosphoglycan*
Lactococcus lactis	*Lipopolysaccharide (LPS)*
Listeria monocytogenes	*Panton-Valentine leukocidin*
Mannheimia haemolytica	
Mycobacterium tuberculosis/canettii	**Inflammatory mediators and cytokines**
Serratia marcescens	*Antibodies*
Shigella flexneri	*Calcium ions*
Staphylococcus aureus	*GM-CSF + C5a/ LPS*
Streptococcus dysgalactiae/pneumoniae	*Hydrogen peroxide*
Yersinia enterocolitica	*Interferon + eotaxin*
Fungi	*Interferon-α/γ + C5a*
Aspergillus fumigatus	*Interleukin 1-β/8/23*
Candida albicans	*Nitric oxide*
Cryptococcus gattii/neoformans	*Platelet activating factor*
Protozoa	*Platelets through TLR-4*
Leishmania	*TNF-α*
amazonensis/donovani/major/chagasi	**Other stimuli**
Virus	*Phorbol-12-myristate-13-acetate (PMA)*
Feline Leukemia Virus	*PMA + ionomycin*
HIV-1	*Statins*
Influenza A	

DOI:10.14753/SE.2015.1738

1.3.2. Formation of NETs

1.3.2.1. NET formation as a form of cell death

NETs are the results of a unique cell death program that is different from apoptosis or necrosis (228). It is characterized by the loss of intracellular membranes before the plasma membrane integrity is compromised (NETosis). To release NETs, activated neutrophils undergo dramatic morphological changes (229). Minutes after activation by PMA, they flatten and firmly attach to the substratum, while showing a multitude of granules and a lobulated nucleus (230). During the next hour, the nucleus loses its lobules, the chromatin decondenses and swells, and the inner and outer nuclear membranes progressively detach from each other. Concomitantly, the granules disintegrate. After one hour, the nuclear envelope seems to disaggregate into vesicles and the contents of nucleoplasm, cytoplasm and granules are able to freely mix. After approximately 4 hours, the cells round up and seem to contract until the cell membrane ruptures and the internal components are ejected to the extracellular space (230,231). It is important to note, that depending on stimuli and donor, only a certain percentage of the activated neutrophils make NETs (230).

Apoptosis, another form of programmed cell death, is characterized by membrane blebbing, phosphatidylserine exposure on the cell surface, nuclear chromatin condensation and DNA fragmentation *without* membrane disintegration (225). Necrosis is characterized by PS exposure during the early steps, cellular swelling and bursting, and plasma membrane damage/rupture *without* nuclear membrane disintegration. The program of NETosis, on the other hand, shows disintegration of the nuclear envelope *without* DNA fragmentation; loss of internal membranes and organelles, and membrane rupture (and therefore PS exposure) *after* mixing of the nuclear and cytoplasmic elements.

1.3.2.2. Alternative ways of extracellular trap formation

Besides the above described, first observed form of NETosis (also called *'suicidal' NETosis*), several other types have been reported (232).

In contrast with the PMA-induced 3-4 hour-long cell death program, a recently described form, *'vital' NETosis,* leads to rapid NET formation without neutrophil cell death (233-235): Staphylococcus aureus appears to induce NETs in a rapid fashion (233), and LPS-activated platelets are also capable of inducing NETosis within minutes (236). 'Vital' NETosis does not only spare the neutrophil from 'suicidal' lysis, but transforms them into anuclear cytoplasts capable of chasing and imprisoning live bacteria (235). The third difference between 'suicidal' and 'vital' forms (besides timing and functional capacity of the involved neutrophils) is the mechanisms employed to create and cast out NETs: in contrast to the above described form, vital NETosis requires budding of the nuclear envelope, and vesicular trafficking of nuclear components to the plasma membrane, thereby delivering the NET out of the cell without requiring membrane perforation (233). *Mitochondrial ETosis* originally observed in eosinophils, and later in neutrophils could also be considered as a subtype of the 'vital' form (237,238).

1.3.3. Structure and composition of NETs

NETs released from neutrophils into the extracellular space consist of nuclear DNA and various histones decorated with granular proteins. NETs are fragile, complex structures (Fig. 11) composed of smooth 'threads', approximately 15-25 nm in diameter, which are likely to represent chains of nucleosomes from unfolded chromatin. High-resolution scanning electron microscopy (SEM) revealed that the NET threads are studded to variable extent with globuli of 30-50 nm (231) that contain the multiple cathelicidin

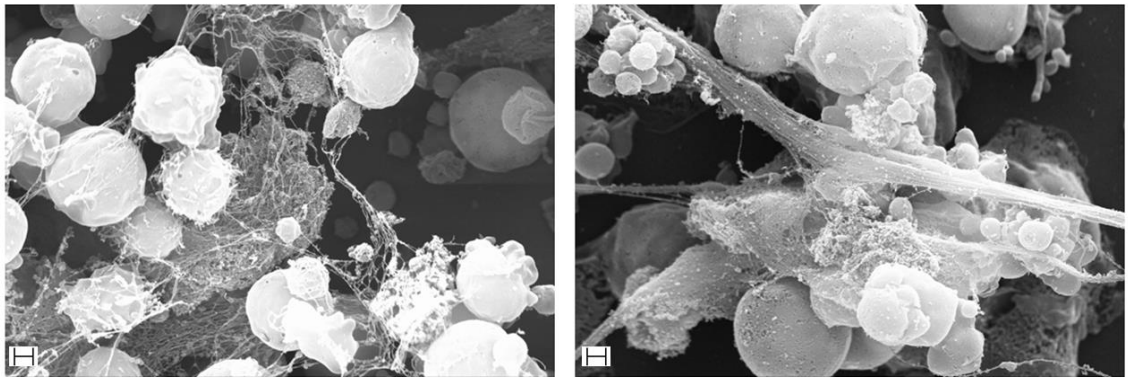

Figure 11. **SEM images of NETs produced by PMA-activated neutrophils.** *Samples were prepared as described in 3.3.1. Images were taken at 10.000x magnification. Scale bars = 1 μm.*

antimicrobial peptides which originate from the neutrophil granules (or lysosomes). Several ‘threads’ can be wound into ‘cables’ that can be up to 100 nm in diameter (Fig. 11). These cables then form complex three-dimensional structures that, using SEM, can be hard to distinguish from fibrin networks (239). Analysis of cross sections of NETs by transmission electron microscopy (TEM) revealed that fibres are not surrounded by membranes (5). When produced in multiwell plates in vitro, NETs float within the medium, rather like a spider’s web does in moving air (240). The fact that they are ‘sticky’ as a result of their electrostatic charge and that they extend over areas of several microns makes them very effective at trapping (241), and possibly killing microorganisms (240).

DNA is a major structural component, because several intercalating dyes stain NETs strongly, and deoxyribonuclease (DNAse) treatment results in the disintegration of NETs, whereas protease treatment has no such effect (5). Accounting for approximately 70%, the most abundant component of NETs are *histones* (242). All core histones (H2A, H2B, H3, H4) as well as linker histones (H1) can be found in NETs, although in an enzymatically processed form (see later). The aforementioned globuli contain proteins and enzymes from the primary (azurophilic) granules (e.g. neutrophil elastase, cathepsin G, myeloperoxidase (MPO), bactericidal permeability increasing protein BPI), secondary (specific) granules (e.g. lactoferrin), and tertiary granules (e.g. gelatinase or MMP-9, peptidoglycan recognition proteins PGRPs (243)) of neutrophils (244). Calprotectin, a heterodimer of cytosolic S100A8 and S100A9, represents one of the few examples for cytoplasmic components, which are rarely found in NETs (242).

These proteins exert various antimicrobial actions (245): MPO is responsible for microbicidal HOCl generation; serine proteases (neutrophil elastase NE, cathepsin G, proteinase 3, tryptase, neutrophil serine protease 4 NSP4 (246)) are able to inactivate bacteria by cleaving their virulence factors (5); cathelicidin LL37, BPI, defensins, and histones can disintegrate pathogen cell membranes challenging their viability (247,248); calprotectin (242,249), calgranulin and lactoferrin chelate ions that are vital for microbial growth, altogether making NETs an effective tool virtually against all types of microbes.

NETs produced from mitochondrial DNA release have a slightly different structure (238). NE and MPO co-localize with mitochondrial DNA, but certain nuclear

(lamin B, nuclear matrix protein-45, poly-ADP-ribose polymerase, histones) and other (cytoplasmic caspase-3, beta-actin, mitochondrial cytochrome c, membrane markers CD15 and 16) elements are absent, which suggests a different type of host-NET interaction in the case of mitochondrion-derived NETs.

1.3.4. Intracellular events leading to NET formation

A unifying theory describing the subsequent steps of NET formation is still missing, but many mechanisms have been identified to contribute to NET expulsion.

1.3.4.1. Signalling events

The signalling mechanisms leading to the formation of NETs are poorly understood, and it is very likely that different triggers are able to induce NETosis through different pathways (Fig. 12,(250)).

The protein kinase C (*PKC*) enzyme family is comprised of conventional, novel and atypical isoforms (251). There are at least four conventional isoenzymes: PKCα, PKCβI, PKCβII and PKCγ. The novel isoenzyme group has four subtypes: PKCδ, PKCε, PKCη and PKCθ. The third group, atypical isoenzymes, consists of PKCζ and PKCι (251). PMA (phorbol-12-myristate-13-acetate), a widely used inducer of NETs, stimulates conventional (α, βI, βII, γ) and novel (δ, ε, η, θ) PKC by mimicking the activating ligand diacylglycerol (DAG) (251). PKC isoforms of all classes have been reported in neutrophils from healthy donors (252), and activation of PKC is critical in the generation of NETs (253). Nevertheless, an intricate antagonism is present between PKC isoforms in the regulation of a crucial element of NETosis, histone deimination: PKCα has a dominant role in the repression of histone deimination, whereas PKCζ is essential in the activation of peptidyl arginine deiminase 4 (PAD4, see 1.3.4.3.) and the execution of NETosis. The precise balance between opposing PKC isoforms in the regulation of NETosis affirms the idea that NET release underlies specific and vitally important evolutionary selection pressures (254).

PKC activation (e.g. by PMA) is upstream of the *Raf-MEK-ERK* pathway (255) leading to phosphorylation of gp91phox (256) and p47phox (257) which initiates the assembly of the cellular or phagosomal membrane-bound and the cytosolic subunits of

another key player of NET formation, NADPH oxidase (see 1.3.4.2.). An alternative route for activation of ERK is also suggested through generation of reactive oxygen species (ROS) (258). The Raf-MEK-ERK pathway also upregulates the expression of antiapoptotic protein Mcl-1, which contributes to the inhibition of apoptosis and redirects the death program to NETosis (255).

The monomeric G-protein (rho small GTPase) *Rac2* is also activated upstream of NADPH oxidase activation (259).

The role of *PI3K-Akt-mTOR* pathway is contradictory. Inhibition of mTOR leads to enhancement of fMLP-induced NETosis, because the pathway inhibits autophagy, a process that seems to enhance NET formation (e.g. by blocking apoptosis) (227). If a different trigger, lipopolysaccharide (LPS) is used, however, mTOR seems to support NETosis by exerting translational enhancement of HIF1α (260).

Certain triggers of NETosis act through a PKC/ROS-independent pathway, possibly mediated by *Src* kinase (261), which may be able to directly activate PAD4.

Cytoskeletal elements may also play a role in transmitting signals from the cell surface to the nucleus, e.g. inhibition of the cell surface receptor integrin *Mac1-cytohesin1* (a guanine exchange factor)-*actin* cytoskeleton pathway results in inhibition of PAD4 activation and NET formation (262).

1.3.4.2. NADPH oxidase and ROS formation

Most signalling pathways activated by the triggers of NETosis converge to activate *NADPH oxidase* as a key enzyme of the process (263). Neutrophils isolated from patients with chronic granulomatous disease (CGD) caused by mutations in NADPH oxidase fail to produce NETs upon PMA-stimulation (230). Inhibition of the oxidase with diphenyleneiodonium (DPI) also prevents NETosis in response to several factors (264). Assembly of the NADPH oxidase responsible for the generation of ROS during the respiratory burst requires phosphorylation of the four cytosolic subunits (p47-phox, p40-phox, p67-phox and Rac) to enable their association with the membrane bound gp91phox-p22phox (cytochrome b558) complex. Once being in the active form, the enzyme generates ROS, out of which the most important seem to be the superoxide ions (O_2^-). O_2^- dismutates (either spontaneously or by superoxide dismutase (SOD) catalysis) to form H_2O_2. Further metabolization of H_2O_2 can lead to a variety of toxic oxygen de-

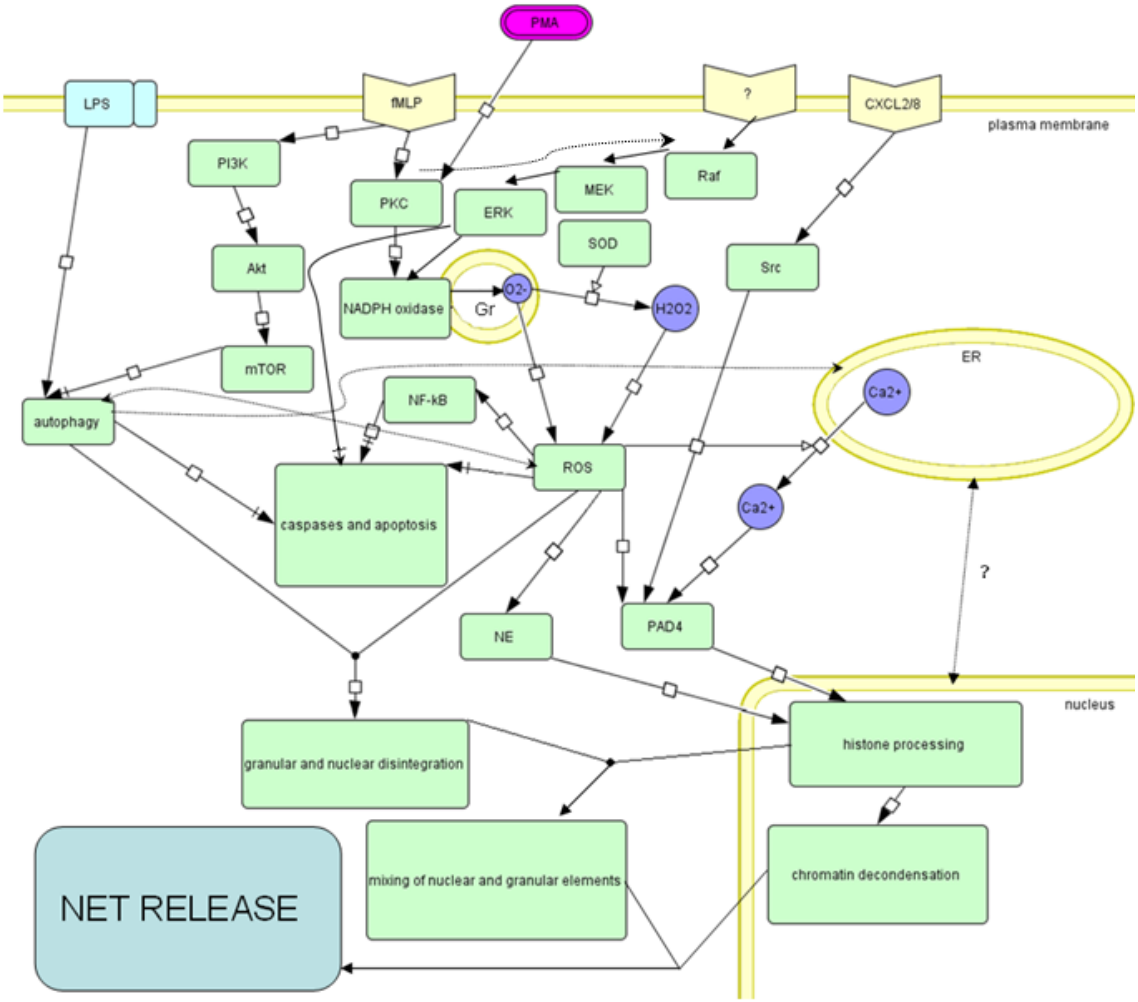

Figure 12. Intracellular steps leading to NET formation. *Several signalling pathways can lead to NADPH oxidase activation and ROS formation, which triggers NE and PAD4 action on nuclear histones. Nuclear disintegration and decondensation leads to mixing of the granular and nuclear components, which are later expelled from the cell in the form of NETs. Dashed-end arrows represent inhibition, arrows pointing to the middle of another arrow represent activation of a step. Arrows with dotted lines stand for ambiguous relations. Gr: granule. For other abbreviations and explanation: see text. Modified from (250).*

rivatives, like the primary mediator of oxidative killing in the phagosome, HOCl, formed by *myeloperoxidase* (MPO) action. The importance of the latter enzyme is underlined by studies in patients suffering from MPO deficiency: the level of NETs they produced correlated negatively with the degree of the enzyme deficiency (265). How ROS generated during an oxidative burst contribute to NETosis is controversial. One

possibility is that they contribute directly to the observed morphological changes by causing direct membrane destruction (266). A proposed alternative is that ROS directly and indirectly (through activation of NF-κB) inactivate caspases (267-270), while exerting a possible autophagy-enhancing effect (250). Both mechanisms lead to an inhibition of apoptosis, ensuring that the already ongoing cell death program does not take an apoptotic route. ROS also play a crucial role in initializing the events that lead to chromatin decondensation, another key component of this type of cell death (Fig. 12.).

1.3.4.3 Chromatin decondensation

One option to weaken the interaction between DNA and highly positively charged histones is the enzymatic processing. At this moment, two enzymes seem to be of greatest importance: PAD4 (peptydilarginine deiminase 4) and NE (neutrophil elastase).

Peptydilarginine deiminases are enzymes catalysing citrullination (deimination), a posttranslational modification of arginine to citrulline. The process results in the loss of positive charge and hydrogen bond acceptors, therefore leading to weakened protein-protein, RNA-protein, and DNA-protein interactions. Out of the five PAD enzymes expressed in humans and mice (PAD1-4 and 6) (271), PAD2 and 4 are the most abundant in neutrophil granulocytes, and the latter seems to be critical in NET formation: PAD4-deficient mice are unable to decondense chromatin or form NETs (272), whereas overexpression of PAD4 is sufficient to drive chromatin decondensation to form NET-like structures in cells that normally do not form NETs (273).

PAD4, a 74 kDa protein that exists as a head-to-tail dimer (274,275) is the only member of the peptydilarginine deiminase family containing a nuclear localization signal that ensures its trafficking to the nucleus (274,276,277) (although not the only one to be found inside, e.g. PAD2 is also reported to be localized intranuclearly (278)). The activation of PAD4 is calcium-dependent: binding of calcium to the C-terminal catalytic domain induces conformational changes that lead to the adequate positioning of critical active site residues (274). The calcium-dependency of the enzyme also serves as a possible connection between ROS generation (possibly leading to calcium release from the endoplasmic reticulum) and PAD4 activation. In addition, ROS are possible direct regulators of PAD4 (279). Cytoskeletal activity and autophagy may also be

involved in PAD4 activation, since both processes have been shown to be required for chromatin decondensation during NET generation.

The main nuclear substrates of PAD4 are arginyl residues of PRMT1 (protein arginine methyltransferase 1) (277), PAD4 itself (autocitrullination downregulating the activity of the enzyme (280,281)), and, most importantly regarding the process of NETosis, histones (H2A and B, H3Arg-2, -8 and -17 or H4Arg3) (280,282). Hypercitrullination of arginil residues in histones (283) weakens their interactions with DNA resulting in the dissociation of heterochromatin protein 1-β (273), and the extensive chromatin decondensation that leads to nuclear delobulation and swelling of the nuclear content (282,284).

In concert with PAD4, *neutrophil elastase* (NE), a serine protease that is able to cleave histones, also promotes nuclear decondensation. H1 is cleaved early during the process of NETosis, but nuclear decondensation coincides with degradation of H4 (266). ROS may play a possible role in the translocation of NE from the azurophilic granules into the nucleus by disrupting the association of NE with the proteoglycan (e.g. serglycin) matrix that is thought to down-regulate protease activity in resting cells (285-287). The similar, but later occurring translocation route of myeloperoxidase (MPO) supports the process, which seems to be independent of its enzymatic activity (266). Once in the nucleus, NE activity is reduced by DNA, which could help in protecting certain NET-components from losing their antimicrobial activity by proteolytic digestion (266). Interestingly, serpinb1, an inhibitor of neutrophil proteases is also being transported to the nucleus during NETosis, possibly setting a brake of NE action (288). While NE knockout mice fail to form NETs in a pulmonary model of *Klebsiella pneumoniae* infection (266), serpinb1-deficient neutrophils produce overt NETosis in vivo during Pseudomonas aeruginosa lung infection (288), which points to the importance of the fine regulation of NE activity during the process of NET formation.

1.3.4.4. Reorganization of membrane structures-the role of autophagy in NETosis

While the decondensated nuclear content expands, the space between the two membranes of the delobulated nuclear envelope starts growing, this eventually leads to formation of vesicles and disintegration of nuclear membranes. During the final stage, nuclear and granular integrity is completely lost, which allows mixing of the chromatin

and the granular components, and a rupture in the plasma membrane causes the release of extracellular chromatin traps.

However, vesicle formation is also seen in neutrophils isolated from CGD patients, which are unable to produce NETs (289). This observation suggests that vesicles do not necessarily originate from the nuclear envelope, but ER membranes are likely to be assembled as a source of autophagic vesicles (250), in addition to possible *de novo* vesicle formation. A decrease in perinuclear ER membranes may result in lower morphological constraints on nuclear collapse, and calcium leaking form the ER may activate PAD4. Taken together, these events could partially explain that autophagy is needed for nuclear decondensation and NET formation (289). These speculations are supported by the finding that inhibition of mTOR, a suppressor of autophagy, also leads to enhanced NET production (see 1.3.4. and (227)).

1.3.5. NETs and haemostasis

NETs represent a newly recognized scaffold of venous (290) and arterial (291) thrombi (besides fibrin and von Willebrand Factor vWF) that allows cell localization (neutrophils, red blood cells), platelet adhesion, activation and aggregation, and promotion of both (extrinsic and intrinsic) pathways of coagulation. Thus, NETs are a focus of cross-talk between immunity, inflammation and haemostasis.

The concentration of cell-free DNA is generally low in the circulation, 50-100 ng/ml, but is higher in some conditions such as lupus, pulmonary embolism and cancer (292). In malignancy very high levels may be observed: 0.5-5 μg/ml (293). However, this only serves as a baseline, as the important consideration is rather the amount of DNA present in a clot, released from dying cells going through necrosis or NETosis. A starting point for the amount of DNA available for release from neutrophils can be estimated by multiplying the concentration of neutrophils in blood (~1.5 million per ml) and the amount of DNA per cell (8-10 pg) to arrive at 12-15 μg/ml DNA. However, inflammatory signals associated with thrombosis may cause the accumulation of white blood cells in clots (294) increasing the total amount of DNA available. Furthermore, and most importantly, DNA will be released from a cell to form NETs and, like fibrin, will be present as a heterogeneous component of a clot at a very high local concentration. Indeed, as previously shown in deep vein thrombosis (DVT) (295),

DNA stains both as dotted pattern of nuclear DNA plus a diffuse DNA distribution in clots, indicating the potential for widespread distribution and also extremely high local concentrations within a clot.

Sepsis models of baboons treated with *E. coli* suggest histone concentrations up to 70 μg/ml (296), however, the determination of their local concentration within a clot raises similar issues and questions.

This section discusses the interaction among the various players of the haemostatic system and NET components.

1.3.5.1. NETs and the vessel wall

The classic view of the intact endothelial surface emphasizes its anticoagulant role. While endothelial damage is a common initiator of arterial thrombosis, in the case of DVT, activation of endothelium and Weibel-Palade Body (WPB) release play a crucial role. NETs induce endothelial cell damage and death (234,297-299), an effect that is likely to be assigned to NET-associated proteases, defensins and, most importantly, histones (298,300). Binding of histones to membrane phospholipids results in pore formation and influx of ions (296,301,302), this may lead to elevated endothelial calcium levels, vWF release from WPBs (303), activation of endothelium, or even endothelial cell death. Endothelial ROS formed under these circumstances may, in turn, trigger NET formation by neutrophils (297). Perfusion of iliac artery cross sections with NE results in increased thrombogenicity of the arterial wall (304), although it is not clear if NET-bound NE is able to reproduce this effect at the site of vascular damage.

NETs also contribute to the progression of atherosclerotic plaque formation in the subendothelial layer of arteries: neutrophils infiltrate arteries during early stages of atherosclerosis (305), and NETs can be detected in murine and human atherosclerotic lesions (306).

1.3.5.2. NETs and platelets

NET fibres bind platelets directly and/or indirectly, and support their aggregation (307). When perfused with blood, NETs bind platelets serving as an alternative scaffold for platelet adhesion and activation (295).

The first step of platelet binding involves either electrostatic interactions between NET histones and platelet surface phospholipids (301)/heparan sulphate (308), or histone binding to Toll-like receptors 2 and 4 (309). Platelets also bind double and single stranded DNA in vitro (310,311). Adhesion molecules may also play a role in thrombocyte-NET interactions, such as vWF (binding histones through its A1 domain) (312), fibronectin or fibrinogen (295,303). The interaction of histones with platelets results in calcium influx either by pore formation (313) or by opening of existing channels (314), a process, which triggers activation of αIIbβ3 (315). This chain of events raises the possibility of a sequential histone-induced activation of platelets (first binding to platelet surface, then, following platelet activation, binding to adhesion molecules (307)), which could explain the unsaturable nature of histones binding to platelets (307). When infused into mice, histones co-localize with platelets and induce thrombocytopenia and thrombosis (296,303,307), possibly partially through potentiation of thrombin-dependent platelet-activation (316).

Serine proteases may also play a role in platelet activation: NETs contain enzymatically active NE and cathepsin G (5), and these proteases potentiate platelet aggregation through proteolitically activating platelet receptors (317,318). Some of these elements, however, play an ambiguous role in the modulation of platelet functions: e.g. NE is also an effective enzyme for the cleavage of vWF under high shear stress (319), helping the detachment of platelets from thrombogenic surfaces.

NETs also seem to bind certain interleukins that may enhance platelet activation and aggregation: the presence of IL17A and -F was shown in NET regions of acute myocardial infarction thrombus specimens (320).

Platelet-NET interaction seems to be bidirectional in many ways. Serotonin released from platelets promotes the recruitment of neutrophils (321). Activated platelets generate ROS, such as superoxide (322), and secrete human β-defensin 1 (323), both of which can trigger formation of NETs (230,324). Platelets pre-stimulated with LPS or collagen also induce NETosis in neutrophils (234,325), contributing to the formation of a vicious cycle of NET formation and platelet activation (290).

Interaction between platelets and NETs might also be involved in pathological situations like transfusion-related acute lung injury (TRALI) (326,327), thrombotic microangiopathies (328), or heparin-induced thrombocytopenia (HIT). During HIT,

possible binding of NETs to platelet factor 4 (PF4) forming an antigenic complex may offer an explanation for disease progression even after immediate removal of heparin (329).

1.3.5.3. NETs and red blood cells

Red blood cells (RBCs) are no longer considered as passively entrapped elements of thrombi, but cells that may promote thrombosis by exposing phosphatidylserine and altering blood viscosity (330); furthermore, their presence modulates structural parameters of the forming fibrin meshwork through integrin-mediated fibrin(ogen)-red blood cell interactions (1.2.3., (217)).

Similarly to platelets, RBCs avidly bind to NETs after perfusion of whole blood (295), possibly through direct and indirect mechanisms. RBCs can bind DNA, since it was eluted from the surface of isolated RBCs from cancer patients (331). Activated neutrophils or platelets (e.g. in NETs) can also recruit RBCs at very low venous shear in vitro (332). NETs are predominantly found in the red, RBC-rich part of experimental mice DVT thrombus, suggesting that NETs could be important for RBC recruitment to venous thrombi (303).

1.3.5.4. NETs and the coagulation system

NETs offer a variety of activators for both the extrinsic and the intrinsic (contact-) pathways of the coagulation cascade (333,325) stimulating fibrin formation and deposition in vitro ((295,325,333), (Fig. 13)).

NE and cathepsin G, two serine proteases that are in the NETs, degrade inhibitors of coagulation (229). NE is known to cleave tissue factor pathway inhibitor (TFPI) of the extrinsic pathway, and enhance factor Xa activity (334). The cleavage of TFPI by NE is supported by activated platelets that attach to the surface of neutrophils and facilitate NET formation (325). Neutrophil-expelled nucleosomes also bind TFPI and serve as a platform for the NE-driven degradation of TFPI (325). NETs do not only release brakes of the extrinsic pathway, but also trigger it: TF was identified as a NET component (333,335); and disulphide isomerase (PDI) released from damaged or activated endothelial cells and platelets (e.g. in NETs) participates in bringing the

inactive (encrypted) TF (e.g. in neutrophils (291,336) and platelets (337,338) to its active (decrypted) form (339).

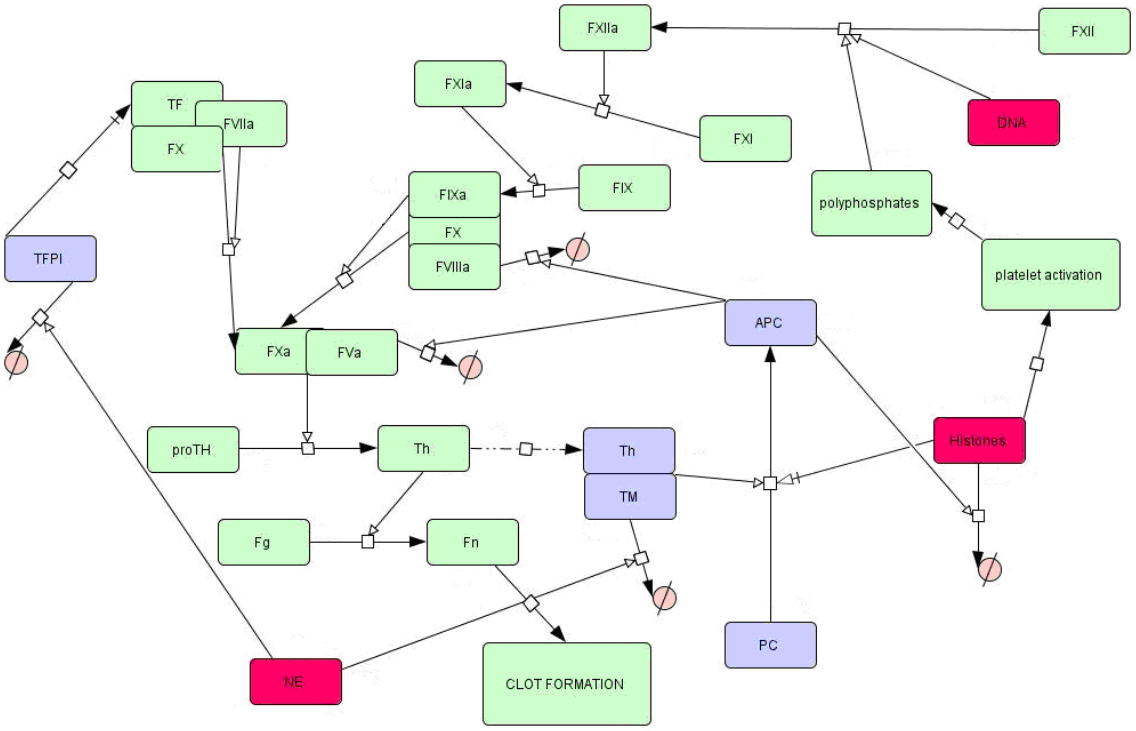

Figure 13. Examples of NET-coagulation interactions. *Green boxes indicate prothrombotic elements/steps of the cascade. Blue represents antithrombotic systems. Red boxes stand for NET components. Dashed pink circles symbolize degradation of the respective protein. Dashed arrows represent inhibition, while arrows pointing to the middle of another arrow represent activation of a process. For further explanation, see text.*

NETs also bind factor XII and stimulate fibrin formation via the intrinsic coagulation pathway (333). Factor XII can be activated following contact with pathogens (e.g. entrapped in NETs), damaged cells (e.g. endothelial damage by NETs), and negatively charged surfaces (such as the NET component DNA, which also enhances the activity of certain coagulation serine proteases (340)). Polyphosphates released from activated platelets following stimulation by histones may also serve as coagulation-triggering negatively charged molecules (309,341).

Besides its crucial role in NET-driven thrombosis (342), PAD4 has also been shown to citrullinate antithrombin (ATIII) in vitro (343), which weakens its thrombin-

inhibiting efficiency and this may be an additional factor contributing to increased thrombin generation associated with NETs. Histones also bind to fibrinogen and prothrombin (344) and can aggregate vWF (312), the significance of which is not clear.
NET components also interfere with the anticoagulant systems in plasma. Despite the historically attributed anticoagulant properties of histones (345,346) (prolonging the plasma based standard clotting assays, probably due to their affinity for negatively charged phospholipids, such as phosphatidylserine (301)), nowadays they are viewed as clear pro-coagulant substances, due to their platelet-activating nature (see before) and their modulatory effects on the thrombin-thrombomodulin(TM)-activated protein C (APC) pathway. Histones interact with TM and protein C and inhibit TM-mediated protein C activation (347). Interestingly, in return, APC cleaves histones (H2A, H3, H4) and reduces their cytotoxicity (296), possibly serving as a basis for a counter-regulatory process. Cleavage of histones is relatively slow, but is augmented substantially by membrane surfaces, particularly those that best support APC anticoagulant activity (296), although NET-bound histones may be more difficult to cleave (298). Thrombomodulin is also cleaved by NE and may also be rendered inactive by neutrophil oxidases (such as MPO) (348,349) present in NETs.

Heparin, a highly sulphated polyanion (GAG) is able to remove histones from NET chromatin fibres, leading to their destabilization (295,333): NETs are dismantled after perfusion with heparinized blood (333). Heparin also blocks the interaction between the positively charged histones and platelets (307), in this way adding newly recognized elements to its long-known anticoagulant effects.

1.3.5.5. NETs, thrombolysis, NET lysis

In vitro and in vivo observations indicate that fibrin, vWF and chromatin form a co-localized network within the thrombus, the structure of which is similar to that of extracellular matrix (302,303,333), and it is likely that each of these components should be cleaved by their own appropriate enzyme (plasmin, ADAMTS-13, and DNAses, respectively). Therefore, in addition to summarizing the interactions between NETs and the fibrinolytic system, this section attempts to assess current knowledge on the possible ways of NET degradation in blood plasma.

Whilst there are extensive studies on the interaction between NET components and coagulation, little is known about their effects on fibrinolysis. Nevertheless, certain NET components may promote thrombolysis: in vitro studies have shown that NE and cathepsin G can degrade fibrin (350), and in plasminogen-knockout mice, more neutrophils infiltrate the clot (351), possibly serving as an auxiliary mechanism when plasmin-mediated fibrinolysis is impaired (352). Histone 2B can serve as a receptor to recruit plasminogen on the surface of human monocytes/macrophages (353), and perhaps in NETs as well, where the co-localization of NE and plasmin(ogen) could result in amplified formation of mini-plasmin, a plasmin-derivative that bears a catalytic efficiency on cross-linked fibrin that exceeds that of plasmin (354). NE is also able to efficiently disable the major plasmin-inhibitor, α2-antiplasmin, further supporting plasmin action (355). PAD4 is eventually secreted from neutrophils during NET formation and was shown to citrullinate fibrin in rheumatoid arthritis (356) (although less efficiently than PAD2 (357)), but the significance of this related to thrombolysis is not known.

NETs can be degraded by DNases in vitro. There are two main DNases in human plasma: DNase1 and DNase1-like family, out of which, DNase1-like 3 (DNase1l3) is the most characterized. Both enzymes show calcium/magnesium dependency. DNase1 is secreted into circulation by a variety of exocrine and endocrine organs (358-360), whereas DNase1l3 is released from liver cells, splenocytes, macrophages and kidney cells (361). DNase1 and DNase1l3 cooperate during in vitro chromatin breakdown (chromatin fragmentation is completely absent if DNase1 and DNase1l3 is inhibited) (362), and pre-processing of NETs by DNAse1 also facilitates NET clearance by macrophages (363). Plasmin is able to cleave histones (364), thus helping DNase action, since DNase1 prefers protein-free DNA. In addition, NE already present in NETs, APC (see before), thrombin (365) and an unidentified protease (366) may also assist in histone degradation. The in vivo relevance of plasmin-DNase cooperation is reflected in the elevated levels of plasma DNA in patients with DVT (290). As a possible counter-regulatory mechanism, NETs seem to protect themselves from bacterial and perhaps human DNases by limiting the availability of divalent cations (see calprotectin) and consequently the activity of these enzymes (367).

DOI:10.14753/SE.2015.1738

2. OBJECTIVES

2.1. Effects of mechanical stress

In light of the gross structural alterations in in vitro stretched fibrin as discussed in 1.1.4., the present study was undertaken in an attempt to understand the relationship between clot structure and lytic susceptibility of clots exposed to similar mechanical stress. In the first part of this work, our aims were therefore:

-To examine thrombi from patients to seek for possible effects of intravascular mechanical forces
-To build a model system in which fibrin structure approximates that of the external region of certain thrombi exposed to shear stress exerted by blood flow
-To assess structural and lytic properties of stretched fibrin clots

2.2. Effects of NET components

Given the various known interactions of NET components and the haemostatic system, and taking into consideration, that DNA and histones may also accumulate in clots in a NETosis-independent manner, in the second part of the work presented here, we focused on the following:
-To detect DNA and histone content in arterial thrombi from patients
-To investigate the effect of NET components on fibrin structure in pure fibrin clots and more complex plasma systems
-To assess mechanical properties of clots containing DNA, histones, or their combinations
-To study the process of fibrinolysis in plasma clots containing DNA ± histones or NETs derived from activated neutrophils

DOI:10.14753/SE.2015.1738

3. MATERIALS AND METHODS

3.1. Patients

Ten patients (4 men and 6 women, mean age: 66 years; range: 49–91) subjected to thrombectomy were enrolled in the study regarding the effects of mechanical stress. Eight of them had obliterative thrombosis localized in large arteries (femoral, ileac, popliteal and brachial) based on atherosclerosis (in four cases the thrombus was in a previously implanted graft). One patient had venous thrombosis and the pulmonary embolizing thrombus was removed, one thrombus was from a resected aorta aneurysm. To study the abundance of DNA and histones in thrombi, three additional representative specimens were selected: a thrombus from popliteal artery, a thrombus from infrarenal aorta aneurysm, and a thrombus from femoro-popliteal graft. No inherited or acquired thrombophilic state could be diagnosed in the patients. At the time of thrombectomy all patients received heparin treatment. Written informed consent was obtained from all patients and the study protocol was approved by the institutional and regional ethical board.

3.2. Preparation of basic materials

3.2.1. Preparation of fibrin clots exposed to mechanical stress

Elastic silicon rubber tubes (3 mm internal diameter) were soaked in 25% (v/v) Triton X-100 solution for 60 min and thoroughly washed with water. Human fibrinogen (plasminogen-depleted; Calbiochem, LaJolla, CA, USA) at 30 μM in 10 mM HEPES-NaOH 150 mM NaCl pH 7.4 buffer was clotted in these tubes with 30 nM thrombin (thrombin from Serva Electrophoresis GmbH [Heidelberg, Germany] was further purified by ion-exchange chromatography on sulfopropyl-Sephadex yielding preparation with specific activity of 2100 IU/mg (368)) at 37 °C for 30 min. Thereafter 1.5 cm long pieces of fibrin were cut and used for SEM imaging or fibrinolytic measurements as non-stretched (NS fibrin with 106 μl volume and 140 mm^2 surface area). For fibrinolytic experiments with stretched fibrin, 2.25 or 1.5 cm long pieces of the rubber tubes with fibrin inside were stretched to a final length of 4.5 cm and used as 2S fibrin (16 μl volume and 94.7 mm^2 surface area) and 3S fibrin (10.6 μl volume and

77.4 mm^2 surface area), respectively. The volume and surface area of fibrin were estimated from the initial dimensions of the rubber mould and the data reported in (80) for the volume changes of stretched fibrin. For SEM imaging and confocal microscopy the fibrin clots were removed from the mould, stretched and kept in this state with compression under the clamps of Bürker chambers during glutaraldehyde fixation or under glass coverslips of self-designed confocal microscopic chambers.

3.2.2. Plasmin generation

Plasmin was generated using plasminogen (isolated from human plasma (369) activated by streptokinase (Calbiochem, LaJolla, CA, USA) at 172.5 U/mg zymogen. For plasmin inactivation assays, 40 μM plasminogen was activated by 70 nM tissue-type plasminogen activator (tPA, Boehringer Ingelheim, Ingelheim am Rhein, Germany) at 37 °C for 25 min. Determination of active enzyme concentration was carried out before each experiment by measuring the hydrolysis rate of synthetic peptide Spectrozyme-Plasmin (SPPL, H-D-norleucyl-hexahydrotyrosyl-lysine-p-nitroanilide, American Diagnostica, Pfungstadt, Germany) substrate at eight different concentrations. Calculation was performed on the basis of the Michaelis-Menten equation using an extinction coefficient of 8820 M^{-1} cm^{-1} for p-nitroaniline, and k_{cat}=13.5 s^{-1} (determined in a separate experiment with active site-titrated enzymes (370)).

3.2.3. Preparation of fibrin degradation products (FDP)

Clotting and fibrinolysis were initiated simultaneously in transparent reaction tubes with a diameter of 0.8 cm using 2 ml volumes of mixtures of thrombin, fibrinogen and plasmin (all components in 25 mM NaH_2PO_4/Na_2HPO_4 75 mM NaCl pH 7.4 buffer) incubated at room temperature. The final concentration of fibrinogen was 6 μM in the first set of tubes (for extensively degraded products of fibrin digestion) and 12 μM in the second set (for partial digestion and generation of large FDP). Final concentrations of thrombin (90 nM) and plasmin (5 nM) were identical in the two set of tubes. 15 seconds after setting up the mixture, a steel ball with a diameter of 2 mm and a weight of 0.13 g was placed on the surface of the clot. In the case of tubes with higher concentration of fibrinogen, plasmin action was stopped by the addition of 4-(2-

aminoethyl)-benzenesulphonyl fluoride (Pefabloc® from Boehringer Mannheim, Germany) at a final concentration of 0.05 mM immediately after the ball reached the bottom of the tube (approximately 16-18 hours after the start of lysis). In the case of tubes with lower concentrations of fibrinogen, Pefabloc® was added 2-4 hours later, when the visible fibrin gel had totally disappeared. The fluid phases were withdrawn from each of the tubes after centrifugation at 6,000*g* for 5 min, and the total protein contents were determined from the values of absorbance of the supernatants at 280 nm (A_{280} of 1.6 corresponds to 1 g/l non-clottable fibrin degradation products measured under identical conditions (371). The supernatant was subjected to SDS electrophoresis on 4-15 % polyacrylamide gel under non-reducing and reducing conditions and silver-stained. Concentrations of large degradation fragments (over 150 kDa) were calculated as a fraction of total protein based on quantitative gel analysis using SigmaGel software (Jandel Scientific, Erkrath, Germany).

3.2.4. Preparation of neutrophil DNA

Neutrophil granulocytes were isolated from buffy coat fraction of human blood (Hungarian Blood Supply Service, Budapest, Hungary) (372) which was mixed with an equal volume of 2 w/v% Dextran T500 (GE Healthcare Bio-Sciences, Uppsala, Sweden) in saline followed by a centrifugation at 150*g* for 5 min. Platelet-rich supernatant was discarded and the residual fraction was mixed again with an equal volume of 2 w/v% Dextran T500 in saline and erythrocytes were allowed to sediment for 45 min. The supernatant was mixed with an equal volume of PBS (1.5 mM KH_2PO_4, 8.1 mM Na_2HPO_4 buffer pH 7.4 containing 137 mM NaCl, 2.7 mM KCl and 5 mM glucose) and centrifuged for 3 min at 400*g*. The cell pellet was washed with an equal volume of PBS-glucose followed by centrifugation for 3 min at 400*g*. The polymorphonuclear (PMN) leukocyte-rich fraction was layered on an equal volume of Percoll (GE Healthcare Bio-Sciences, Uppsala, Sweden) and centrifuged for 5 min at 400*g*. The supernatant was removed and further centrifuged for 15 min at 800*g*. The PMN-rich pellet was washed in PBS twice and centrifuged for 3 min at 400*g*. Isolated neutrophils were lysed in 20 mM HEPES-NaOH pH 7.9 buffer containing 400 mM NaCl, 1 mM EDTA, 1 mM EGTA and 1 w/v% NP-40 non-ionic detergent ($2x10^5$ cell/ml). Following cell lysis DNA was extracted using phorbol:chloroform:isoamyl

alcohol 25:24:1 reagent (Sigma-Aldrich Kft, Budapest, Hungary), precipitated out of the water phase in 0.3 M Na-acetate pH 5.2 and 96 v/v% ethanol and resuspended in 25 mM NaH_2PO_4/Na_2HPO_4 pH 7.4 buffer containing 75 mM NaCl. The ratio of absorbance at 260 and 280 nm was 1.88-1.95 in the final preparation. The concentration of DNA was determined from absorbance at 260 nm using calf thymus DNA as a reference. Human granulocyte DNA was used for certain confocal studies, for other experiments, calf thymus DNA was applied.

3.2.5. Expression and characteristics of fluorescent chimeric tPA variants

Recombinant human tPA-jelly fish green and yellow fluorescent proteins (GFP/YFP) were constructed and expressed using the Bac-to-Bac baculovirus expression system as a tPA-C-terminal fusion with Enhanced Green/Yellow Fluorescent Protein (EGFP/EYFP) isolated from the pEGFP/pEYFP plasmid (Clonetech, Mountain View, CA, USA), as described in (373,374).

3.3. Structural studies

3.3.1. Scanning electron microscope (SEM) imaging of thrombi and clots

Immediately (within 5 min) after the surgery, 5x5x10 mm pieces of thrombi were placed into 10 ml 100 mM Na-cacodylate pH 7.2 buffer for 24 h at 4 °C, followed by repeated washes with the same buffer.

Fibrin clots were prepared in duplicate from mixtures of 6 μM fibrinogen and various concentrations of DNA (from calf thymus, Calbiochem, LaJolla, CA, USA) and histones (Histone IIIS from calf thymus (lysine rich fraction containing H1), Sigma-Aldrich, Budapest, Hungary) clotted with 30 nM thrombin at 37 °C for 60 min.

Plasma clots were prepared in duplicate from mixtures of human plasma (citrated, fresh frozen plasma obtained from Hungarian Blood Supply Service, Budapest, Hungary, 2-fold diluted in 10 mM HEPES buffer pH 7.4 containing 150 mM NaCl) supplemented with 12.5 mM $CaCl_2$, and additives (various concentrations of DNA and/or histone) clotted with 16 nM thrombin at 37 °C for 60 min. Clots were washed 7 times with distilled water at 4 °C for 5 minutes.

Granulocytes at $5x10^4$/μl (in PBS containing 5 mM glucose) were pipetted into culture plate wells containing cover slips with a diameter of 6 mm at the bottom. Cells were activated with 50 nM PMA (phorbol 12-myristate 13-acetate; SIGMA, St Louis, MO, USA) for 4 hours at 37 °C. After the incubation, the fluid phase was withdrawn. In certain cases, cover slips were thereafter dipped in a mixture of 10 nM thrombin and 6 μM fibrinogen.

Stretched fibrin clots and their controls were prepared as mentioned in *3.2.1*.

All samples above were fixed in 1% (v/v) glutaraldehyde (in 100 mM Na-cacodylate pH 7.2 buffer) for 16 h. The fixed samples were dehydrated in a series of ethanol dilutions (20 – 96%(v/v)), 1:1 mixture of 96%(v/v) ethanol/acetone and pure acetone followed by critical point drying with CO_2 in E3000 Critical Point Drying Apparatus (Quorum Technologies, Newhaven, UK). The specimens were mounted on adhesive carbon discs, sputter coated with gold in SC7620 Sputter Coater (Quorum Technologies, Newhaven, UK) and images were taken with scanning electron microscope EVO40 (Carl Zeiss GmbH, Oberkochen, Germany).

3.3.2. Morphometric analysis of fibrin structure in SEM images

The SEM images of certain thrombi and clots were analysed to determine the diameter of the fibrin fibres and area of the fibrin network pores using self-designed scripts running under the Image Processing TOOLBOX v. 7.0 of Matlab 7.10.0.499 (R2010a) (The Mathworks, Natick, MA, USA) (375). The diameters were measured by manually placing the pointer of the Distance tool over the endpoints of transverse cross sections of 300 fibres from each image (always perpendicularly to the longitudinal axis of the fibres). Pores of the gels were identified with a boundary tracing algorithm of the Image Processing Toolbox working on the whole area of the image as a region of interest. With this approach the area of the plane projections of the gel pores was measured and these values were used as dimensionality-reduced indicators of the pore size. For each measurement, 2 images of 2 independent samples were analysed in a single global procedure.

3.3.3. Immunohistochemistry

After surgery, certain removed thrombus samples were frozen immediately at -70 °C and stored until examination. Cryosections (6 μm thickness) of these thrombi were attached to lysine-coated slides. Sections were fixed in acetone at 4 °C for 10 min and air-dried for 5 min at room temperature, followed by incubation in 100 mM Na-phosphate 100 mM NaCl pH 7.5 buffer (PBS) containing 5 w/v% bovine serum albumin (BSA from Sigma, St. Louis, MO, USA) to eliminate nonspecific binding of antibodies. Subsequently slides were washed in PBS 3 times and DNA was stained with the dimeric cyanine nucleic acid dye TOTO-3® (T-3604, Life Technologies, Budapest, Hungary; excitation 640 nm, emission 660 nm) at 1:5000 dilution with PBS containing 10 % glycerol and 0.02 % Tween 20 for 15 minutes followed by 3 washes in 50 mM TRIS-HCl, 100 mM NaCl, 0.02 %(w/v) NaN_3 pH 7.4 (TBS). For double immunostaining the sections were incubated with 2 μg/ml mouse monoclonal anti-human fibrin antibody (ADI313, American Diagnostica, Pfungstadt, Germany) and 2 μg/ml rabbit anti-human histone H1 antibody (Sigma-Aldrich, Budapest, Hungary) in TBS. Following washing with TBS, sections were treated with Alexa Fluor 488 (excitation 495 nm, emission 519 nm) goat anti-mouse immunoglobulin antibody (Life Technologies, Budapest, Hungary) at 1:100 dilution and Alexa Fluor 546 (excitation 556 nm, emission 573 nm) goat anti-rabbit immunoglobulin antibody (Life Technologies, Budapest, Hungary) at 1:100 dilution. Following 3 washes glass coverslips were affixed over a drop of 50 %(v/v) glycerol in TBS. Confocal fluorescent images were taken using a Zeiss LSM710 confocal laser scanning microscope equipped with a 20x1.4 objective (Carl Zeiss, Jena, Germany) at 488-nm excitation laser line (20 % intensity) and emission in the 500–530 nm wavelength range, 543-nm excitation laser line (100 % intensity) and emission in the 565–615 nm wavelength range, 633-nm excitation laser line (100 % intensity) and emission in the range over 650 nm wavelength.

3.3.4. Clot permeability assays

Fibrin clots containing 8 μM fibrin and 16 nM thrombin ± additives (50 μg/ml DNA and/or 250 μg/ml histone) were prepared in 100 μl volumes at the bottom of 5 ml plastic

pipette tips. After 70 mins of incubation at 37 °C, the tips were filled up with buffer(10 mM HEPES 150 mM NaCl pH 7.4), and a stopper was used to close the upper end of the tip. An additional syringe stabbed the stopper through; the inside of the syringe was removed and filled up with 2 ml buffer. Pressure was kept unchanged by continuously refilling the syringe with buffer to the 2 ml mark.

Plasma clots (supplemented with 20 mM $CaCl_2$, clotted with 16 nM thrombin) ± additives (45 μg/ml DNA and/or 220 μg/ml histone) were prepared in 1 ml plastic pipette tips the internal surface of which had been previously scratched. After 70 min of incubation at 37 °C, the tips were filled with buffer. Pressure was kept constant by refilling the buffer to the top of the tip.

A silicon tube with 3 mm internal diameter was attached to the exit of each pipette tip, and the permeated volume was calculated from mm values of fluid front movement (15 mm corresponds to 100 μl). Fluid front movement was measured for every 10 minutes after 160 μL buffer had washed the clot through. Values measured for plasma clots after more than 3 hours were discarded, since an abrupt increase of permeability was seen in all cases (possibly due to slow endogenous lysis mediated by tPA). Ks (permeability coefficient) was calculated from the equation $K_S = \frac{Q \cdot L \cdot \eta}{t \cdot A \cdot \Delta P}$ where Q = permeated volume of buffer (cm^3); η = viscosity of buffer (10^{-2} poise = 10^{-7} N s cm^{-2}); L = clot length (1.5 cm for fibrin clots, 1.7 cm for plasma clots); A = average cross-sectional area of the clot (0.102 cm^2 for fibrin clots, 0.057 cm^2 for plasma clots); t = time (s); ΔP = pressure drop (0.209 N cm^{-2} for fibrin clots, 0.056 N cm^{-2} for plasma clots).

3.4. Mechanical studies-evaluation of fibrin rigidity

140 μl 30 μM fibrinogen was pre-mixed with 60 or 120 μl 0.5 mg/ml DNA and supplemented with 10 mM HEPES pH 7.4 buffer containing 150 mM NaCl to 500 μl final volume. Clotting was initiated with 50 μl 100 nM thrombin added to 410 μl fibrinogen solution and 360 μl of the clotting mixture was transferred to the plate of HAAKE RheoStress 1 oscillation rheometer (Thermo Scientific, Karlsruhe, Germany) thermostatted at 37 °C. The cone (titanium, 2° angle, 35 mm diameter) of the rheometer was lowered and strain (γ) of 0.015 was imposed exactly at 2.5 min after the addition of thrombin. Measurements of storage modulus (*G'*) and loss modulus (*G''*) were taken at

1 Hz in the course of 15 min with HAAKE RheoWin data manager software v. 3.50.0012 (Thermo Scientific, Karlsruhe, Germany) (23Colin). Following this 15-min clotting phase determination of the flow limit of the fibrin gels was performed in the same samples increasing the applied shear (τ) from 0.01 to 500.0 Pa stepwise (100 steps in 60 s) and the measured resulting strain was used for calculation of the viscosity modulus (the critical shear τ_0 resulting in fall of viscosity to 0 was used as indicator of the gel/fluid transition in the fibrin structure).

3.5. Intermolecular interactions-isothermal titration calorimetry (ITC)

The enthalpy changes accompanying the interaction of DNA and proteins (fibrin degradation products (FDP), fibrinogen, histones, plasminogen) were measured using isothermal titration method on VP-ITC microcalorimeter (MicroCal Inc., Northampton, MA). The proteins were injected in a series of 25 aliquots (10 µl each) into the cell of the calorimeter containing DNA or histones and the heat increment of each addition was recorded by the instrument. Dilutions of protein into buffer were carried out in separate series of injections and these heat increments were subtracted from the raw data. The heat data for the interactions were evaluated according to the single-site algorithm with ITC Data Analysis version 7.0 software (MicroCal). For the calculation of equilibrium parameters the mass concentration of DNA was converted to molar concentration of nucleotides using average molecular weight of 500 Da. The molar concentration of the fibrin degradation products (FDP) of 150 kDa size or larger was estimated from the mass concentration and densitometric data of the polyacrylamide gel electrophoretic (PAGE) pattern of the FDP used for the binding experiments.

3.6. Studies of fibrinolysis

3.6.1. Confocal microscopic imaging

Clots were prepared from 6/30 µM fibrinogen or 2-fold diluted human plasma, supplemented with 50/90 nM Alexa Fluor® 546-conjugated fibrinogen (Invitrogen Life Technologies, Budapest, Hungary), 0.2/1.5 µM plasminogen, clotted with 16/30 nM thrombin for 30 minutes at room temperature in 0.5 mm high chambers constructed from glass slides, or uncoated IBIDI VI 0.4 µ-slides (Ibidi GmbH, Martinsried,

Germany). In certain cases, 50 or 100 μg/ml human granulocyte DNA and/or 45/280 μg/ml histone were also added to the mixture. Thereafter 55 nM tPA-GFP or 85 nM tPA-YFP supplemented with 3 μM plasminogen was added to the edge of the clot and the fluorescence (excitation wavelength 488 nm, emission wavelength 525 nm for tPA-GFP/tPA-YFP detection and excitation wavelength 543 nm, emission wavelength 575 nm for Alexa546-fibrinogen detection) was monitored with Confocal Laser Scanning System LSM710 (Carl Zeiss GmbH, Jena, Germany) taking sequential images of the fluid-fibrin interface at a distance of approximately 50 μm from the glass surface with identical exposures and laser intensities using a Plan-NeofluarX20/0.5 objective.

3.6.2. Plasminogen activation assays

In 96-well microtiter plates, 2-times diluted plasma supplemented with 12.5 mM $CaCl_2$ ± additives (50 μg/ml DNA and/or 250 μg/ml histone) was clotted with 16 nM thrombin in a volume of 80 μl. After 45 min at 37 °C 60 μl of 28 nM tPA and 0.6 mM Spectrozyme-PL in 10 mM HEPES, 150 mM NaCl pH 7.4 were placed on the surface of the clot. The forming plasmin generated p-nitroaniline, the absorbance of which was continuously recorded at 405 nm (A_{405}) with Zenith 200rt spectrophotometer. The measured values were plotted versus time squared (t^2) yielding a linear relationship according to the equation $\Delta A_{405} = 0.5\varepsilon k_1 k_{cat}[tPA]t^2$ (376), where ε = 12.6 mM^{-1} cm^{-1} is the extinction coefficient of p-nitroaniline , k_1 = 350 min^{-1} is the turn-over number of plasmin on Spectrozyme-PL (377), k_{cat} and $[tPA]$ are the catalytic constant for plasminogen activation and the concentration of tPA in the reactive layer on the surface of fibrin, respectively (378). The term $V_{app} = k_{cat}[tPA]$ is equivalent to the apparent maximal rate of plasminogen activation in the reactive layer of fibrin and was determined from linear regression according to the abovementioned equation (Curve fitting toolbox v. 3.3.1 of Matlab 2013a).

For the detection of plasminogen activation on a stretched substrate, 20 μg/ml plasminogen was added to fibrinogen before clotting in elastic silicon rubber tubes (performed as described in 3.2.1.). After stretching, a shell filled with buffer was formed around the retracted fibrin in the rubber tube and it was replaced with 1.2 μM tPA using two needles pierced at the clamped ends of the tube. After incubation at 37 °C for various times, the total fluid phase was removed and its volume was measured. The

concentration of plasmin in the fluid phase was determined from the enzyme activity measured on 0.1 mM Spectrozyme-PL using active site-titrated plasmin with accurately known concentration as a reference (at dilutions yielding linear dependence of amidolytic activity on enzyme concentration) (379). The amount of generated plasmin was calculated as the product of this concentration and the measured volume of the fluid surrounding fibrin and expressed in pmol per unit surface of fibrin (the area of fibrin surface after stretching was calculated as described in 3.2.1.). In order to account for plasmin retention in fibrin, plasminogen activation was also measured in the presence of plasmin substrate Spectrozyme-PL at 0.2 mM (33-fold higher concentration than its Km (377)). After various incubation times, the fluid surrounding the fibrin was withdrawn and its volume and absorbance at 405 nm were measured. The amount of p-nitroaniline released from the plasmin substrate was normalized for unit surface area of the fibrin clots in the same way as the amount of plasmin.

3.6.3. Turbidimetry assays

tPA-driven lysis of plasma clots was studied in 96-well microtiter plates. 2-fold diluted plasma supplemented with 8 μM plasminogen and 12.5 mM $CaCl_2$ and DNA and/or Histone at various concentrations were mixed with 16 nM thrombin in a total volume of 80 μl (all substances diluted in 10 mM HEPES buffer pH 7.4 containing 150 mM NaCl). In another set of experiments, $5x10^3$/μl granulocytes were incorporated into to clots (instead of pure DNA and histones), in certain cases activated by 100 nM PMA in the presence/absence of 0.2 mM Cl-Amidine (Calbiochem, San Diego, CA, USA). Lysis was initiated by addition of 100 μl of tPA (0.2 μM) to the clot surface, following 60 min clotting. In the case of experiments with neutrophils, the time for clotting was prolonged up to 240 min to allow for NET formation. Clot formation and dissolution was followed by measuring the light absorbance at 340 nm at 37 °C with a Zenyth 200rt microplate spectrophotometer (Anthos Labtec Instruments GmbH, Salzburg, Austria). For adequate comparison of lytic rates from measurements, in which different maximum turbidity values were reached despite the identical quantities of fibrin, the absorbance values were normalized as follows: clot integrity = $100*(A-A_i)/(A_{max}-A_i)$ where A_i is the initial- and A_{max} is the maximal absorbance at 340 nm. The time needed to reduce the turbidity of the clot to a given fraction of the maximal value (T50 to reach

0.5A_{max}, T10 to reach 0.1A_{max}) was used as a quantitative parameter of fibrinolytic activity.

3.6.4. Examination of clot lysis in microslide channels

Plasmin-induced plasma clot lysis was examined in IBIDI VI 0.4 μ-slides. Two-fold diluted plasma supplemented with 12.5 mM $CaCl_2$ and 50 μg/ml DNA and/or 250 μg/ml histone were mixed with 16 nM thrombin. The mixtures were quickly pipetted into the 30 μl channnels of IBIDI slides, and incubated at 37 °C for 30 min. Lysis was initiated by the addition of 60 μl of 5 μM plasmin introduced to the opening of the channels. (All substances were diluted in 10 mM HEPES buffer pH 7.4 containing 150 mM NaCl). Lysis of plasma clots was followed by time lapse photoscanning of the transparent fluid/opaque clot boundary.

3.6.5. Release of soluble fibrin degradation products (FDP) in the course of fibrinolysis

Stretched fibrin containing 0.2 μM plasminogen was prepared as described in *3.2.1*. and fibrinolysis was initiated with 15 nM tPA added to the surface. For some measurements plasminogen-free fibrin was prepared and fibrinolysis was initiated with 1 μM plasmin. At 15-min intervals the fluid surrounding the fibrin was withdrawn, its volume was measured and ice-cold ethanol was added at 20% (v/v) final concentration. After centrifugation at 20,000*g* for 5 min, the protein content of the supernatant was determined from the values of its absorbance at 280 nm. After adjustment for protein concentration, certain samples were subjected to SDS electrophoresis on 12.5% polyacrylamide gel under non-reducing conditions and silver-stained.

3.7. Enzyme inactivation assays

3.7.1. Defibrinogenated plasma-induced inactivation of plasmin

0.1 v/v% acetic acid (in distilled water) and plasma were mixed in a 1:4 volume ratio. After 35 min incubation at 58 °C, the mixture was placed on ice for 10 min. After 15 min centrifugation at 800 g, the supernatant was withdrawn, and was used as defibrinogenated plasma. A 20 μl mixture of plasmin, 12.5 mM $CaCl_2$, 4-fold diluted

defibrinogenated plasma ± 250 μg/ml DNA were incubated at room temperature for 10 seconds, and then diluted 11-fold in 0.1 mM Spectrozyme-PL. All substances were in 10 mM HEPES buffer pH 7.4 containing 150 mM NaCl. The change of absorbance at 405 nm (ΔA/minute) was measured with a Beckman DU 7500 spectrophotometer. Initial plasmin activity (in the absence of inhibitors and DNA) was set to yield a ΔA/minute value between 0.12 and 0.2. All obtained A_{405} values were normalized for this value**.**

3.7.2. Inactivation of thrombin by antithrombin

Mixtures of 55 nM antithrombin (American Diagnostica, Stamford, CT, USA or NIBSC, S. Mimms, UK, concentration of active antithrombin titrated with thrombin is reported), 170 nM thrombin, 0/25 μg/ml histone ± 25 μg/ml DNA in the presence or absence of 0.025 U/ml heparin (NIBSC, S. Mimms, UK) were incubated for 1/5/10/15 minutes at room temperature. For another set of experiments, mixtures of 2.5 μM antithrombin, 180 nM thrombin, 0/0.5/1/2/2.5/10/20 μg/ml histone ± 5/25/50 μg/ml DNA in the presence of 0.15 U/ml heparin were incubated for 15 seconds at room temperature. Thereafter, samples from the incubation mixtures were 3-fold diluted with fibrinogen so that the final concentration of fibrinogen was 6 μM. Clotting time was measured with a coagulometer KC-1A (Amelung, Lemgo, Germany) at 37 °C. All substances above were diluted in 10 mM HEPES 150 mM NaCl pH 7.4, for the dilution of thrombin, the buffer also contained 1 mg/ml bovine serum albumin (SIGMA, St. Louis, MO, USA).

3.8. Statistical procedures

The distribution of the data on fibre diameter and pore area measured in SEM images was analysed using the algorithm described in (379): theoretical distributions were fitted to the empirical data sets and compared using Kuiper's test and Monte Carlo simulation procedures. The statistical evaluation of other experimental measurements in this work was performed with the Kolmogorov–Smirnov test (Statistical TOOLBOX 7.3 of Matlab); values of $p < 0.05$ were considered statistically significant. Detailed description of statistical analysis of measurements is given in figure legends in the respective section of 'RESULTS'.

DOI:10.14753/SE.2015.1738

4. RESULTS

4.1. Stressed fibrin lysis

4.1.1. Structural features of thrombi from patients

In order to evaluate fibrin architecture at a microscopic scale in relation to the exposure of shear stress, SEM images were taken from the surface and interior core regions of surgically removed thrombi (Fig. 14A). In four (two in grafts, one in popliteal artery and the single pulmonary embolus) out of the 10 examined specimens a significant difference could be observed regarding the arrangement of fibres in the interior and exterior regions of the clot: while in all cases the core of the thrombi contained a random fibrin network, in 4 thrombi the gel pores on the surface were elongated in one direction resulting in longitudinal alignment of the fibres accompanied by their tighter packing in the transverse direction (in the remaining six cases the surface of the clot appeared similar to the core).

Morphometric analysis of the fibrin structure (Fig. 14B) showed that both fibre diameter and gel pore area were significantly lower (by about 16% and twofold, respectively) in the exterior regions of these clots. Since the appearance of fibrin on the surface of thrombi was reminiscent of the fibrin structure reported for clots exposed to mechanical stretching 80) stretched clots were used (Fig. 15) as a model system to evaluate the impact of mechanical stress on the structure and lytic susceptibility of fibrin.

4.1.2. Structural features of stretched fibrin clots

Stretching changed the arrangement of the fibres (Fig. 15A) to a pattern similar to the one observed on the surface of thrombi (Fig. 14A); both the median fibre diameter and the pore area of the clots decreased two- to three-fold and the distribution of these morphometric parameters became more homogeneous (Fig. 15B).

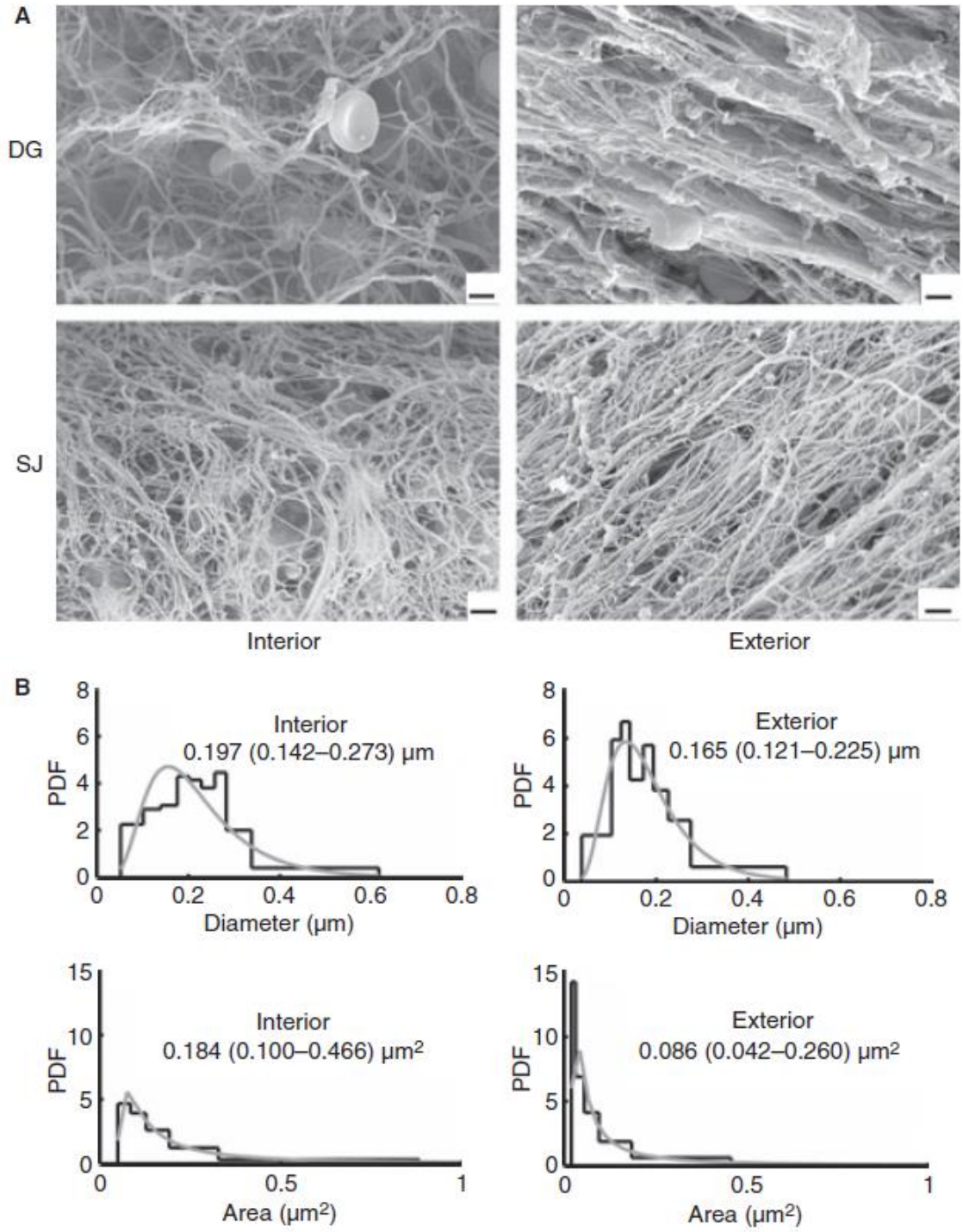

Figure 14. Fibrin structure on the surface and in the core of thrombi. *A: After thrombectomy thrombi were washed, fixed and dehydrated as detailed in 3.3.1. Scanning electron microscopic (SEM) images were taken from the surface and transverse section of the same thrombus sample, scale bar = 2 µm. DG: a thrombus from popliteal artery, SJ: a thrombus from aorto-bifemoral by-pass Dacron graft. B: Fibre diameter (upper graphs) and fibrin pore area (lower graphs) were measured from*

the SEM images of the DG thrombus shown in (A) using the algorithms described in 3.3.2.. The graphs present the probability density function (PDF) of the empirical distribution (black histogram) and the fitted theoretical distribution (gray curves). The numbers under the location of the observed fibrin structure show the median, as well as the bottom and the top quartile values (in brackets) of the fitted theoretical distributions. The parameters of the fitted distributions differ between the interior and exterior data sets at p<0.01 level according to Kuiper's test-based evaluation as described in 3.8.

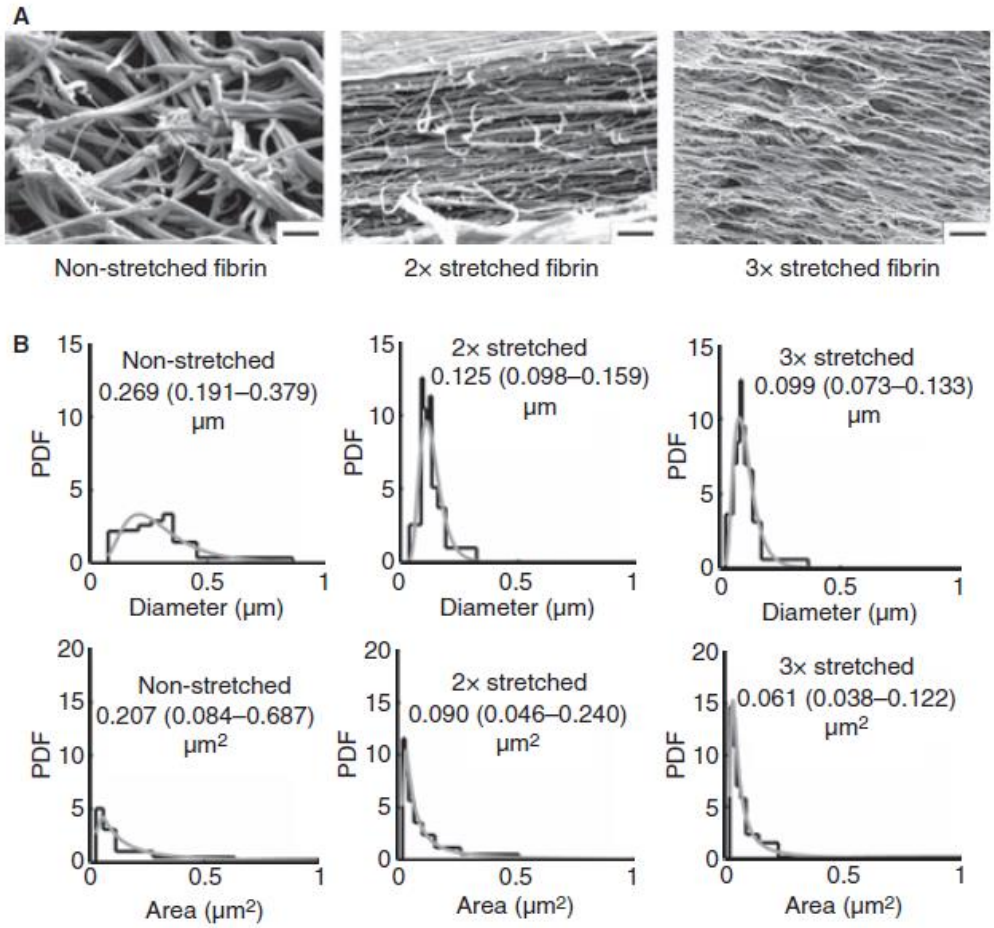

Figure 15. Changes in fibrin network structure caused by mechanical stretching. *A: Scanning electron microscopic (SEM) images of fibrin clots prepared from 30 µM fibrinogen clotted with 30 nM thrombin. Fibrin samples were fixed with glutaraldehyde before stretching or after two- and three-fold stretching as indicated, scale bar = 2 µm. B: Fibre diameter (upper graphs) and fibrin pore area (lower graphs) were measured*

from the SEM images illustrated in (A) using the algorithms described in 3.3.2.. The graphs present the probability density function (PDF) of the empiric distribution (black histogram) and the fitted theoretical distribution (gray curves). The numbers under the fibrin type show the median, as well as the bottom and the top quartile values (in brackets) of the fitted theoretical distributions. The parameters of the fitted distributions differ between any two data sets at p<0.001 level according to Kuiper's test-based evaluation as described in 3.8.

4.1.3. Lysis of stretched fibrin

The amount of plasmin generated by tPA on the surface of fibrin and released in the fluid phase decreased two- to three-fold, if stretched fibrin was used as a template instead of its non-stretched counterpart (Fig. 16A-left). When plasminogen activation

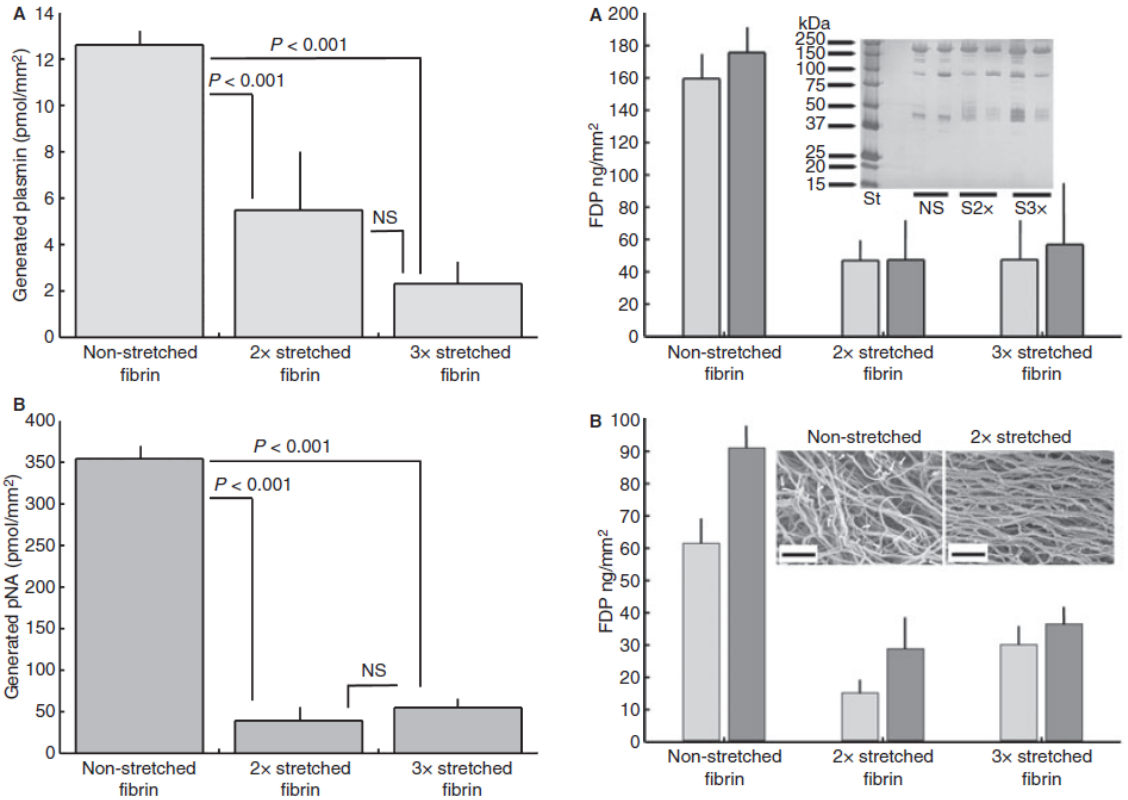

Figure 16. Plasminogen activation on the surface of fibrin (left) and the release of soluble fibrin degradation products (FDP) from the surface of clots (right). *A-left: Plasminogen (200 nM) was added to fibrinogen before clotting performed as in Figure 15. After stretching, the buffer around the retracted fibrin in the rubber tube was replaced with 1 nM tissue-type plasminogen activator (tPA) and after 30-min*

incubation at 37 °C the plasmin activity in the fluid phase was measured on 0.1 mM Spectrozyme-PL. Using a series of accurately known plasmin concentrations as a reference, the amount of generated plasmin is shown (normalized for unit surface area of the fibrin clots as described in 3.6.2.). B-left: Plasminogen activation was initiated under the same conditions as in A-left, but the tPA solution contained 0.2 mM Spectrozyme-PL. After 150-min incubation the fluid surrounding the fibrin was withdrawn and its volume and absorbance at 405 nm were measured. The amount of p-nitroaniline released from the plasmin substrate is shown (normalized for unit surface area of the fibrin clots as described in 3.2.1.). Data are presented as mean and SD (n = 6–9), the p-values refer to Kolmogorov–Smirnov test for the linked pairs of data sets (NS indicates p>0.05). A-right: Fibrin containing 200 nM plasminogen was prepared as in Figure 16A-left and fibrinolysis was initiated with 15 nM tissue type plasminogen activator (tPA). B-right: Plasminogen-free fibrin was prepared as in Figure 15 and fibrinolysis was initiated with 1 μM plasmin. At 15-min intervals the fluid surrounding the fibrin was withdrawn and its ethanol-soluble FDP content was measured as described in 3.6.5.. The amount of released FDP is shown (normalized for unit surface area of the fibrin clots) for the 1st (light gray bars) and 3rd (dark gray bars) 15-min period of the lysis. Data are presented as mean and SD (n = 4) and the differences between the non-stretched and stretched fibrins are significant at the p<0.01 level according to the Kolmogorov–Smirnov test. Inset A: After adjustment for protein concentration the samples in A-right were subjected to SDS electrophoresis on 12.5% polyacrylamide gel under non-reducing conditions and silver-stained. Inset B: After withdrawal of the fluid phase after 45-min digestion the samples in B were fixed in glutaraldehyde and SEM images were taken as described in 3.3.1.; truncated fibres are indicated by white arrows, scale bar = 2 μm.

was evaluated in the presence of a low-molecular-weight plasmin substrate Spectrozyme-PL, which is able to penetrate into the clot, the detected plasmin activity was similarly lower on stretched fibrin (Fig. 16B-left). Thus, the effect of the modified fibrin structure on the apparent plasmin generation is based on changes in plasminogen activation rather than in plasmin retention in the clot.

In agreement with the conclusion for restricted tPA-dependent plasminogen activation on the surface of stretched fibrin detected with synthetic plasmin substrate, the non-stretched fibrin lysed completely in the time range of 65–70 min, whereas the stretched clots were observed to fracture only after 80 min into large fragments that remained visible for at least 60 min more. The release of soluble FDP from stretched fibrin clots was also slower (Fig. 16A-right). However, this assay measures the activity of the generated plasmin on fibrin substrates of different structure (Fig. 15) and thus the FDP release reflects changes not only in plasminogen activation, but in susceptibility of fibrin to plasmin too.

In order to evaluate separately the direct fibrin solubilisation by plasmin, plasminogen-free fibrin clots were treated with plasmin and the course of their dissolution was monitored (Fig. 16B-right). The SEM images of non-stretched plasmin digested for 45 min with plasmin showed many truncated fibres in the remnant fibrin, whereas only few fibres presented signs of digestion in the stretched fibrin (Fig. 16B-right, Inset). These experiments confirm that FDP release from stretched fibrin was slower but the effect was weaker than in the case of tPA-induced fibrinolysis. These results indicate that the stretched fibrin structure hinders both stages of fibrinolysis, plasminogen activation and fibrin lysis.

In spite of the differences in the time-course of fibrinolysis, the molecular-size pattern of FDP released from different fibrins was essentially identical (Fig. 16A-right, Inset).

The mechanism of fibrinolytic resistance induced by stretched fibrin was approached with the help of fluorescent confocal microscopy (Fig. 17.). When tPA-GFP was applied to the surface of non-stretched fibrin, a distinct zone of tPA accumulation was formed at the fluid/fibrin interface within several minutes, which moved a distance of about 75 μm in 50 min as plasmin was formed and it dissolved the fibrin. The interfacial tPA-enriched zone was definitely less sharp and of smaller depth on the surface of stretched fibrin and it did not move at all in the first hour of observation. Thus, the modified ultrastructure of fibrin in clots exposed to mechanical stress impedes tPA binding/penetration into fibrin and consequently delays the lytic process in this experimental setup.

DOI:10.14753/SE.2015.1738

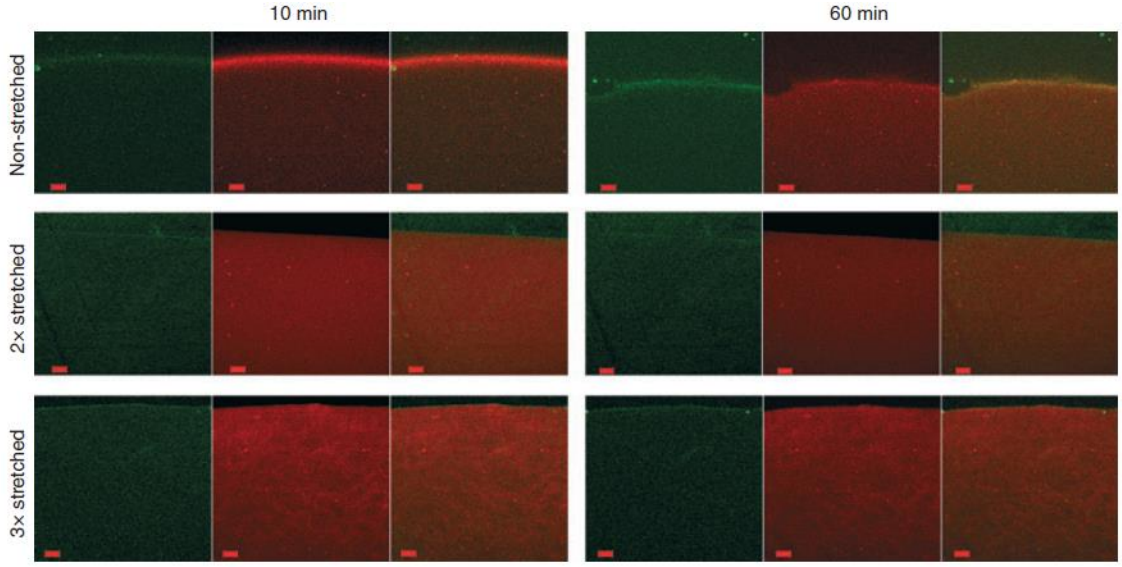

Figure 17. Lysis of fibrin monitored with confocal laser microscopy. *Fibrin clots were prepared from 30 μM fibrinogen containing 50 nM Alexa546-labeled fibrinogen and 200 nM plasminogen, clotted with 30 nM thrombin and stretched as indicated. Thereafter 55 nM tPA-GFP was added to fibrin and the fluid/fibrin interface was monitored with a confocal laser scanning microscope using dual fluorescent tracing: green channel for tPA and red channel for fibrin (the third panel in each image presents the overlay of the green and red channels), scale bar = 50 μm. The time after addition of tPA-GFP is indicated.*

4.2. Effect of neutrophil extracellular trap constituents on clot structure and lysis

4.2.1. Thrombi from patients

Since little is known about the distribution of DNA and histones in arterial thrombi, images of surgically removed thrombi were analysed using immunohistochemistry and SEM. Fig. 18 shows staining for DNA and histones found in 3 representative thrombi recovered from patients. There was variable but widespread staining for DNA, and histones were also present though not so widely dispersed and in some cases were coincident with fibrin aggregates. The thrombi rich in red blood cells (TO) or in fibrin (GI) according to the SEM images showed limited DNA- and histone-positive regions in contrast to the extensively stained areas in the leukocyte-rich (TJ) thrombus. Based on these findings, model thrombi containing activated neutrophils or DNA ± histones were used to study the effect of NET components on clot structure and fibrinolysis.

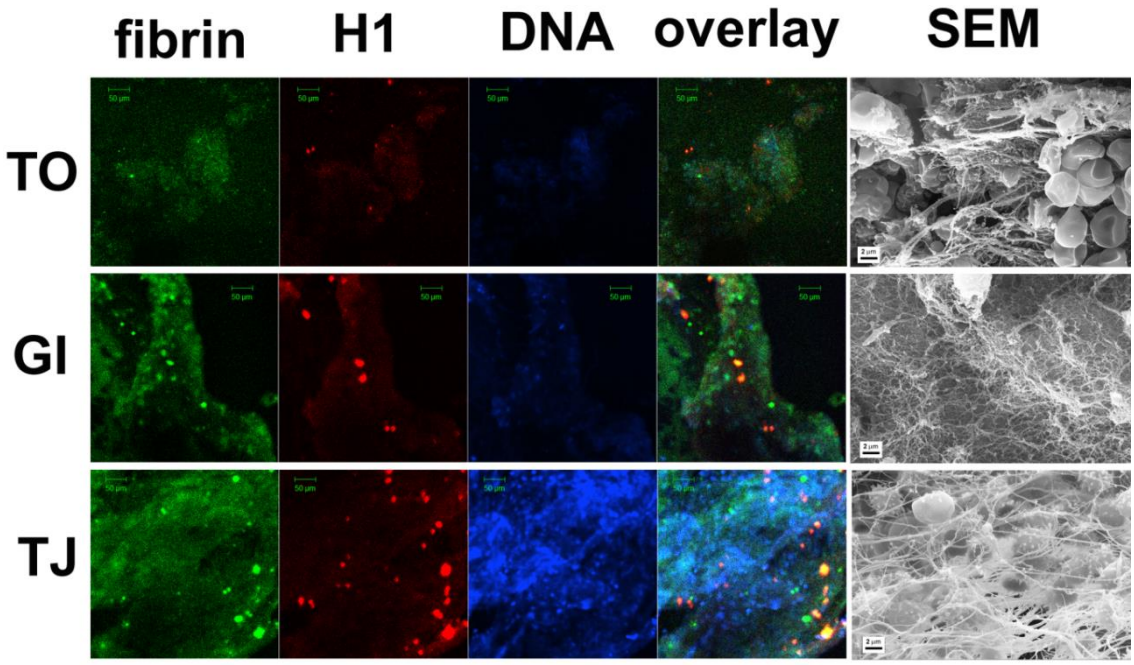

Figure 18. **Fibrin, histone and DNA content of arterial thrombi.** *Following thrombectomy thrombus samples were either frozen for immunostaining or washed, fixed and dehydrated for SEM processing as detailed in 3.3.1.. Sections of frozen samples were double-immunostained for fibrin (green) and histone 1 (H1, red) as well as with a DNA-dye, TOTO-3 (blue). Images were taken at original magnification of ×20 with confocal laser microscope. SEM images were taken from the fixed samples of the*

same thrombi. TO: a thrombus from popliteal artery, GI: a thrombus from infrarenal aorta aneurysm, TJ: a thrombus from femoro-popliteal graft. Scale bars: 50 μm in confocal panels, 2 μm in SEM panels.

4.2.2. Structural studies

In order to gain visual information on clots formed in an environment where NETting granulocytes are present, experimental systems were set up to generate fibrin in the presence of PMA-activated neutrophils, in which clotting was initiated after 4 hours of activation. SEM studies of the samples evidenced that PMA-activated neutrophils formed NETs: a meshwork of fine fibres (Fig. 19A, B) (diameter in the range of 10 nm)

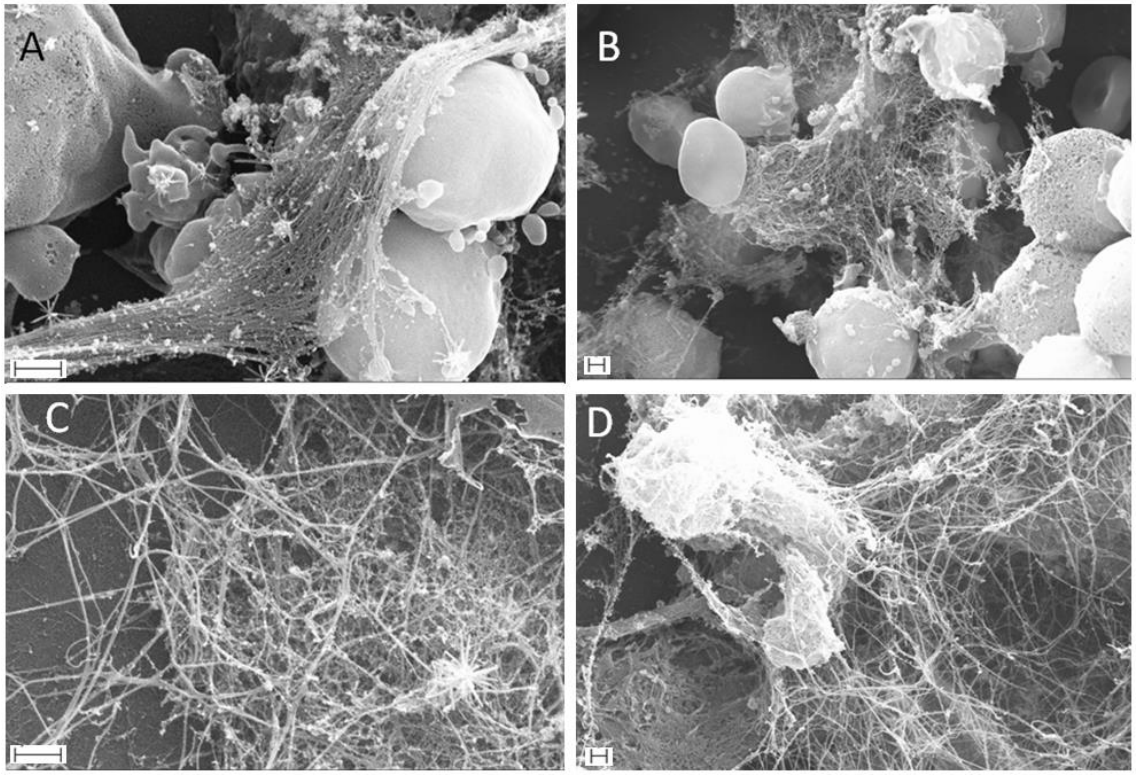

Figure 19. SEM images of NETs produced by PMA-activated neutrophil granulocytes. *A-B: Web-like structures trapping cells and cell-derived debris. C-D: NETs in a fibrin-rich environment in samples coated with a mixture of 10 nM thrombin and 6 μM fibrinogen. The thicker, coarse fibrin (C: in the foreground, D: to the right) merges with the fine structure of NETs (C: in the background, D: left bottom corner). Samples were prepared as described in 3.3.1., bars indicate 1 μm.*

decorated with protein aggregates and cell debris was seen. These fine structures were tangled in the pores surrounded by about 10-fold thicker fibrin fibres (in the range of 100 nm) in fibrin-rich regions of samples.

Since –in agreement with earlier findings (239)– the distinction between NET and fibrin fibres was not overall obvious in these heterogeneous regions (Fig 19C, D), this meshwork was modelled by the addition of NET components (DNA and/or histones) to clotting fibrinogen or blood plasma. Statistical analysis of fibrin fibre diameter was performed and probability density distributions were calculated for clots with no additives or with DNA ± histones as indicated in Table 2. When fibrinogen or

Table 2. Effect of DNA and histones on fibre diameter. *SEM images of fibrin- and plasma clots containing the indicated additives were used for the measurement of fibre diameter as described in (374). The fibre size is reported in nm as median and bottom - top quartile values (in brackets) of the theoretical distributions fitted to the measured diameter values (data from 4 SEM images per slot with 300 measured diameters in each, * stands for p<0.05 according to the Kolmogorov-Smirnov test, in comparison with control without additives). H1: histone H1, Th: thrombin.*

Fibrin clots (16 nM Th)	**No H1**	**50 µg/ml H1**	**100 µg/ml H1**
No DNA	84 (64-110)	119 (91-154)*	108 (88-132)*
50 µg/ml DNA	94 (74-120)*	122 (97-153)*	122 (93-157)*
100 µg/ml DNA	92 (76-111)*	114 (92-140)*	123 (98-149)*

Plasma clots	**16 nM Th**		**60 nM Th**	
	No H1	**250 µg/ml H1**	**No H1**	**250 µg/ml H1**
No DNA	108 (87-136)	119 (98-146)*	118 (93-157)	115 (95-141)*
50 µg/ml DNA	121 (97-150)*	129 (104-159)*	130 (105-159)*	111 (92-134)*

plasma was clotted in the presence of DNA and/or histones, morphometric analysis of SEM images showed significant changes in fibrin fibre diameter. The general trend in clots formed with low concentrations of thrombin was that the presence of histones enhanced the otherwise small effects of DNA on fibre diameter values resulting in the appearance of thicker fibres, while at higher thrombin concentrations DNA and histones alone had opposing effects in a plasma environment: DNA caused thickening of fibres, while histones caused a decrease of diameter values.

Fibre diameter values provide indirect information about the average pore size of the sample (fibre diameter values are in a positive correlation with pore area data (381,382), which is a major determinant of clot permeability. Therefore, plasma- and fibrin clots containing DNA ± histones were subjected to clot permeation studies. Clots were prepared in pipette tips and the Darcy constant (Ks, which provides information about the average pore area) was calculated from flow rate values of HEPES buffer permeating through them. As Table 3 shows, in the purified system, the presence of histones increased the permeability constant approximately 4-fold, even in the presence of additional DNA, as expected from thicker fibre diameter values. In the more complex plasma environment, however, the opposite effect was seen: the presence of histones reduced the Darcy constant by almost 50%. The effect of DNA alone on clot permeability was consistent in both examined systems: a significant negative effect was seen.

Table 3. Effect of DNA and histones on permeability of clots. *Clots were prepared from either 8 μM fibrinogen or citrated plasma supplemented with 20 mM $CaCl_2$ and the indicated additives and clotted with 16 nM thrombin. The Darcy constant (Ks) was calculated as described in 3.3.4.. * stands for $p<0.05$ according to the Kolmogorov-Smirnov test, in comparison with control. SD: standard deviation, H1: histone H1.*

Ks (10^{-9} cm^2) ±SD	Control (no additives)	45 μg/ml DNA	220 μg/ml H1	45 μg/ml DNA +220 μg/ml H1
Fibrin clots	0.62±0.13	0.45±0.08*	2.43±0.81*	2.09±0.38*
Plasma clots	6.43±2.58	3.13±1.13*	3.68±0.91*	5.14±1.68

DOI:10.14753/SE.2015.1738

4.2.3. Inactivation kinetics of thrombin

Since thrombin concentrations alone are also able to influence structural parameters of clots (as described in 1.1.3.), the effects of NET constituents on the inactivation of thrombin by antithrombin were investigated (Fig. 20-21). Histones, DNA, heparin, and

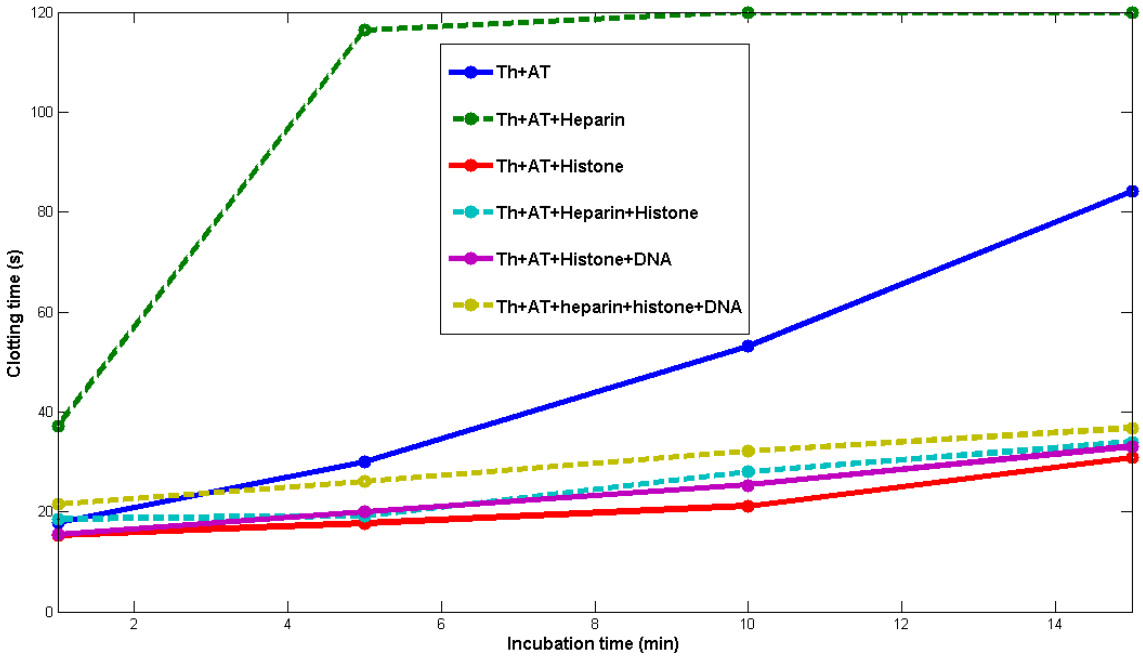

Figure 20. Effects of histones and DNA on clotting times in the course of thrombin inactivation. *Mixtures of 55 nM antithrombin, 170 nM thrombin, 0/25 μg/ml histone ± 25 μg/ml DNA in the presence or absence of 0.025 U/ml heparin were incubated for 1/5/10/15 minutes at room temperature. Residual thrombin activity-induced clotting times were measured after addition of 6 μM fibrinogen. Figure points are calculated from at least 4 independent experiments. Clotting times above 120 sec are shown as 120 sec. Th: thrombin, AT: antithrombin.*

their combinations were added to mixtures of thrombin and antithrombin, and after various incubation times the residual thrombin activity was detected by measuring the clotting times in a coagulometer. Histones were effective in protecting thrombin from inactivation even in the presence of heparin. Titration curves obtained from measurements using a range of histone and DNA concentrations showed that increasing

concentrations of DNA were able to partially attenuate this effect in the presence of physiological antithrombin concentration (2.5 µM) (Fig. 21).

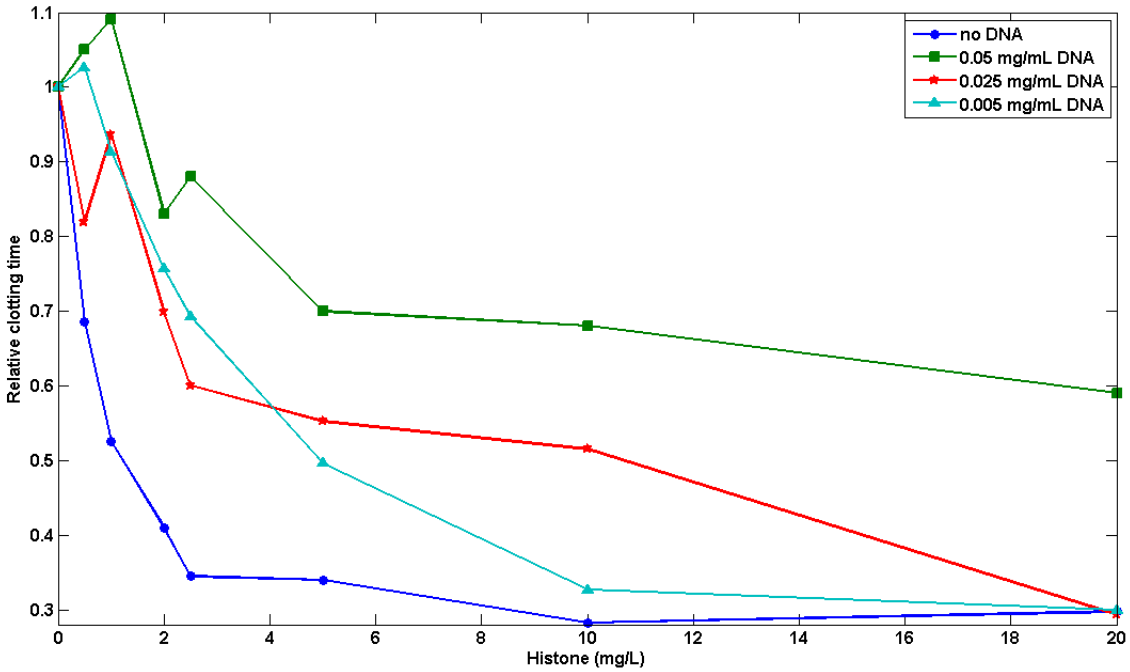

Figure 21. Effect of increasing concentrations of histones and DNA on relative clotting times. *Mixtures of 2.5 µM antithrombin, 180 nM thrombin, 0/0.5/1/2/2.5/10/20 µg/ml histone ± 5/25/50 µg/ml DNA in the presence of 0.15 U/ml heparin were incubated for 15 s at room temperature. Clotting times were measured as described above. Figure points are calculated from 3 experiments with 3 replicas each. Average clotting time values were divided by clotting time values of control experiments (no DNA and histones added), and are expressed as relative values.*

4.2.4. Viscoelastic properties of fibrin

Further evidence that DNA and histones can affect the behaviour of fibrin clots was obtained from rheology studies. Fibrin clots were formed so as to contain pure fibrin or 50/100 µg/ml DNA, and the effect of added histones (300 µg/ml) was also investigated. The most striking differences seen in rheology parameters was in the shear stress necessary to disassemble the fibrin as presented in Fig. 22, where two opposing effects are clearly demonstrated. In the presence of DNA alone the curves can be interpreted as increased sensitivity of fibrin to mechanical shear so that the shear stress needed to

disassemble fibrin (where viscosity approaches zero) is reduced in comparison to the situation without DNA. However, when histones are added to fibrin, and to a greater extent when histones are added to fibrin+DNA, the clots became more stable and resistant to shear forces.

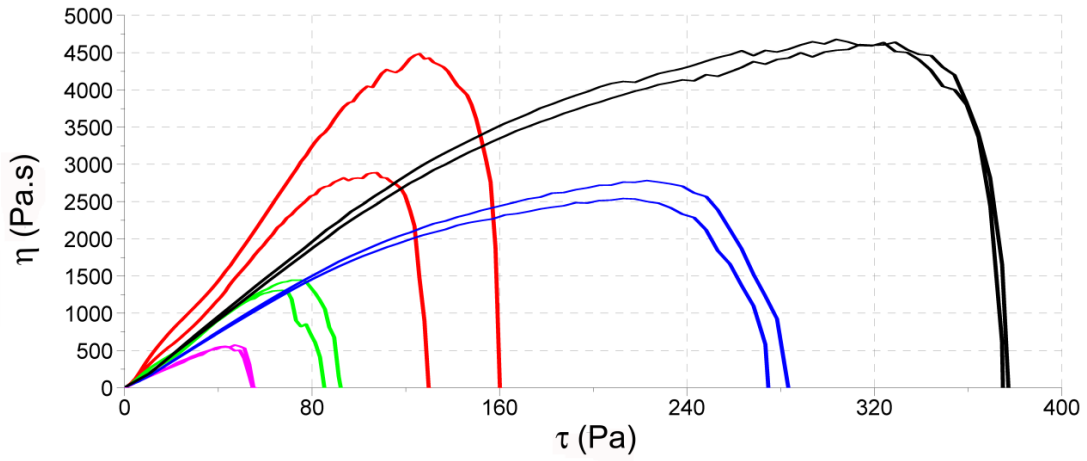

Figure 22. Rheometer studies showing the effect of DNA and histones on the critical shear stress needed to disassemble fibrin. *Curves are shown for pure fibrin (red), fibrin containing increasing DNA concentrations (green: 50 µg/ml; magenta: 100 µg/ml), histone (300 µg/ml, blue) and histone+100 µg/ml DNA (black). The figure shows the two extreme measurements of an experiment performed in 3 replicas. τ: shear stress, η: viscosity.*

4.2.5. Studies on lysis of plasma clots

To study the microscale pattern of lysis in the presence of NET components, DNA ± histones were incorporated in clots supplemented with fluorescent fibrinogen, and the movement of the lysis front with accumulated fluorescent tPA-YFP was measured using images taken with a confocal laser scanning microscope (Fig. 23). DNA and histones alone had a negligible effect on the tPA-front penetration in plasma clots, however, when both components were added simultaneously, the relative run distance of the lysis front after 30 minutes was reduced by approximately 25%. The hindered progress of lysis was accompanied by subtle changes regarding the microscopic pattern of the clot-tPA interface: unlike the rough granular surface seen in clots without any additives, a

fine granular structure showing less aggregate formation was present in the case of clots formed in the presence of NET components (Fig. 23A and 23D).

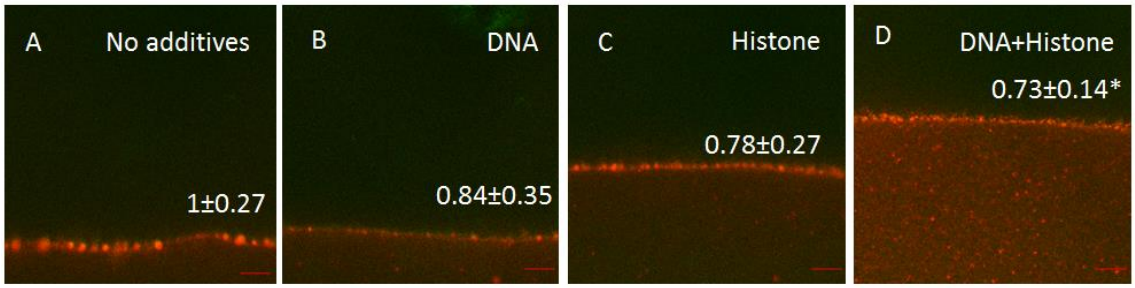

Figure 23. Penetration of tissue plasminogen activator (tPA)-YFP into plasma clots in the course of lysis. *Clots were prepared from human plasma supplemented with Alexa546-labeled fibrinogen, plasminogen, thrombin and the indicated additives (for concentrations, see 3.6.1.). After 30-min clotting tPA-YFP and plasminogen were added to fibrin and the movement of the fluid/fibrin interface was monitored by confocal laser scanning microscopy using double fluorescent tracing (excitation 488 nm/emission 525 nm for tPA-YFP and excitation 543 nm/emission 575 nm for fibrin). Images are shown for the 30th min after the application of tPA-YFP. The tPA-related fluorescence stains in vague green, whereas the fibrin is shown in red. At 0 time the edges of the clots were approximately at the same position near the top of each field of observation. The numbers indicate the relative distance for penetration of tPA-YFP in the clot at 30 min (all values are normalized by the mean value of clots with no additives): mean and standard deviation from at least 6 samples are shown. Asterisk indicates a difference significant at $p<0.05$ according to Kolmogorov-Smirnov test in comparison to control. Scale bar = 50 μm.*

Macroscale lysis was studied using turbidimetry assays measuring A_{340} during lysis of plasma clots containing DNA ± histones prepared in microplate wells (see Fig. 24). Analysis of lysis curves revealed that DNA and histones prolonged the average time elapsed until 90% clot lysis (T10) when added separately or together (Fig. 24), while the time needed for 50% lysis (T50) remained mostly unchanged (except for clots including histones alone).

DOI:10.14753/SE.2015.1738

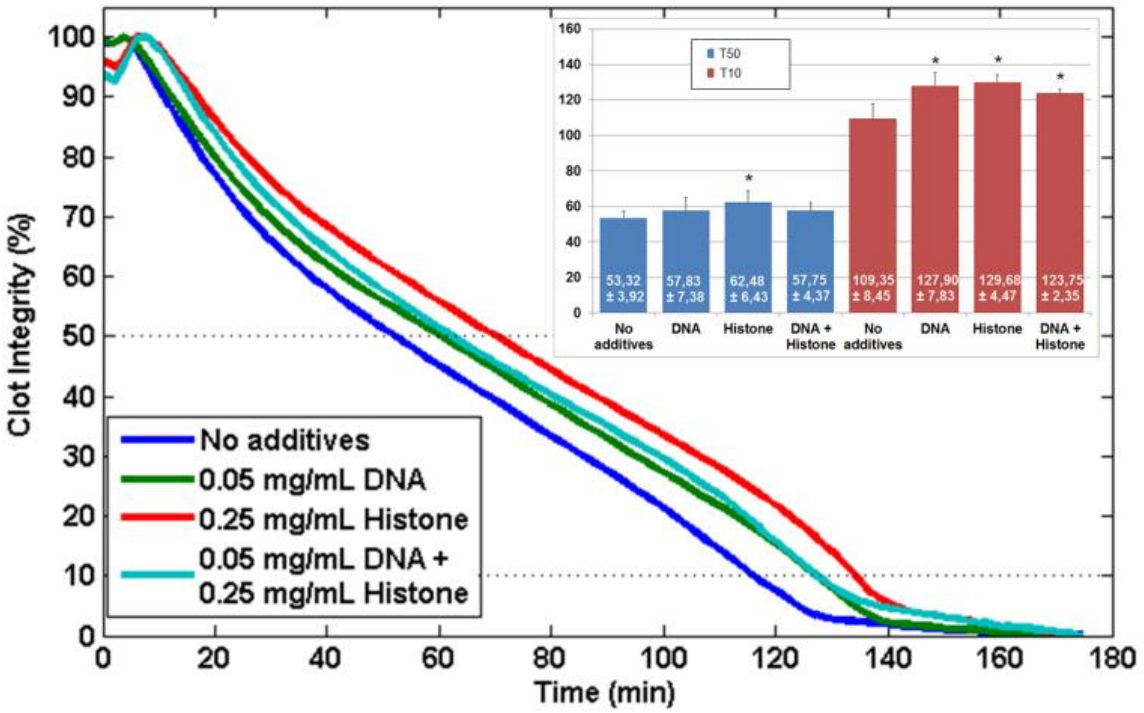

Figure 24. tPA-induced lysis of clots containing NET constituents. *Plasma clots supplemented with plasminogen and the indicated additives were prepared in microplate wells, tPA was added to the surface, and the absorbance was continuously measured at 340 nm. A_{340} turbidity values were normalized for maximal value of absorbance of each individual curve after extraction of the lowest measured A_{340} values from the raw data. Mean curves of 8 measurements from a representative experiment are shown. Dotted lines indicate origin of T50 and T10 parameters shown in the inset (time (min) elapsed until 50% and 90% lysis, respectively). Inset: T50 and T10 values and standard deviation were calculated from mean values of 3 independent experiments with 6-8 parallels each. Asterisk indicates a difference significant at $p<0.05$ according to Kolmogorov-Smirnov test in comparison with control.*

Presence of NETs generated by PMA-activated granulocytes incorporated in the clots reproduced the effect of isolated components (Fig. 25): presence of NETs increased T10 approximately 2-fold (from 50.5 min for PMA-free control to 106 min for clots containing PMA-activated cells), while T50 was unaffected. NETosis inhibitor Cl-Amidine moderated the NET effects exerted on T10 values (Fig. 25, inset).

To assess the influence of NET components on tPA-induced plasminogen activation, clots containing DNA ± histones were prepared in microplate wells, and a

DOI:10.14753/SE.2015.1738

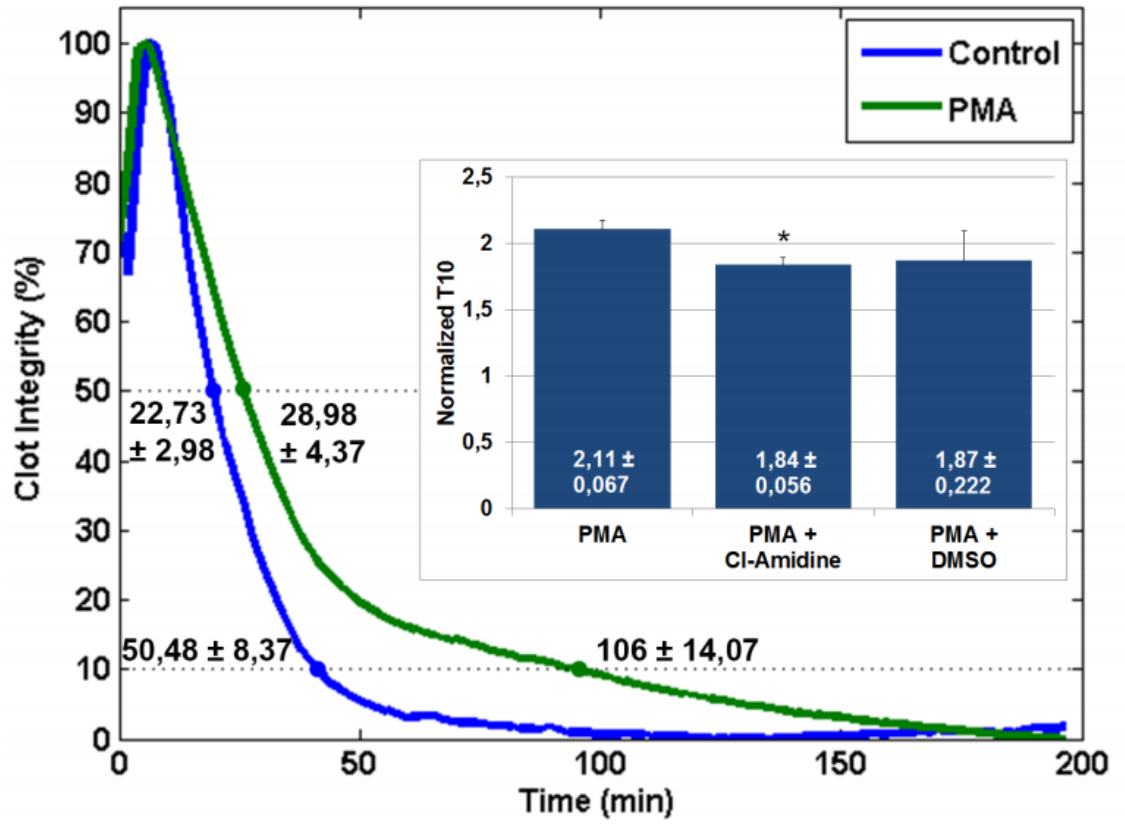

Figure 25. tPA-induced lysis of clots containing activated neutrophils. *Plasma clots containing 5x10^3/µl granulocytes, plasminogen and the indicated additives were prepared, tPA was added to the surface and the absorbance was continuously measured at 340 nm. A_{340} turbidity values were normalized as described in 3.6.3. Dotted lines indicate the origin of T50 and T10 values (time elapsed until 50% and 90% lysis, respectively). Mean values of 8 measurements from a representative experiment are shown. Numbers next to the dotted lines show the respective lysis time in min±SD, averaged from mean values of three independent experiments containing 6-8 replicas each, p<0.05 according to the Kolmogorov-Smirnov test for T10. Inset: Effect of Cl-Amidine (middle bar) and DMSO (vehiculum for Cl-Amidine) on T10 in clots containing PMA-activated neutrophils. T10 values were normalized for control to give relative units. Bars show mean values and black lines represent SD of means of 3 experiments with 6-8 parallels each.*

chromogenic plasmin substrate (Spectrozyme-PL) was added to the clot surface together with tPA. Apparent velocity of plasmin formation (V_{app}) on the clot surface was

DOI:10.14753/SE.2015.1738

calculated from the quantity of the generated *p*-nitroaniline detected at A_{405} during the course of activation (Fig. 26). While DNA alone reduced slightly the V_{app} values for plasmin formation by 20%, histones ± DNA increased the velocity of plasmin generation (Fig. 26, inset).

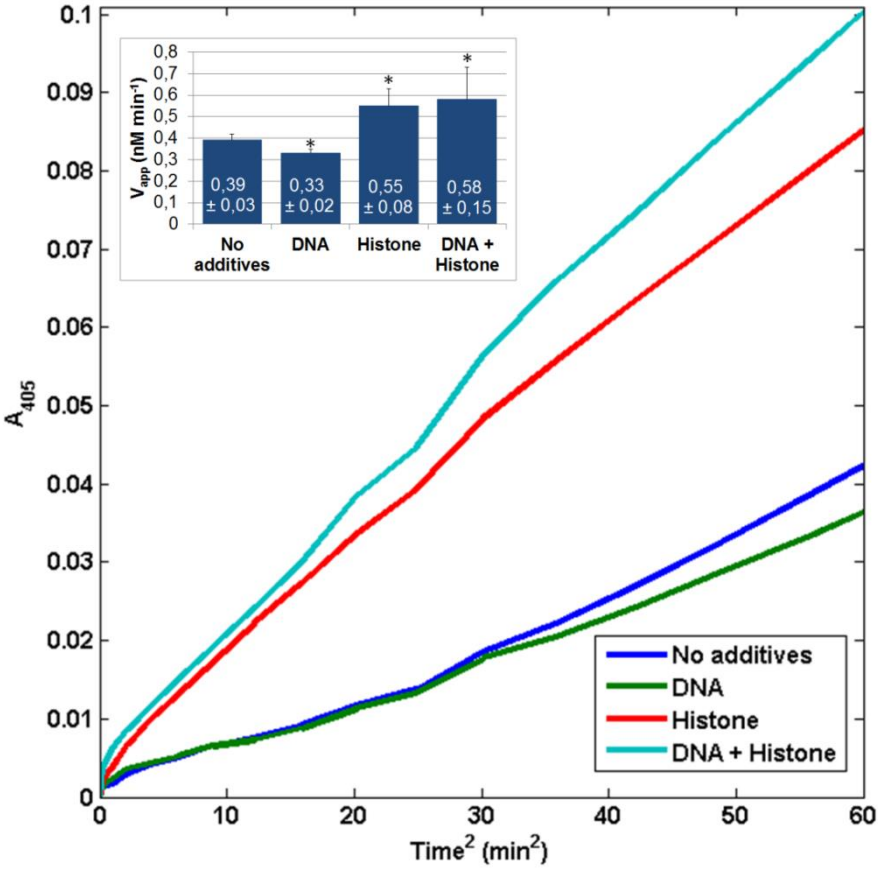

Figure 26. tPA-induced plasminogen activation on clot surface. *Plasma clots containing plasminogen and the indicated additives were prepared and thereafter tissue plasminogen activator (tPA) and the plasmin substrate Spectrozyme-PL were added. The absorbance of the liberated p-nitroaniline was continuously measured at 405 nm (A_{405}), and plotted against time squared. Baseline A_{405} was extracted from each of the data sets. The figure shows mean values of eight measurements from a representative experiment. Inset: apparent maximal activation rates (V_{app}) were calculated using the equation $\Delta A_{405}=0.5\varepsilon k_1 V_{app} t^2$ (see 3.6.2.). Mean values and standard deviation presented here are calculated from mean values of 3 independent experiments with 6-8 parallels each. Asterisk indicates a difference significant at $p<0.05$ according to Kolmogorov-Smirnov test in comparison with control.*

DOI:10.14753/SE.2015.1738

To study plasmin-induced lysis of plasma clots, clots were prepared in channels of IBIDI-microslides, and the lysis front movement was followed by time-lapse photoscanning of the transparent fluid/opaque clot boundary. Incorporation of DNA in the clots reduced front movement velocity by 40%, while histones ± DNA did not influence run distance values (Fig. 27).

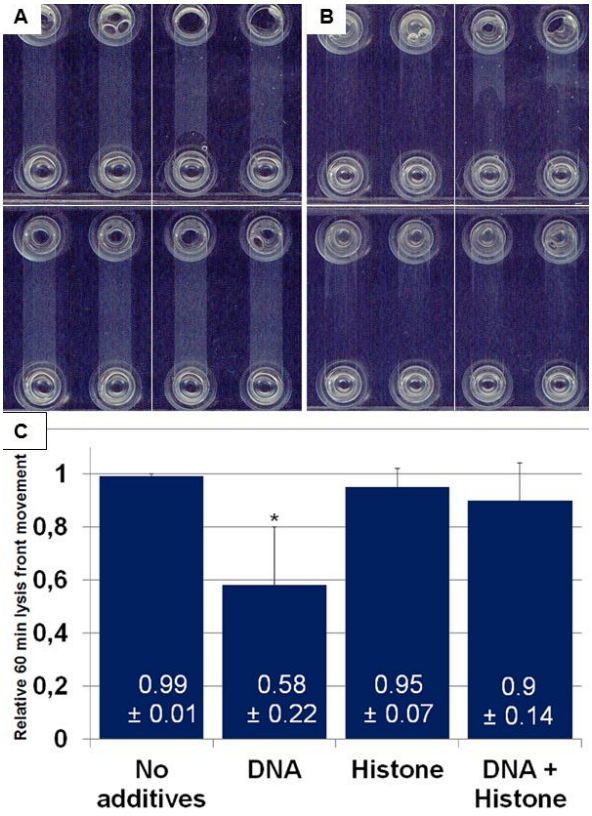

Figure 27. Plasmin-induced lysis of clots. *Mixtures of plasma supplemented with 12.5 mM $CaCl_2$,16 nM thrombin, and the indicated additives were injected in 0.4 mm high channels of microslides (IBIDI™) through the upper orifice, and 5 µM plasmin was applied through the lower orifice after 60 mins of clotting. A: initial stage. B: lysis fronts after 60 mins. Additives: Upper left box: none, upper right box: DNA, lower left box: histone, lower right box: histone+DNA. C: Lysis front movement was registered every 15 minutes by photoscanning the samples and measured mm values of 60 min lysis front (opaque clot /transparent fluid interface) movement were normalized for channel length (13 mm) to give relative units. The data represent means and standard deviation of at least 7 measured values from 3 independent experiments. * indicates a difference significant at $p<0.05$ according to Kolmogorov-Smirnov test in comparison with control.*

The effect of DNA on the course of plasmin inactivation was investigated using defibrinogenated plasma and chromogenic plasmin substrate Spectrozyme-PL, measuring for 60 seconds the A_{405} of *p*-nitroaniline liberated by the enzyme after 10 seconds of incubation. DNA enhanced the defibrinogenated plasma-induced inactivation of plasmin: after 10 s a 0.72±0.15 fraction of initial plasmin activity was retained in the control and DNA decreased this value to 0.52±0.16 (averages and SD values calculated from 4 independent measurements; ΔA_{405} values were normalized as described in 3.7.1.; $p<0.05$ according to the Kolmogorov-Smirnov test).

4.2.6. Binding studies on fibrin degradation products and NET constituents

Given the apparent widespread distribution of DNA in thrombi noted in Fig. 18 and the effects of DNA and/or histones observed in fibrinolytic assays, further studies were performed to investigate the interactions between DNA and histones with fibrin degradation products (FDPs) using ITC (Table 4, Fig. 28). These studies, illustrated in Fig. 28, clearly showed that FDP bind to both DNA (Kd=136.1 nM) and histones (Kd=190.7 nM) with a higher affinity than fibrinogen and plasminogen (Table 4).

Table 4. Binding data from isothermal titration calorimetry. *The intermolecular interactions of the indicated ligands were measured as described in 3.5. and illustrated in Fig. 28. Abbreviations: FDP, fibrin degradation products; Fg, fibrinogen; Plg, plasminogen; N, size of binding size (in number of nucleotides, when DNA is the binding partner or number of molecules, when histone is used); Kd, dissociation equilibrium constant; ΔH, enthalpy change. Mean and standard deviation (SD) of at least 4 measurements are shown.*

	FDP/DNA		FDP/histone		Fg/DNA		Plg/DNA	
	mean	SD	mean	SD	mean	SD	mean	SD
N	1315.8	136.3	1.6	0.5	2145.9	1903.0	682.0	110.9
K_d (nM)	136.1	111.7	190.7	91.7	534.3	52.8	524.1	72.7
ΔH (kcal/mole)	-239.5	28.8	-12.8	2.9	-1116.3	1874.4	-153.0	135.6

DOI:10.14753/SE.2015.1738

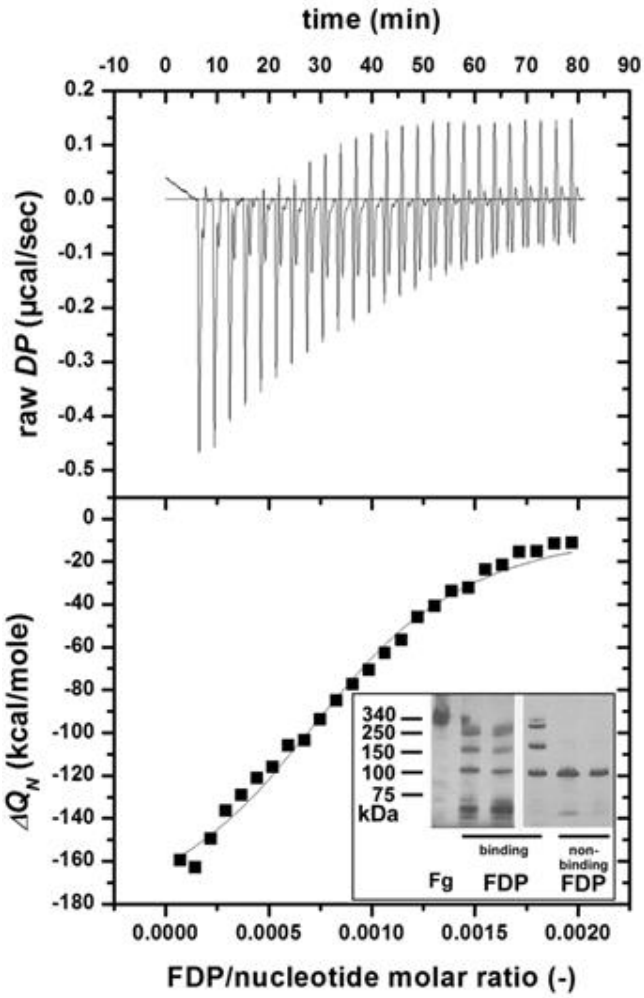

Figure 28. Binding of FDP and DNA studied using ITC. *The cell (1.43 ml) of the titration calorimeter is filled with 0.5 mg/ml DNA, 25 successive aliquots (10 µl each) of 6 µM FDP are injected into the cell at 25 °C and the heat increments of each addition (raw differential power, DP) are measured (top panel). The baseline-corrected, peak-integrated and concentration-normalized enthalpy changes (ΔQN, symbols, bottom panel) are evaluated according to the single-site algorithm and the best-fitting binding isotherm is shown. The inset shows a non-reducing SDS PAGE gel of typical FDP preparations consisting of high molecular weight fibrin fragments (binding) and low molecular weight fibrin fragments (non-binding).*

The size of the binding site in the DNA correlated with the size of the interacting ligand; fibrinogen required the largest one (2146 nucleotides) and plasminogen the smallest one (682 nucleotides). Further studies (not shown) indicated that only larger FDP (> 150 kDa) demonstrated this high affinity binding and smaller FDP did not.

DOI:10.14753/SE.2015.1738

5. DISCUSSION

5.1. The effect of mechanical stress on structure and lytic susceptibility of fibrin

Our ex vivo exploration of the ultrastructure of fibrin at different locations of surgically removed thrombi (Fig. 14) provided some evidence to support the prediction of longitudinal alignment of fibres exposed to shear stress as described in 1.1.4.. In 40% of the examined thrombi the surface fibres were aligned along one preferred axis and closer together in the perpendicular direction, whereas the fibrin meshwork in the interior parts showed random arrangement in all three dimensions of space. Although in these thrombi the individual surface fibres became thinner compared with the core of the thrombi, they formed rough bundles because of the smaller inter-fibre pore size (Fig. 14B). Our SEM data of oriented fibres at the thrombus/blood interface extended the former report on longitudinal alignment of fibrin bundles of about 20 μm diameter observed in coronary thrombi and aortic aneurysms at the lower resolution of polarized light microscopy (383). The surface localization of the oriented fibres reported here resolved the issue of the organizational factor for this alignment (shear stress vs. structural elements of the blood vessel wall) in favour of the flow-related forces. The fact that such a striking difference between the exterior and interior fibrin architecture was not observed in the majority of the sampled thrombi can be attributed to the variability in the magnitude of the shear stress, to which they were exposed in the blood vessels. Elaborate mathematical modelling (79) shows that the mechanical forces differ significantly even at different points of a single stenotic site, whereas the thrombi evaluated in the present study were derived from different anatomical locations and from patients with rather heterogeneous clinical background. Thus, the rheological conditions and consequently the local shear stress presumably differed significantly at the time of thrombus formation.

These ultrastructural findings raised the question about the impact of the altered fibrin architecture on the clot susceptibility to lysis. It has been well documented that thinner individual fibres are lysed more easily than thicker ones (91,354,384). However, as mentioned in 1.2.1., the macroscopic lytic rate does not automatically follow the trend of the individual fibres; so that in parallel with the faster individual fibre lysis evidence is provided for slower dissolution of clots composed of thin fibres in a dense

conformation compared with clots composed of thicker fibres in a more open arrangement (93). Such discrepancies can be accounted for by differences in tPA binding (208) and permeation (385) in clots of various compactness. Thus, the lytic susceptibility of the fibrin structures in thrombi reported in the present study needed to be addressed with an adequate in vitro model. The previously described structural properties of mechanically stretched fibrin clots (80) appeared to resemble the orientation and lateral packing of the surface fibres observed in some thrombi (Fig 14). The appropriateness of stretched fibrin as a model of these observed structures was verified by the analogous changes in fibre diameter and gel pore area (Fig 15). The application of stretched fibrin as a model system for the evaluation of the modifications in lytic susceptibility caused by mechanical stress has the advantage that these structures have been quantitatively characterized in terms of supra- and submolecular morphology and extensibility (80). Thus, the reported geometric parameters could be used directly in our calculations of area-normalized rates of plasmin generation and fibrin dissolution. Although stretching of pre-formed fibrin results in similar fibrin architecture to the morphology observed on the surface of thrombi, the *in vivo* mechanism might be different. There is evidence that similar fibrin fibre alignment can be observed if fibrin polymerizes under flow (386,387). Independently of the formation mechanism, however, the identical final structure supports the adequateness of the applied model for assessment of the lytic susceptibility of fibrin exposed to shear forces either at the stage of clotting or later.

Our data evidenced that the stretched conformation of the clots is resistant to both tPA- and plasmin-induced lysis (Fig. 16). In spite of the reported changes in the conformation of individual fibrin monomers (80) no essential differences in the molecular-weight pattern of FDP from stretched and non-stretched fibrins could be observed (Fig. 16A-right, inset). Importantly, tPA-induced fibrinolysis was apparently more sensitive to the effects of mechanical stress than the direct digestion of fibrin by plasmin (Fig. 16A-right vs. B-right) in line with additivity of altered plasminogen activation on the surface of stretched fibrin (Fig. 16-left) and modified plasmin susceptibility of the clot. Monitoring of the remnant fibrin clot on a microscopic scale showed that the movement of the tPA-enriched lytic front was completely blocked in stretched fibrin in the first hour of lysis (Fig. 17). In the experiments with a fluorescent

chimera variant of tPA both the fluorescence intensity and the depth of the interfacial layer of tPA accumulation were smaller in the stretched fibrins suggesting weaker binding and impeded permeation as the mechanism of impaired fibrinolysis with this activator. Thus, taking a coherent view of ultrastructural and activity assays we conclude that mechanical stress, which results in higher density of re-oriented fibrin fibres confers lytic resistance related to both impaired plasminogen activation on the surface of the denser fibrin network and reduced rates of fibrin lysis by plasmin. The previously described unfolding of individual monomers in stretched fibrin (80) might possibly contribute to the hindered lysis through exposure of hydrophobic regions and expulsion of water with consequent blocking of tPA-binding and plasmin-cleavage sites in fibrin.

Based on the similarities in ultrastructure, we have correlated the lytic properties of stretched fibrin to the physical changes induced by shear stress on the surface of thrombi, but our findings may have some broader implications arising from alternative sources of mechanical stress. As mentioned before (1.1.3 and 1.2.3.), platelets cause clot retraction and in the vicinity of platelets the fibrin network is oriented, denser and more resistant to lysis (58). When the platelet content of 10 ml of blood is compacted in 400 μl of arterial thrombi (207), clots experience a large amount of mechanical strain. It has long been known that retracted clots are very resistant to fibrinolysis (208,388,389), and this resistance has been correlated with impaired tPA binding and expulsion of plasminogen. Our results gained in stretched fibrin extend the previously known factors contributing to the lytic resistance of peri-platelet zones of thrombi exposed to contractile forces of cellular origin. Together, our present findings point to the need to appreciate the role of biomechanical and rheological factors in the variable therapeutic response of patients treated with thrombolysis.

5.2. The effects of DNA, histones and neutrophil extracellular traps on structure, mechanical stability, and lytic properties of clots

Besides mechanical stress, structure and lytic susceptibility of clots are influenced by a variety of enzymatic (e.g. thrombin concentration), soluble, and cellular (e.g. red blood cells) factors (see 1.1.3.). NETs, representing a recently recognized source of pro-thrombotic components, add new elements to the already existing complexity. Based on

the demonstration of neutrophil elastase-specific fibrin degradation products, our group has previously provided *ex vivo* evidence for the proteolytic contribution of neutrophils to fibrinolysis in arterial thrombi (390). A different aspect of leukocyte functionality in thrombolysis is suggested by the presence of DNA and histones in clots from arteries revealed by the present study (Fig. 14). These observations on arterial clots add to previous work on the contribution of DNA and histones to the pathogenesis of deep vein thrombosis in animal models, for example baboons (295) and mice (303), as well as other conditions such as sepsis (296) and inflammatory and autoimmune diseases (391). The influence of DNA and histones on thrombi warranted further investigation, and our results presented above suggest that neutrophil extracellular traps and their components (DNA, histones, DNA+histones) can have different, sometimes opposing, effects, which are now considered below in turn.

5.2.1. DNA

Fibre diameter and clot pore area are thought to be positively correlated (381,382). Our results show however, that fibrin and plasma clots formed in the presence of DNA alone are less permeable despite being composed of thicker fibres (Table 2 and 3). The consistent negative effect of DNA on clot permeability may be attributed to its pore-filling property suggested by confocal laser-microscopic images of thrombi stained for DNA (not shown here).

The SEM data characterize the protein content of individual fibrin fibres, but this technique cannot resolve nanometre-scale structure of fibrin in its natural hydrated state. Small-angle X-ray and neutron scattering proved to be a powerful tool in the characterization of the longitudinal arrangement of the monomers in the protofibrils and the lateral alignment of protofibrils in fibres (392). The general decay trend of the scattering curves (Fig. 29) reflects the fractal structure of the fibrin clot and its effect can be modelled as a background signal with empirical power-law functions in the form of $C0+C4*q^{-\alpha}$ for clots containing fibrin, DNA and heparin or with an additional function with a fixed exponent of -1 for samples with histones. The peaks arising above this background reflect longitudinal and cross-sectional alignment of fibrin monomers. A small, but sharp peak in pure fibrin at *q*-value of ≈ 0.285 nm^{-1} (Fig. 29) corresponds to the longitudinal periodicity of $d = 2\pi/q' = 22$ nm that is in agreement with earlier SAXS

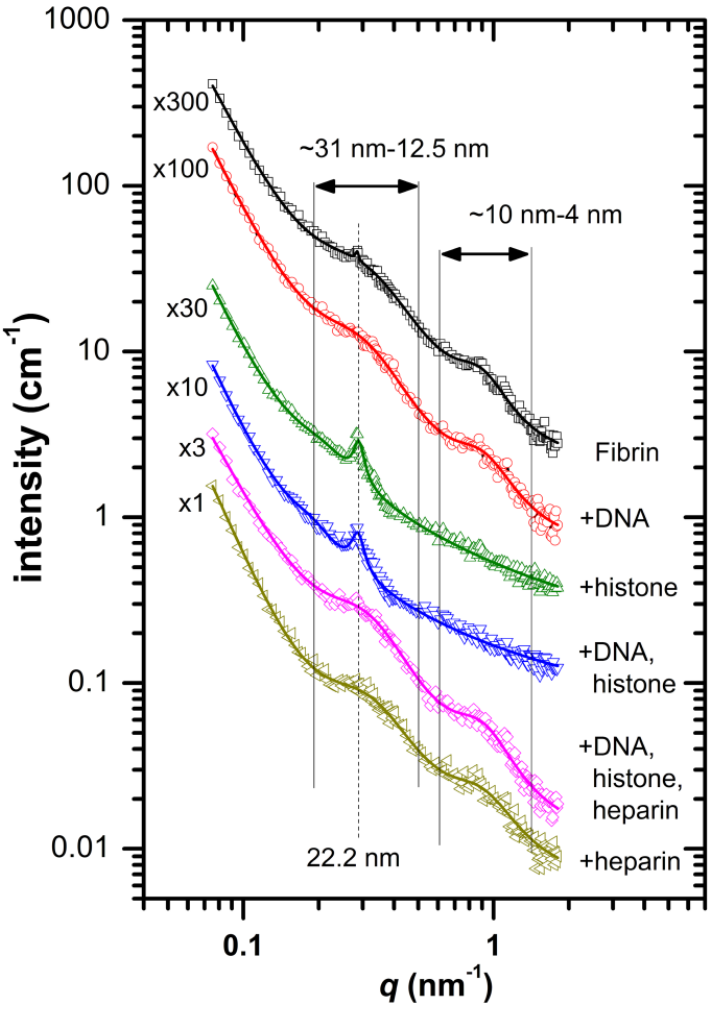

Figure 29. Small angle x-ray scattering in fibrin clots. *Clots contain 100 μg/ml DNA, 300 μg/ml histone, 10 IU/ml heparin, or their combinations. Curves are shifted vertically by the factors indicated at their origin for better visualization. Symbols represent the measured intensity values, while solid lines show the fitted empirical functions. The dashed vertical line indicates the longitudinal periodicity of fibrin of about 22 nm (representing the approximate half-length of a fibrin monomer), while the solid vertical lines show the boundaries of the broad peaks that characterize the lateral structure of the fibrin fibres. q (momentum transfer)= 4π/λ sinθ , where θ is half the scattering angle and λ is the wavelength of the incident X-ray beam.*

studies (392) and a little bit lower than the values reported for dried samples in transmission electron microscopic investigations (393). This peak cannot be resolved in

fibrin containing DNA (or heparin) indicating that these additives disrupt the regular longitudinal alignment of the monomeric building blocks.

Rheology data suggest that fibrin clots containing DNA alone were less stable in response to mechanical shear stress suggesting "weak, floppy" clots (Fig. 22), which is in line with the disrupted longitudinal alignment of the monomers revealed by SAXS studies (Fig. 29).

As expected from the higher fibre diameter values, tPA-mediated plasminogen activation was retarded on the surface of plasma clots containing DNA alone, and tPA induced lysis was delayed, as reflected in higher T10 values (Fig. 24 and 26). When plasma clot lysis was initiated with plasmin, DNA alone was effective in hindering clot lysis (Fig. 27), which is in line with the enhancement of defibrinogenated plasma-induced inactivation of plasmin. The examined interactions between DNA and large FDPs (molecular weight > 150 kDa) might be among the factors responsible for retarding clot lysis, suggesting that further digestion of large FDPs to lower molecular weight forms is required to achieve complete clot dissolution.

5.2.2. Histones

When fibrinogen or re-calcified plasma was clotted with 16 nM thrombin, presence of histones alone increased median diameter values of fibrin fibres, in line with results from SAXS studies. In pure fibrin two broad scattering peaks can be resolved spanning over the *q*-ranges of ≈0.2 to 0.5 nm^{-1} and ≈0.6 to 1.5 nm^{-1}. The first peak can be attributed to periodicity of ≈12.5 to 31 nm in cluster units of the fibres, while the second one corresponds to periodicity of ≈4 to 10 nm characteristic for the mean protofibril-to-protofibril distances based on the structural models of Yang et al. (394) and Weisel (393). Both of these broad peaks are profoundly affected by the presence of histones (Fig. 29) suggesting that this additive interferes with the lateral organization of protofibrils resulting in lower protofibril density. Earlier studies (28) have shown that lower protofibril density can correspond to thicker fibre diameter, which is in qualitative agreement with our SEM results (Table 2).

In plasma clots clotted with 60 nM thrombin, however, the opposite effect was seen: histones decreased fibre thickness. This finding indicates that in a more complex plasma environment, histones might have effects that oppose their interference with

lateral organization of fibrin strands. Impairment of antithrombin-induced inactivation of thrombin may be such an effect (Fig. 20). Given the bell-shaped dependence of fibre diameter on thrombin concentrations (see 1.1.3.), it is not surprising that histone-mediated protection of thrombin results in opposing trends regarding diameter values in the presence of lower (16 nM) and higher (60 nM) thrombin concentrations. As expected from increased fibre thickness, permeability constant values referring to average pore size were higher in fibrin clots containing histones, however, in plasma clots, the opposite effect was seen, possibly due to interactions of histones with other plasma components outside the scope of this investigation.

The trend in alterations of mechanical properties of clots containing histones alone is the opposite of that seen with DNA: fibrin clots showed increased mechanical stability in the presence of histones, as reflected in higher shear stress values needed for clot disassembly (Fig. 22).

Lytic susceptibility of plasma clots containing histones alone for plasmin-induced lysis showed no significant differences compared to clots with no additives (Fig. 27). In the case of the in vivo more relevant tPA-induced lysis, however, histones, like DNA, also proved to be inhibitory (Fig. 24), despite the increased velocity of plasmin activation on clot surface (Fig. 26). Similarly to DNA, histones were also able to bind large FDPs, possibly contributing to delayed lysis times.

5.2.3. DNA and histones, NETs

Structural changes in fibrin clots seen with histones were retained with the addition of DNA as shown in SEM (Table 2), permeability (Table 3), and SAXS (Fig. 29) studies in fibrin clots. In plasma clots, DNA enhanced the trends seen with histones alone contributing to formation of thicker (with 16 nM thrombin) and thinner (with 60 nM thrombin) fibres.

According to SAXS studies, the structure modifying effects of histones are preserved in the presence of DNA, but these effects are completely reversed in the quaternary system of fibrin/DNA/histone/heparin (Fig. 29).

Clot stability was enhanced in rheology studies (Fig. 22) by the addition of DNA to histone, in line with increased fibre diameter having been previously identified as a significant factor in increasing clot stability and network stiffness (395). This finding is

in line with the fact that clot rigidity has been proposed as a predisposing factor for increased myocardial infarction (396).

While histones were able to nullify certain effects of DNA (e.g. permeability of plasma clots and plasmin-dependent lysis), the combination of the two substances retained decelerating effects on tPA-induced lysis on both micro- and macroscopic scales. DNA ± histones disturbed the pattern and retarded the movement of the tPA-induced lysis front examined with confocal microscopy (Fig. 23) and the combination of DNA and histones resulted in a significant, 25% decrease in the average run distance of tPA fronts (despite the enhanced velocity of plasmin formation on the clot surface detected by spectrophotometry (Fig. 26)). These microscale data are in line with results of the turbidimetry assay, in which the presence of NET constituents (alone and together) prolonged the time elapsed until 90% lysis (T10) by approximately 15% while initial fibrinolysis remained mostly unaffected (as reflected in values of the time elapsed until 50% lysis (T50), Fig. 24).

The effects of NETs produced by PMA-activated granulocytes incorporated in plasma clots supported the findings of the simplified models. Co-localization of NETs and fibrin as seen in SEM images (Fig. 19) resulted in a two-fold increase of T10 in comparison with clots containing non-activated cells, (Fig. 25), while the NETosis inhibitor Cl-Amidine partially reversed this effect supporting a role for PAD4-dependent formation of NETs in the prolongation of lysis times. The lack of complete restoration of the baseline fibrinolytic profile in the presence of the inhibitor could be explained by the contribution of other plasma components, which –in concert with PMA– could overcome the effect of Cl-Amidine. Thrombin may reinforce the activation of neutrophils through PAR-4 receptors (397) (leading to an increased Ca^{2+}-signal, which is known to activate PAD4 (274), although currently there is no direct evidence for the participation of PARs in NETosis.

5.2.4. In vivo implications

Although the diverse methods in the current work were utilized in systems of increasing complexity (from fibrin clots with purified components to plasma clots with activated neutrophils), caution is required when extrapolating these findings to the *in vivo* situation. Nevertheless, these data add novel facts to previous work implicating DNA

and histones in disturbances of coagulation and promotion of deep vein thrombosis (295,309,347). We have extended these studies to include arterial clots and now focus on fibrinolysis.

The heterogeneous distribution of DNA and histones observed in arterial clots shown in Fig. 18 suggests that it will be difficult to predict how they affect clot stability and lysis *in vivo*. The earlier studies involved histones within a similar concentration range used in the present study (around 40 μg/ml for example (309,347)), and concentrations up to 70 μg/ml have been suggested by measurements carried out in baboon models of sepsis (296). It is difficult to estimate the amounts of DNA that might be found in venous or arterial blood clots. Although circulating cell-free DNA concentrations are generally low (50-100 ng/ml), under certain pathological conditions (e.g. malignancy) this can rise up to a 0.5-5 μg/ml range (293), but very high local concentrations around dead cells are also likely as observed previously (295). In addition to the fact that NETs are today being viewed as a supplementary scaffold of thrombi, DNA and histones may accumulate in the vicinity of atherosclerotic plaques, which contain dead cells. Thrombosis is believed to occur here after necrotic core expansion causes weakening of the atheroma cap to generate thrombogenic debris (398). Inflammatory signals may also recruit additional leukocytes to blood clots, providing an increased pool of DNA and histones (294). Therefore, the ranges applied in this study (5-100 μg/ml for DNA and 0.5-300 μg/ml for histones) give a fair estimation of possible DNA and histone concentrations of clots.

Here we propose that DNA release may result in weakened clots more prone to embolize, whereas histones might strengthen clot structure. DNA and histones decelerate the breakdown of plasma clots containing DNA ± histones, which appear to stabilize the network by binding large FDPs. Prolonged clot lysis in the presence of NETs from PMA-activated neutrophils mirrored the findings in systems using purified components. Taken together, these observations raise the prospect that, besides agents activating the fibrinolytic system, utilization of supplementary substances capable of disrupting the DNA-histone matrix (e.g. DNAses and aPC) may lead to improved therapeutic outcomes of thrombolysis.

DOI:10.14753/SE.2015.1738

6. CONCLUSIONS

The studies reported in this work demonstrate that mechanical stress as well as the presence of NET components renders clots more resistant to fibrinolysis. Our most important *conclusions* are the following:

(1) Stretching of fibrin clots results in structural changes: a meshwork composed of thinner fibres and diminished pores is formed, in which the distribution of these parameters becomes more homogeneous, compared to that of non-stretched clots.
(2) Structural changes are accompanied by decreased lytic susceptibility of stretched fibrin clots: tPA- as well as plasmin-mediated lysis is hindered on the stretched substrate.

(3) Major NET components (DNA and histones) are present in arterial thrombi.
(4) Presence of DNA and histones in fibrin- and plasma clots formed with low concentrations of thrombin results in the formation of thicker fibres and alterations in clot porosity: DNA alone decreases permeability, while histones have opposing effects in the purified and plasma systems.
(5) Histones slow down the antithrombin-mediated inactivation of thrombin even in the presence of heparin, while the addition of DNA partially reverses this effect.
(6) While DNA alone contributes to decreased mechanical stability of fibrin clots, histones ± DNA increase clot resistance against shear forces.
(7) Plasma clots containing either NETs from activated neutrophils or purified NET components (DNA ± histones) are resistant to tPA-mediated lysis, while DNA alone hinders plasmin-induced lysis.
(8) Retardation of fibrinolysis by NET constituents is partially elucidated by their affinity towards fibrin degradation products. Binding of DNA and histone to these clot fragments may contribute to hindered disassembly of thrombi.

Implications:

(1) Our findings indicate that intravascular thrombi exposed to increased circulatory shear forces (e.g. in bifurcations) might be more difficult to dissolve. Our results also

add to the earlier observations that aging thrombi going through the process of retraction are less susceptible to fibrinolysis.

(2) Disruption of the DNA-histone matrix of thrombi (e.g. by DNAses or histone-degrading proteases like aPC) may enhance the effectiveness of current thrombolytic therapies aiming the dissolution of the fibrin meshwork.

DOI:10.14753/SE.2015.1738

7.1. SUMMARY

Intravascular thrombi, the underlying causes in the majority of cerebro- and cardiovascular diseases, are complex structures composed of fibrin meshwork and a variety of cells and other soluble blood-borne elements. They are exposed to shear stress exerted by circulating blood. Thrombolysis aiming at degradation of the fibrin network is a therapeutic modality that is able to reduce damage caused by blockage of blood flow. From the numerous elements influencing the effectiveness of fibrinolysis in thrombolytic therapy, the work here concentrates on two main aspects: *mechanical stress* and the role of neutrophil extracellular traps (*NET)* constituents.

Thrombi formed in stenotic vessels are exposed to both external (blood flow) and internal (contraction of platelets) sources of mechanical stress, and SEM images obtained from thrombi of patients (presented in this work) provided additional indirect evidence that these shear forces can be strong enough to modify fibrin alignment in vivo. Our findings expanded the previous observation that mechanical stress induces structural changes in the fibrin network: fibre diameter and pore area values were decreased. These structural changes were accompanied by increased lytic resistance of the stretched fibrin clots, which could be attributed to the observed impaired tPA accumulation on fibrin surface and decreased lytic susceptibility of fibrin to plasmin.

A role for NETs is emerging as fundamental components of venous and arterial thrombi. In the present work we addressed the effects of NET components on the structural and lytic properties of clots in systems of increasing complexity: from fibrin clots supplemented with purified components (DNA ± histones) to plasma clots containing activated neutrophil-derived NETs. Our results showed that incorporation of NET components increased fibre thickness and decreased permeability in plasma clots formed with low concentrations of thrombin. Investigation of the lytic properties of plasma clots containing NET constituents revealed that these model-thrombi bear increased resistance against tPA-mediated lysis and DNA also hinders plasmin-induced digestion.

In summary, our work revealed novel determinants of the mechanical and chemical stability of thrombi and substantiated the need for more complex thrombolytic strategies (e.g. including agents disrupting the DNA-histone-NET-matrix).

DOI:10.14753/SE.2015.1738

7.2. ÖSSZEFOGLALÁS

A cerebro- és kardiovaszkuláris betegségek többségének hátterében meghúzódó oki tényezők az intravaszkuláris trombusok, melyek fibrinhálóból, sejtekből, és egyéb vér-eredetű szolubilis elemekből felépülő, komplex struktúrák, kitéve a keringő vér által kifejtett nyíróerőknek. A fibrin alapváz lebontását célzó trombolízis olyan terápiás eszköz, mely képes csökkenteni az akadályozott véráramlás okozta szöveti károsodást. Jelen disszertáció a terápiás trombolízis hatékonyságát befolyásoló számos tényező közül kettőre fókuszál: egyrészt a *mechanikai stressz*, másrészt a neutrofil extracelluláris csapdák (*NET*ek) komponenseinek szerepére.

Az érszűkületben fekvő trombusokat mind külső (véráramlás), mind belső (vérlemezke kontrakció) forrásból származó mechanikai hatások érik, és az itt közzé tett, betegek trombusairól készült pásztázó elektronmikroszkópos felvételek további, indirekt bizonyítékot szolgáltatnak arra nézve, hogy ezen hatások elég nagy mértékűek ahhoz, hogy a fibrin *in vivo* elrendezését befolyásolni tudják. Eredményeink kiterjesztették azon korábbi megfigyeléseket, melyek szerint a mechanikai stressz a fibrin szerkezetének megváltozását okozza: csökkent az átlagos pórusnagyság és fibrinszál-átmérő. Ezen szerkezeti változások a nyújtott fibrinalvadékok megnövekedett lítikus ellenállásával jártak együtt.

A NETek jelenléte egyre inkább alapvetőnek tekintendő mind a vénás-, mind az artériás trombusokban. Jelen munkánkban a NETek komponenseinek az alvadékok szerkezetére és lítikus tulajdonságaira kifejtett hatásait vizsgáltuk növekvő komplexitású rendszerekben: a tisztított komponensekkel (DNS±hiszton) kiegészített fibrinalvadékoktól egészen az aktivált neutrofilekből származó NETeket tartalmazó plazmaalvadékokig. A NET komponensei a szálátmérő növekedését és a permeabilitás csökkenését okozzák alacsony trombin-koncentráció mellett létrejött alvadékokban. Ezen trombus-modellek megnövekedett ellenállással bírnak a tPA-indukálta lízissel szemben, a DNS pedig hátráltatja a plazmin-indukálta alvadékemésztést is.

Összefoglalva, jelen disszertációban közölt munka új, a trombusok szerkezeti és kémiai stabilitását meghatározó elemeket tár fel, és rámutat egy komplexebb trombolítikus stratégia kidolgozásának szükségességére (olyan anyagok segítségével, melyek a DNS-hiszton-NET-mátrix integritását képesek megszüntetni).

REFERENCES

1. World Health Organization, Global Health Observatory Data Repository. Number of deaths: WORLD By cause Available at: http://apps.who.int/gho/data/node.main.CODWORLD?lang=en Accessed 2014. Apr 06.
2. Smith SC Jr, Benjamin EJ, Bonow RO, Braun LT, Creager MA, Franklin BA, Gibbons RJ, Grundy SM, Hiratzka LF, Jones DW, Lloyd-Jones DM, Minissian M, Mosca L, Peterson ED, Sacco RL, Spertus J, Stein JH, Taubert KA. (2011) AHA/ACCF secondary prevention and risk reduction therapy for patients with coronary and other atherosclerotic vascular disease: 2011 update: a guideline from the American Heart Association and American College of Cardiology Foundation endorsed by the World Heart Federation and the Preventive Cardiovascular Nurses Association. J Am Coll Cardiol, 58(23):2432-46.
3. Verstraete M. (2003) Overview of new therapeutic agents. In: New therapeutic agents in thrombosis and thrombolysis (Sasahara, A.A., and Loscalzo, J.L., eds), Marcel Dekker, Inc., New York, NY, pp. 477-478.
4. Newman, David. Thrombolytics for Acute Ischemic Stroke – No benefit found. The NNT group. Available at: http://www.thennt.com/nnt/thrombolytics-for-stroke Accessed 2014. Apr 20.
5. Brinkmann V, Reichard U, Goosmann C, Fauler B, Uhlemann Y, Weiss DS, Weinrauch Y, Zychlinsky A (2004) Neutrophil extracellular traps kill bacteria. Science, 303: 1532–1535.
6. Mosesson MW. (2005) Fibrinogen and fibrin structure and functions. J Thromb Haemost, 3(8):1894-904.
7. Henschen A, Lottspeich F, Kehl M, Southan C. (1983) Covalent structure of fibrinogen. Ann N Y Acad Sci, 408:28-43.
8. Blombäck B, Hessel B, Hogg D. (1976) Disulfide bridges in nh2-terminal part of human fibrinogen. Thromb Res, 8(5):639-58.
9. Huang S, Cao Z, Davie EW. (1993) The role of amino-terminal disulfide bonds in the structure and assembly of human fibrinogen. Biochem Biophys Res Commun, 190(2):488-95.

10. Zhang JZ, Redman CM. (1992) Identification of B beta chain domains involved in human fibrinogen assembly. J Biol Chem, 267(30):21727-32.
11. Hoeprich PD Jr, Doolittle RF. (1983) Dimeric half-molecules of human fibrinogen are joined through disulfide bonds in an antiparallel orientation. Biochemistry, 22(9):2049-55.
12. Medved L, Weisel JW. (2009) Fibrinogen and Factor XIII Subcommittee of Scientific Standardization Committee of International Society on Thrombosis and Haemostasis. Recommendations for nomenclature on fibrinogen and fibrin. J Thromb Haemost, 7(2):355-9.
13. Scheraga HA, Laskowski M Jr. (1957) The fibrinogen-fibrin conversion. Adv Protein Chem, 12:1-131.
14. Blombäck B. (1958) Studies on the action of thrombotic enzymes on bovine fibrinogen as measured by N-terminal analysis. Ark Kemi, 12:321–35.
15. Blombäck B, Hessel B, Hogg D, Therkildsen L. (1978) A two-step fibrinogen-fibrin transition in blood coagulation. Nature, 275(5680):501-5.
16. Weisel JW, Veklich Y, Collet JP, Francis CW. (1999) Structural studies of fibrinolysis by electron and light microscopy. Thromb Haemost,82(2):277-82.
17. Ferry JD. (1952) The mechanism of polymerization of fibrinogen. Proc Natl Acad Sci USA, 38: 566–9.
18. Krakow W, Endres GF, Siegel BM, Scheraga HA. (1972) An electron microscopic investigation of the polymerization of bovine fibrin monomer. J Mol Biol, 71: 95–103.
19. Fowler WE, Hantgan RR, Hermans J, Erikson HP. (1981) Structure of the fibrin protofibril. Proc Natl Acad Sci USA, 78: 4872–6.
20. Müller MF, Ris H, Ferry JD. (1984) Electron microscopy of fine fibrin clots and fine and coarse fibrin films. Observations of fibers in cross-section and in deformed states. J Mol Biol, 174(2):369-84.
21. Spraggon G, Everse SJ, Doolittle RF. (1997) Crystal structures of fragment D from human fibrinogen and its crosslinked counterpart from fibrin. Nature, 389: 455-462.
22. Brown JH, Volkmann N, Jun G, Henschen-Edman AH, Cohen C. (2000) The crystal structure of modified bovine fibrinogen. Proc Natl Acad Sci USA, 97: 85-90.

23. Baradet TC, Haselgrove JC, Weisel JW. (1995) Three-dimensional reconstruction of fibrin clot networks from stereoscopic intermediate voltage electron microscope images and analysis of branching. Biophys J, 68: 1551-1560.
24. Veklich YI, Gorkun OV, Medved LV, Niewenhuizen W, Weisel JW. (1993) Carboxyl-terminal portions of the α-chains of fibrinogen and fibrin. J Biol Chem 268: 13577–85.
25. Gorkun OV, Veklich YI, Medved LV, Henschen A, Weisel JW. (1994) Role of the αC domains of fibrin in clot formation. Biochemistry, 33: 6986–97.
26. Carr ME Jr, Hermans J. (1978) Size and density of fibrin fibers from turbidity. Macromolecules, 11: 46-50
27. Voter WA, Lucaveche C, Blaurock A, Erickson HP. (1986) Lateral packing of protofibrils in fibrin fibers and fibrinogen polymers. Biopolimers, 25: 2359-2373.
28. Guthold M, Liu W, Stephens B, Lord ST, Hantgan RR, Erie DA, Taylor Jr RM, Superfine R. (2004) Visualization and mechanical manipulations of individual fibrin fibers suggest that fiber cross section has fractal dimension 1.3. Biophys J, 87: 4226-4236.
29. Blombäck B, Carlsson K, Hessel B, Liljeborg A, Procyk R, Aslund N. (1989) Native fibrin gel networks observed by 3D microscopy, permeation and turbidity. Biochim Biophys Acta, 997(1-2):96-110.
30. Rellick LM, Becktel WJ. (1995) Molecular volume. Meth Enzymol, 259:377-95.
31. Matveyev MY, Domogatsky SP. (1992) Penetration of macromolecules into contracted blood clot. Biophys J, 63: 862-863.
32. Macfarlane RG. (1964) An Enzyme Cascade in the Blood Clotting Mechanism, and Its Function as a Biochemical Amplifier. Nature, 202: 498-499.
33. Davie EW, Ratnoff OD. (1964) Waterfall Sequence for Intrinsic Blood Clotting. Science, 145: 1310-1312.
34. Hoffman MM, Monroe DM. (2005) Rethinking the coagulation cascade. Curr Hematol Rep, 4: 391-396.
35. Wood JP, Silveira JR, Maille NM, Haynes LM, Tracy PB. (2011) Prothrombin activation on the activated platelet surface optimizes expression of procoagulant activity. Blood, 117(5):1710-8.

36. Krishnaswamy S, Mann KG, Nesheim ME. (1986) The prothrombinase-catalyzed activation of prothrombin proceeds through the intermediate meizothrombin in an ordered, sequential reaction. J Biol Chem, 261: 8977-8984.
37. Huntington JA. (2014) Natural inhibitors of thrombin. Thromb Haemost, 111(4): 583-9..
38. Pechik I, Madrazo J, Mosesson MW, Hernandez I, Gilliland GL, Medved L. (2004) Crystal structure of the complex between thrombin and the central „E“ region of fibrin. Proc Natl Acad Sci USA, 101: 2718-2723.
39. Fuentes-Prior P, Iwanaga Y, Huber R, Pagila R, Rumennik G, Seto M, Morser J, Light DR, Bode W. (2000) Structural basis for the anticoagulant activity of the thrombin-thrombomodulin complex. Nature, 404: 518-525.
40. Gandhi PS, Chen Z, Di Cera E. (2010) Crystal structure of thrombin bound to the uncleaved extracellular fragment of PAR1. J Biol Chem, 285: 15393-15398.
41. Myles T, Yun TH, Hall SW, Leung LL. (2001) An extensive interaction interface between thrombin and factor V is required for factor V activation. J Biol Chem, 276: 25143-25149.
42. Myles T, Yun TH, Leung LL. (2002) Structural requirements for the activation of human factor VIII by thrombin. Blood, 100: 2820-2826.
43. Bukys MA, Orban T, Kim PY, Beck DO, Nesheim ME, Kalafatis M. (2006) The structural integrity of anion binding exosite I of thrombin is required and sufficient for timely cleavage and activation of factor V and factor VIII. J Biol Chem, 281: 18569-18580.
44. Hall SW, Nagashima M, Zhao L, Morser J, Leung LL. (1999) Thrombin interacts with thrombomodulin, protein C, and thrombin-activatable fibrinolysis inhibitor via specific and distinct domains. J Biol Chem, 274: 25510-25516.
45. Janus TJ, Lewis SD, Lorand L, Shafer JA. (1983) Promotion of thrombin-catalyzed activation of factor XIII by fibrinogen. Biochemistry, 22: 6269-6272.
46. De Cristofaro R, De Candia E, Landolfi R, Rutella S, Hall SW. (2001) Structural and functional mapping of the thrombin domain involved in the binding to the platelet glycoprotein Ib. Biochemistry, 40: 13268-13273.

47. Celikel R, McClintock RA, Roberts JR, Mendolicchio GL, Ware J, Varughese KI, Ruggeri ZM. (2003) Modulation of alpha-thrombin function by distinct interactions with platelet glycoprotein Ibalpha. Science, 301: 218-221.
48. Dumas JJ, Kumar R, Seehra J, Somers WS, Mosyak L. (2003) Crystal structure of the GpIbalpha-thrombin complex essential for platelet aggregation. Science, 301: 222-226.
49. Nogami K, Zhou Q, Myles T, Leung LL, Wakabayashi H, Fay PJ. (2005) Exosite-interactive regions in the A1 and A2 domains of factor VIII facilitate thrombin-catalyzed cleavage of heavy chain. J Biol Chem, 280: 18476-18487.
50. Segers K, Dahlbäck B, Bock PE, Tans G, Rosing J, Nicolaes GA. (2007) The role of thrombin exosites I and II in the activation of human coagulation factor V. J Biol Chem, 282: 33915-33924.
51. Baglin TP, Carrell RW, Church FC, Esmon CT, Huntington JA. (2002) Crystal structures of native and thrombin- complexed heparin cofactor II reveal a multistep allosteric mechanism. Proc Natl Acad Sci USA, 99: 11079-11084.
52. Li W, Adams TE, Nangalia J, Esmon CT, Huntington JA. (2008) Molecular basis of thrombin recognition by protein C inhibitor revealed by the 1.6-A structure of the heparin-bridged complex. Proc Natl Acad Sci USA, 105: 4661-4666.
53. Li W, Huntington JA. (2012) Crystal structures of protease nexin-1 in complex with heparin and thrombin suggest a 2-step recognition mechanism. Blood, 120: 459-467.
54. Li W, Johnson DJ, Esmon CT, Huntington JA. (2004) Structure of the antithrombin-thrombin-heparin ternary complex reveals the antithrombotic mechanism of heparin. Nat Struct Mol Biol, 11: 857-862.
55. Huntington JA. (2013) Thrombin inhibition by the serpins. J Thromb Haemost, 11 (Suppl 1): 254-264.
56. Rau JC, Beaulieu LM, Huntington JA, Church FC. (2007) Serpins in thrombosis, hemostasis and fibrinolysis. J Thromb Haemost, 5 (Suppl 1): 102-115.
57. Gettins PG. (2002) Serpin structure, mechanism, and function. Chem Rev, 102: 4751-4804.
58. Collet JP, Montalescot G, Lesty C, Weisel JW. (2002) A structural and dynamic investigation of the facilitating effect of glycoprotein IIb/IIIa inhibitors in dissolving platelet-rich clots. Circ Res, 90(4):428-34.

59. Minton AP. (1983) The effect of volume occupancy upon the thermodynamic activity of proteins: some biochemical consequences. Mol Cell Biochem, 55: 119-140.
60. Rivas G, Fernandez JA, Minton AP. (1999) Direct observation of the self-association of dilute proteins in the presence of inert macromolecules at high concentration via tracer sedimentation equilibrium: theory, experiment, and biological significance. Biochemistry, 38(29):9379-88.
61. Gabriel DA, Smith LA, Folds JD, Davis L, Cancelosi SE. (1983) The influence of immunoglobulin (IgG) on the assembly of fibrin gels. J Lab Clin Med, 101(4):545-52.
62. Carr ME Jr, Dent RM, Carr SL. (1996) Abnormal fibrin structure and inhibition of fibrinolysis in patients with multiple myeloma. J Lab Clin Med, 128(1):83-8.
63. Coleman M, Vigliano EM, Weksler ME, Nachman RL. (1972) Inhibition of fibrin monomer polymerization by lambda myeloma globulins. Blood, 39(2):210-23.
64. O'Kane MJ, Wisdom GB, Desai ZR, Archbold GP. (1994) Inhibition of fibrin monomer polymerisation by myeloma immunoglobulin. J Clin Pathol, 47(3):266-8.
65. Gruber A, Mori E, del Zoppo GJ, Waxman L, Griffin JH. (1994) Alteration of fibrin network by activated protein C. Blood, 83(9):2541-8.
66. Kovács A, Szabó L, Longstaff C, Tenekedjiev K, Machovich R, Kolev K. (2014) Ambivalent roles of carboxypeptidase B in the lytic susceptibility of fibrin. Thromb Res, 133(1):80-7.
67. Rottenberger Z, Komorowicz E, Szabó L, Bóta A, Varga Z, Machovich R, Longstaff C, Kolev K. (2013) Lytic and mechanical stability of clots composed of fibrin and blood vessel wall components. J Thromb Haemost, 11(3):529-38.
68. Carr ME Jr, Hardin CL. (1987) Fibrin has larger pores when formed in the presence of erythrocytes. Am J Physiol, 253(5 Pt 2):H1069-73.
69. Chao FC, Shepro D, Tullis JL, Belamarich FA, Curby WA. (1976) Similarities between platelet contraction and cellular motility during mitosis: role of platelet microtubules in clot retraction. J Cell Sci, 20(3):569-88.
70. Skarlatos SI, Rao R, Dickens BF, Kruth HS. (1993) Phospholipid loss in dying platelets. Virchows Arch B Cell Pathol Incl Mol Pathol, 64(4):241-5.

71. Retzinger GS. (1995) Adsorption and coagulability of fibrinogen on atheromatous lipid surfaces. Arterioscler Thromb Vasc Biol, 15(6):786-92.
72. Kolev K, Longstaff C, Machovich R. (2005) Fibrinolysis at the fluid-solid interface of thrombi. Curr Med Chem Cardiovasc Hematol Agents, 3(4):341-55.
73. Janmey PA, Lind SE, Yin HL, Stossel TP. (1985) Effects of semi-dilute actin solutions on the mobility of fibrin protofibrils during clot formation. Biochim Biophys Acta, 841(2):151-8.
74. Weisel JW. (2004) The mechanical properties of fibrin for basic scientists and clinicians. Biophys Chem, 112(2-3):267-76.
75. Gabriel DA, Muga K, Boothroyd EM. (1992) The effect of fibrin structure on fibrinolysis. J Biol Chem, 267(34):24259-63.
76. Liu W, Jawerth LM, Sparks EA, Falvo MR, Hantgan RR, Superfine R, Lord ST, Guthold M. (2006) Fibrin fibers have extraordinary extensibility and elasticity. Science, 313(5787):634.
77. Liu W, Jawerth LM, Sparks EA, Falvo MR, Hantgan RR, Superfine R, Lord ST, Guthold M. (2006) Supporting Online Material for: Fibrin fibers have extraordinary extensibility and elasticity. Science, 313(5787):634.
78. Eskin SG, McIntire LV. (2006) Rheology of thrombosis. In: Colman RW, Marder VJ, Clowes AW, George JN, Goldhaber SZ, eds. Hemostasis and Thrombosis: Basic Principles and Clinical Practice, 5th edn. Philadelphia: Lippincott Williams & Wilkins, 737–50.
79. Lee KW, Xu XY. (2002) Modelling of flow and wall behaviour in a mildly stenosed tube. Med Eng Phys, 24: 575–86.
80. Brown AE, Litvinov RI, Discher DE, Purohit PK, Weisel JW. (2009) Multiscale mechanics of fibrin polymer: gel stretching with protein unfolding and loss of water. Science, 325(5941):741-4.
81. Brown AE, Litvinov RI, Discher DE, Purohit PK, Weisel JW. (2009) Supporting Online Material for: Multiscale mechanics of fibrin polymer: gel stretching with protein unfolding and loss of water. Science, 325(5941):741-4.
82. Brown AE, Litvinov RI, Discher DE, Weisel JW. (2007) Forced unfolding of coiled-coils in fibrinogen by single-molecule AFM. Biophys J, 92(5):L39-41. Epub 2006 Dec 15.

83. Ferguson EW, Fretto LJ, McKee PA. (1975) A re-examination of the cleavage of fibrinogen and fibrin by plasmin. J Biol Chem, 250(18):7210-8.
84. Walker JB, Nesheim ME. (1999) The molecular weights, mass distribution, chain composition, and structure of soluble fibrin degradation products released from a fibrin clot perfused with plasmin. J Biol Chem, 274(8):5201-12.
85. Sakharov DV, Nagelkerke JF, Rijken DC. (1996) Rearrangements of the fibrin network and spatial distribution of fibrinolytic components during plasma clot lysis. Study with confocal microscopy. J Biol Chem, 271(4):2133-8.
86. Fleury V, Anglés-Cano E. (1991) Characterization of the binding of plasminogen to fibrin surfaces: the role of carboxy-terminal lysines. Biochemistry, 30(30):7630-8.
87. Bok RA, Mangel WF. (1985) Quantitative characterization of the binding of plasminogen to intact fibrin clots, lysine-sepharose, and fibrin cleaved by plasmin. Biochemistry, 24(13):3279-86.
88. Tsurupa G, Medved L. (2001) Identification and characterization of novel tPA- and plasminogen-binding sites within fibrin(ogen) alpha C-domains. Biochemistry, 40(3):801-8.
89. Sakharov DV, Rijken DC. (1995) Superficial accumulation of plasminogen during plasma clot lysis. Circulation, 92(7):1883-90.
90. Veklich Y, Francis CW, White J, Weisel JW. (1998) Structural studies of fibrinolysis by electron microscopy. Blood, 92(12):4721-9.
91. Collet JP, Lesty C, Montalescot G, Weisel JW. (2003) Dynamic changes of fibrin architecture during fibrin formation and intrinsic fibrinolysis of fibrin-rich clots. J Biol Chem, 278(24):21331-5.
92. Meh DA, Mosesson MW, DiOrio JP, Siebenlist KR, Hernandez I, Amrani DL, Stojanovich L. (2001) Disintegration and reorganization of fibrin networks during tissue-type plasminogen activator-induced clot lysis. Blood Coagul Fibrinolysis, 12(8):627-37.
93. Collet JP, Park D, Lesty C, Soria J, Soria C, Montalescot G, Weisel JW. (2000) Influence of fibrin network conformation and fibrin fiber diameter on fibrinolysis speed: dynamic and structural approaches by confocal microscopy. Arterioscler Thromb Vasc Biol, 20(5):1354-61.

94. Garman AJ, Smith RAG. (1982) The binding of plasminogen to fibrin: Evidence for plasminogen-bridging. Thromb Res, 27:311-320.
95. Weisel JW, Nagaswami C, Korsholm B, Petersen LC, Suenson E. (1994) Interactions of plasminogen with polymerizing fibrin and its derivatives, monitored with a photoaffinity cross-linker and electron microscopy. J Mol Biol, 235(3):1117-35.
96. Petersen LC, Suenson E. (1991) Effect of plasminogen and tissue-type plasminogen activator on fibrin gel structure. Fibrinolysis, 5:51-59.
97. Weisel JW, Litvinov RI. (2008) The biochemical and physical process of fibrinolysis and effects of clot structure and stability on the lysis rate. Cardiovasc Hematol Agents Med Chem, 6(3):161-80.
98. Petersen TE, Martzen MR, Ichinose A, Davie EW. (1990) Characterization of the gene for human plasminogen, a key proenzyme in the fibrinolytic system. J Biol Chem, 265(11):6104-11.
99. Castellino FJ, McCance SG. (1997) The kringle domains of human plasminogen. Ciba Found Symp, 212:46-60; discussion 60-5.
100. Hughes AL. (2000) Modes of evolution in the protease and kringle domains of the plasminogen-prothrombin family. Mol Phylogenet Evol, 14(3):469-78.
101. Váli Z, Patthy L. (1982) Location of the intermediate and high affinity omega-aminocarboxylic acid-binding sites in human plasminogen. J Biol Chem, 257(4):2104-10.
102. Knudsen BS, Silverstein RL, Leung LL, Harpel PC, Nachman RL. (1986) Binding of plasminogen to extracellular matrix, J Biol Chem, 261(23):10765-71.
103. Urano T, Chibber BA, Castellino FJ. (1987) The reciprocal effects of epsilon-aminohexanoic acid and chloride ion on the activation of human [Glu1]plasminogen by human urokinase. Proc Natl Acad Sci USA, 84(12):4031-4
104. Wu HL, Chang BI, Wu DH, Chang LC, Gong CC, Lou KL, Shi GY. (1990) Interaction of plasminogen and fibrin in plasminogen activation. J Biol Chem, 265(32):19658-64.
105. Christensen U. (1984) The AH-site of plasminogen and two C-terminal fragments. A weak lysine-binding site preferring ligands not carrying a free carboxylate function. Biochem J, 223(2):413-21.

106. Sinniger V, Merton RE, Fabregas P, Felez J, Longstaff C. (1999) Regulation of tissue plasminogen activator activity by cells. Domains responsible for binding and mechanism of stimulation. J Biol Chem, 274(18):12414-22.

107. Robbins KC, Summaria L, Hsieh B, Shah RJ. (1967) The peptide chains of human plasmin. Mechanism of activation of human plasminogen to plasmin. J Biol Chem, 242(10):2333-42.

108. Pennica D, Holmes WE, Kohr WJ, Harkins RN, Vehar GA, Ward CA, Bennett WF, Yelverton E, Seeburg PH, Heyneker HL, Goeddel DV, Collen D. (1983) Cloning and expression of human tissue-type plasminogen activator cDNA in E. coli. Nature, 301(5897):214-21.

109. van Hinsbergh VW. (1988) Regulation of the synthesis and secretion of plasminogen activators by endothelial cells. Haemostasis, 18(4-6):307-27.

110. Robbie LA, Bennett B, Croll AM, Brown PA, Booth NA. (1996) Proteins of the fibrinolytic system in human thrombi. Thromb Haemost, 75(1):127-33.

111. Booth NA, Bennett B. (1994) Fibrinolysis and thrombosis. Baillieres Clin Haematol, 7(3): 559-72.

112. Camiolo SM, Thorsen S, Astrup T. (1971) Fibrinogenolysis and fibrinolysis with tissue plasminogen activator, urokinase, streptokinase-activated human globulin, and plasmin. Proc Soc Exp Biol Med, 138(1):277-80.

113. Yakovlev S, Makogonenko E, Kurochkina N, Nieuwenhuizen W, Ingham K, Medved L. (2000) Conversion of fibrinogen to fibrin: mechanism of exposure of tPA- and plasminogen-binding sites. Biochemistry, 39(51):15730-41.

114. Horrevoets AJ, Smilde A, de Vries C, Pannekoek H. (1994) The specific roles of finger and kringle 2 domains of tissue-type plasminogen activator during in vitro fibrinolysis. J Biol Chem, 269(17):12639-44.

115. Bakker AH, Weening-Verhoeff EJ, Verheijen JH. (1995) The role of the lysyl binding site of tissue-type plasminogen activator in the interaction with a forming fibrin clot. J Biol Chem, 270(21):12355-60.

116. Tachias K, Madison EL. (1996) Converting tissue-type plasminogen activator into a zymogen. J Biol Chem, 271(46):28749-52.

117. Tachias K, Madison EL. (1997) Converting tissue type plasminogen activator into a zymogen. Important role of Lys156. J Biol Chem, 272(1):28-31.

118. Medved L, Nieuwenhuizen W. (2003) Molecular mechanisms of initiation of fibrinolysis by fibrin. Thromb Haemost, 89(3):409-19.

119. Barlow GH. (1976) Urinary and kidney cell plasminogen activator (urokinase). Methods Enzymol, 45:239-44.

120. Darras V, Thienpont M, Stump DC, Collen D. (1986) Measurement of urokinase-type plasminogen activator (u-PA) with an enzyme-linked immunosorbent assay (ELISA) based on three murine monoclonal antibodies. Thromb Haemost, 56(3):411-4.

121. Vassalli JD, Dayer JM, Wohlwend A, Belin D. (1984) Concomitant secretion of prourokinase and of a plasminogen activator-specific inhibitor by cultured human monocytes-macrophages. J Exp Med, 159(6):1653-68.

122. Sappino AP, Huarte J, Vassalli JD, Belin D. (1991) Sites of synthesis of urokinase and tissue-type plasminogen activators in the murine kidney. J Clin Invest, 87(3):962-70.

123. Pepper MS, Sappino AP, Stöcklin R, Montesano R, Orci L, Vassalli JD. (1993) Upregulation of urokinase receptor expression on migrating endothelial cells. J Cell Biol, 122(3):673-84.

124. Ichinose A, Fujikawa K, Suyama T. (1986) The activation of pro-urokinase by plasma kallikrein and its inactivation by thrombin. J Biol Chem, 261(8):3486-9.

125. Kobayashi H, Schmitt M, Goretzki L, Chucholowski N, Calvete J, Kramer M, Günzler WA, Jänicke F, Graeff H. (1991) Cathepsin B efficiently activates the soluble and the tumor cell receptor-bound form of the proenzyme urokinase-type plasminogen activator (Pro-uPA). J Biol Chem, 266(8):5147-52.

126. Fears R. (1989) Binding of plasminogen activators to fibrin: characterization and pharmacological consequences. Biochem J, 261(2):313-24.

127. Mimuro J, Kaneko M, Murakami T, Matsuda M, Sakata Y. (1992) Reversible interactions between plasminogen activators and plasminogen activator inhibitor-1. Biochim Biophys Acta, 1160(3):325-34.

128. Stephens RW, Bokman AM, Myöhänen HT, Reisberg T, Tapiovaara H, Pedersen N, Grøndahl-Hansen J, Llinás M, Vaheri A. (1992) Heparin binding to the urokinase kringle domain. Biochemistry, 31(33):7572-9.

129. Appella E, Robinson EA, Ullrich SJ, Stoppelli MP, Corti A, Cassani G, Blasi F. (1987) The receptor-binding sequence of urokinase. A biological function for the growth-factor module of proteases. J Biol Chem, 262(10):4437-40.

130. Reddy KN. (1988) Streptokinase--biochemistry and clinical application. Enzyme, 40(2-3):79-89.

131. Boxrud PD, Fay WP, Bock PE. (2000) Streptokinase binds to human plasmin with high affinity, perturbs the plasmin active site, and induces expression of a substrate recognition exosite for plasminogen. J Biol Chem, 275(19):14579-89.

132. Reed GL, Houng AK, Liu L, Parhami-Seren B, Matsueda LH, Wang S, Hedstrom L. (1999) A catalytic switch and the conversion of streptokinase to a fibrin-targeted plasminogen activator. Proc Natl Acad Sci USA, 96(16):8879-83.

133. Lijnen HR, Van Hoef B, De Cock F, Okada K, Ueshima S, Matsuo O, Collen D. (1991) On the mechanism of fibrin-specific plasminogen activation by staphylokinase. J Biol Chem, 266(18):11826-32.

134. Eaton DL, Malloy BE, Tsai SP, Henzel W, Drayna D. (1991) Isolation, molecular cloning, and partial characterization of a novel carboxypeptidase B from human plasma. J Biol Chem, 266(32):21833-8.

135. Strömqvist M, Schatteman K, Leurs J, Verkerk R, Andersson JO, Johansson T, Scharpé S, Hendriks D. (2001) Immunological assay for the determination of procarboxypeptidase U antigen levels in human plasma. Thromb Haemost, 85: 12-7.

136. Buelens K, Hillmayer K, Compernolle G, Declerck PJ, Gils A. (2008) Biochemical importance of glycosylation in thrombin activatable fibrinolysis inhibitor. Circ Res, 102(3):295-301.

137. Mosnier LO, von dem Borne PA, Meijers JC, Bouma BN. (1998) Plasma TAFI levels influence the clot lysis time in healthy individuals in the presence of an intact intrinsic pathway of coagulation. Thromb Haemost, 80(5):829-35.

138. Sakharov DV, Plow EF, Rijken DC. (1997) On the mechanism of the antifibrinolytic activity of plasma carboxypeptidase B. J Biol Chem, 272(22):14477-82.

139. Schneider M, Nesheim M. A study of the protection of plasmin from antiplasmin inhibition within an intact fibrin clot during the course of clot lysis. (2004) J Biol Chem, 279(14):13333-9.

140. Hoylaerts M, Rijken DC, Lijnen HR, Collen D. (1982) Kinetics of the activation of plasminogen by human tissue plasminogen activator. Role of fibrin. J Biol Chem, 257(6):2912-9.

141. Wang W, Boffa MB, Bajzar L, Walker JB, Nesheim ME. (1998) A study of the mechanism of inhibition of fibrinolysis by activated thrombin-activable fibrinolysis inhibitor. J Biol Chem, 273(42):27176-81.

142. Schatteman KA, Goossens FJ, Scharpé SS, Hendriks DF. (2000) Proteolytic activation of purified human procarboxypeptidase U. Clin Chim Acta, 292(1-2):25-40.

143. Wang W, Nagashima M, Schneider M, Morser J, Nesheim M. (2000) Elements of the primary structure of thrombomodulin required for efficient thrombin-activable fibrinolysis inhibitor activation. J Biol Chem, 275(30):22942-7.

144. Bajzar L, Morser J, Nesheim M. (1996) TAFI, or plasma procarboxypeptidase B, couples the coagulation and fibrinolytic cascades through the thrombin-thrombomodulin complex. J Biol Chem, 271(28):16603-8.

145. Bajzar L, Manuel R, Nesheim ME. (1995) Purification and characterization of TAFI, thrombin-activable fibrinolysis inhibitor. J Biol Chem, 270(24):14477-84.

146. Boffa MB, Wang W, Bajzar L, Nesheim ME. (1998) Plasma and recombinant thrombin-activable fibrinolysis inhibitor (TAFI) and activated TAFI compared with respect to glycosylation, thrombin/thrombomodulin-dependent activation, thermal stability, and enzymatic properties. J Biol Chem, 273(4):2127-35.

147. Boffa MB, Bell R, Stevens WK, Nesheim ME. (2000) Roles of thermal instability and proteolytic cleavage in regulation of activated thrombin-activable fibrinolysis inhibitor. J Biol Chem, 275(17):12868-78.

148. Marx PF, Hackeng TM, Dawson PE, Griffin JH, Meijers JC, Bouma BN. (2000) Inactivation of active thrombin-activable fibrinolysis inhibitor takes place by a process that involves conformational instability rather than proteolytic cleavage. J Biol Chem, 275(17):12410-5.

149. Valnickova Z, Thogersen IB, Christensen S, Chu CT, Pizzo SV, Enghild JJ. (1996) Activated human plasma carboxypeptidase B is retained in the blood by binding to alpha2-macroglobulin and pregnancy zone protein. J Biol Chem, 271(22):12937-43.

150. Valnickova Z, Enghild JJ. (1998) Human procarboxypeptidase U, or thrombin-activable fibrinolysis inhibitor, is a substrate for transglutaminases. Evidence for transglutaminase-catalyzed cross-linking to fibrin. J Biol Chem, 273(42):27220-4.

151. Rau JC, Beaulieu LM, Huntington JA, Church FC. (2007) Serpins in thrombosis, hemostasis and fibrinolysis. J Thromb Haemost, 5 Suppl 1:102-15.

152. Brogren H, Karlsson L, Andersson M, Wang L, Erlinge D, Jern S. (2004) Platelets synthesize large amounts of active plasminogen activator inhibitor 1. Blood, 104(13):3943-8.

153. van Mourik JA, Lawrence DA, Loskutoff DJ. (1984) Purification of an inhibitor of plasminogen activator (antiactivator) synthesized by endothelial cells. J Biol Chem, 259(23):14914-21.

154. Sprengers ED, Kluft C. (1987) Plasminogen activator inhibitors. Blood, 969(2):381-7.

155. Fay WP, Murphy JG, Owen WG. (1996) High concentrations of active plasminogen activator inhibitor-1 in porcine coronary artery thrombi. Arterioscler Thromb Vasc Biol, 16(10):1277-84.

156. Keijer J, Ehrlich HJ, Linders M, Preissner KT, Pannekoek H. (1991) Vitronectin governs the interaction between plasminogen activator inhibitor 1 and tissue-type plasminogen activator. J Biol Chem, 266(16):10700-7.

157. Zhou A, Huntington JA, Pannu NS, Carrell RW, Read RJ. (2003) How vitronectin binds PAI-1 to modulate fibrinolysis and cell migration. Nat Struct Biol, 10(7):541-4.

158. Lawrence DA, Ginsburg D, Day DE, Berkenpas MB, Verhamme IM, Kvassman JO, Shore JD. (1995) Serpin-protease complexes are trapped as stable acyl-enzyme intermediates. J Biol Chem, 270(43):25309-12.

159. Thorsen S, Philips M, Selmer J, Lecander I, Astedt B. (1988) Kinetics of inhibition of tissue-type and urokinase-type plasminogen activator by plasminogen-activator inhibitor type 1 and type 2. Eur J Biochem, 175(1):33-9.

160. Stratikos E, Gettins PG. (1999) Formation of the covalent serpin-proteinase complex involves translocation of the proteinase by more than 70 A and full insertion of the reactive center loop into beta-sheet A. Proc Natl Acad Sci USA, 96(9):4808-13.

161. Lawrence DA, Strandberg L, Ericson J, Ny T. (1990) Structure-function studies of the SERPIN plasminogen activator inhibitor type 1. Analysis of chimeric strained loop mutants. J Biol Chem, 265(33):20293-301.

162. Egelund R, Petersen TE, Andreasen PA. (2001) A serpin-induced extensive proteolytic susceptibility of urokinase-type plasminogen activator implicates distortion of the proteinase substrate-binding pocket and oxyanion hole in the serpin inhibitory mechanism. Eur J Biochem, 268(3):673-85.

163. Huntington JA, Read RJ, Carrell RW. (2000) Structure of a serpin-protease complex shows inhibition by deformation. Nature, 407(6806):923-6.

164. Stefansson S, Muhammad S, Cheng XF, Battey FD, Strickland DK, Lawrence DA. (1998) Plasminogen activator inhibitor-1 contains a cryptic high affinity binding site for the low density lipoprotein receptor-related protein. J Biol Chem, 273(11):6358-66.

165. Horn IR, van den Berg BM, Moestrup SK, Pannekoek H, van Zonneveld AJ. (1998) Plasminogen activator inhibitor 1 contains a cryptic high affinity receptor binding site that is exposed upon complex formation with tissue-type plasminogen activator. Thromb Haemost, 80(5):822-828.

166. Stefansson S, Yepes M, Gorlatova N, Day DE, Moore EG, Zabaleta A, McMahon GA, Lawrence DA. (2004) Mutants of plasminogen activator inhibitor-1 designed to inhibit neutrophil elastase and cathepsin G are more effective in vivo than their endogenous inhibitors. J Biol Chem, 279(29):29981-7.

167. Hekman CM, Loskutoff DJ. (1988) Bovine plasminogen activator inhibitor 1: specificity determinations and comparison of the active, latent, and guanidine-activated forms. Biochemistry, 27(8):2911-8.

168. Mottonen J, Strand A, Symersky J, Sweet RM, Danley DE, Geoghegan KF, Gerard RD, Goldsmith EJ. (1992) Structural basis of latency in plasminogen activator inhibitor-1. Nature, 355(6357):270-3.

169. Schar CR, Blouse GE, Minor KH, Peterson CB. (2008) A deletion mutant of vitronectin lacking the somatomedin B domain exhibits residual plasminogen activator inhibitor-1-binding activity. J Biol Chem, 283(16):10297-309.

170. Podor TJ, Campbell S, Chindemi P, Foulon DM, Farrell DH, Walton PD, Weitz JI, Peterson CB. (2002) Incorporation of vitronectin into fibrin clots. Evidence for a

binding interaction between vitronectin and gamma A/gamma' fibrinogen. J Biol Chem, 277(9):7520-8.

171. Seiffert D, Smith JW. (1997) The cell adhesion domain in plasma vitronectin is cryptic. J Biol Chem, 272(21):13705-10.

172. McMahon GA, Petitclerc E, Stefansson S, Smith E, Wong MK, Westrick RJ, Ginsburg D, Brooks PC, Lawrence DA. (2001) Plasminogen activator inhibitor-1 regulates tumor growth and angiogenesis. J Biol Chem, 276(36):33964-8.

173. Devy L, Blacher S, Grignet-Debrus C, Bajou K, Masson V, Gerard RD, Gils A, Carmeliet G, Carmeliet P, Declerck PJ, Nöel A, Foidart JM. (2002) The pro- or antiangiogenic effect of plasminogen activator inhibitor 1 is dose dependent. FASEB J, 16(2):147-54.

174. Kruithof EK, Vassalli JD, Schleuning WD, Mattaliano RJ, Bachmann F. (1986) Purification and characterization of a plasminogen activator inhibitor from the histiocytic lymphoma cell line U-937. J Biol Chem, 261(24):11207-13.

175. Wun TC, Reich E. (1987) An inhibitor of plasminogen activation from human placenta. Purification and characterization. J Biol Chem, 262(8):3646-53.

176. Mikus P, Urano T, Liljeström P, Ny T. (1993) Plasminogen-activator inhibitor type 2 (PAI-2) is a spontaneously polymerising SERPIN. Biochemical characterisation of the recombinant intracellular and extracellular forms. Eur J Biochem, 218(3):1071-82.

177. Kruithof EK, Baker MS, Bunn CL. (1995) Biological and clinical aspects of plasminogen activator inhibitor type 2. Blood, 86(11):4007-24.

178. Wohlwend A, Belin D, Vassalli JD. (1987) Plasminogen activator-specific inhibitors in mouse macrophages: in vivo and in vitro modulation of their synthesis and secretion. J Immunol, 139(4):1278-84.

179. Astedt B, Hägerstrand I, Lecander I. (1986) Cellular localisation in placenta of placental type plasminogen activator inhibitor. Thromb Haemost, 56(1):63-5.

180. Feinberg RF, Kao LC, Haimowitz JE, Queenan JT Jr, Wun TC, Strauss JF 3rd Kliman HJ. (1989) Plasminogen activator inhibitor types 1 and 2 in human trophoblasts. PAI-1 is an immunocytochemical marker of invading trophoblasts. Lab Invest, 61(1):20-6.

181. Belin D, Wohlwend A, Schleuning WD, Kruithof EK, Vassalli JD. (1989) Facultative polypeptide translocation allows a single mRNA to encode the secreted and cytosolic forms of plasminogen activators inhibitor 2. EMBO J, 8(11):3287-94.

182. Ritchie H, Jamieson A, Booth NA. (1995) Thrombin modulates synthesis of plasminogen activator inhibitor type 2 by human peripheral blood monocytes. Blood, 86(9):3428-35.

183. Ritchie H, Booth NA. (1998) Secretion of plasminogen activator inhibitor 2 by human peripheral blood monocytes occurs via an endoplasmic reticulum-golgi-independent pathway. Exp Cell Res, 242(2):439-50.

184. Jensen PH, Schüler E, Woodrow G, Richardson M, Goss N, Højrup P, Petersen TE, Rasmussen LK. (1994) A unique interhelical insertion in plasminogen activator inhibitor-2 contains three glutamines, Gln83, Gln84, Gln86, essential for transglutaminase-mediated cross-linking. J Biol Chem, 269(21):15394-8.

185. Medcalf RL. (2007) Fibrinolysis, inflammation, and regulation of the plasminogen activating system. J Thromb Haemost, 5 Suppl 1:132-42.

186. Collen D, Wiman B. (1979) Turnover of antiplasmin, the fast-acting plasmin inhibitor of plasma. Blood, 53(2):313-24.

187. Mast AE, Enghild JJ, Pizzo SV, Salvesen G. (1991) Analysis of the plasma elimination kinetics and conformational stabilities of native, proteinase-complexed, and reactive site cleaved serpins: comparison of alpha 1-proteinase inhibitor, alpha 1-antichymotrypsin, antithrombin III, alpha 2-antiplasmin, angiotensinogen, and ovalbumin. Biochemistry, 30(6):1723-30.

188. Lindahl TL, Ohlsson PI, Wiman B. (1990) The mechanism of the reaction between human plasminogen-activator inhibitor 1 and tissue plasminogen activator. Biochem J, 265(1):109-13.

189. Kimura S, Aoki N. (1986) Cross-linking site in fibrinogen for alpha 2-plasmin inhibitor. J Biol Chem, 261(33):15591-5.

190. Sharp RJ, Perugini MA, Marcovina SM, McCormick SP. (2004) Structural features of apolipoprotein B synthetic peptides that inhibit lipoprotein(a) assembly. J Lipid Res, 45(12):2227-34.

191. Ernst A, Helmhold M, Brunner C, Pethö-Schramm A, Armstrong VW, Müller HJ. (1995) Identification of two functionally distinct lysine-binding sites in kringle

37 and in kringles 32-36 of human apolipoprotein(a). J Biol Chem, 270(11):6227-34.

192. Weisel JW, Nagaswami C, Woodhead JL, Higazi AA, Cain WJ, Marcovina SM, Koschinsky ML, Cines DB, Bdeir K. (2001) The structure of lipoprotein(a) and ligand-induced conformational changes. Biochemistry, 40(35):10424-35.

193. McLean JW, Tomlinson JE, Kuang WJ, Eaton DL, Chen EY, Fless GM, Scanu AM, Lawn RM. (1987) cDNA sequence of human apolipoprotein(a) is homologous to plasminogen. Nature, 330(6144):132-7.

194. Rouy D, Koschinsky ML, Fleury V, Chapman J, Anglés-Cano E. (1992)Apolipoprotein(a) and plasminogen interactions with fibrin: a study with recombinant apolipoprotein(a) and isolated plasminogen fragments. Biochemistry, 31(27):6333-9.

195. Anglés-Cano E, de la Peña Díaz A, Loyau S. (2001) Inhibition of fibrinolysis by lipoprotein(a). Ann N Y Acad Sci, 936:261-75.

196. Sangrar W, Gabel BR, Boffa MB, Walker JB, Hancock MA, Marcovina SM, Horrevoets AJ, Nesheim ME, Koschinsky ML. (1997) The solution phase interaction between apolipoprotein(a) and plasminogen inhibits the binding of plasminogen to a plasmin-modified fibrinogen surface. Biochemistry, 36(34):10353-63.

197. Anglés-Cano E, Rojas G. (2002) Apolipoprotein(a): structure-function relationship at the lysine-binding site and plasminogen activator cleavage site. Biol Chem, 383(1):93-9.

198. Hajjar KA, Gavish D, Breslow JL, Nachman RL. (1989) Lipoprotein(a) modulation of endothelial cell surface fibrinolysis and its potential role in atherosclerosis. Nature, 339(6222):303-5.

199. Ezratty A, Simon DI, Loscalzo J. (1993) Lipoprotein(a) binds to human platelets and attenuates plasminogen binding and activation. Biochemistry, 32(17):4628-33.

200. Miles LA, Fless GM, Scanu AM, Baynham P, Sebald MT, Skocir P, Curtiss LK, Levin EG, Hoover-Plow JL, Plow EF. (1995) Interaction of Lp(a) with plasminogen binding sites on cells. Thromb Haemost, 73(3):458-65.

201. Hancock MA, Boffa MB, Marcovina SM, Nesheim ME, Koschinsky ML. (2003) Inhibition of plasminogen activation by lipoprotein(a): critical domains in

apolipoprotein(a) and mechanism of inhibition on fibrin and degraded fibrin surfaces. J Biol Chem, 278(26):23260-9.

202. Kang C, Dominguez M, Loyau S, Miyata T, Durlach V, Anglés-Cano E. (2002) Lp(a) particles mold fibrin-binding properties of apo(a) in size-dependent manner: a study with different-length recombinant apo(a), native Lp(a), and monoclonal antibody. Arterioscler Thromb Vasc Biol, 22(7):1232-8.

203. Sottrup-Jensen L. (1989) Alpha-macroglobulins: structure, shape, and mechanism of proteinase complex formation. J Biol Chem, 264(20):11539-42.

204. Harpel PC. (1981) Alpha2-plasmin inhibitor and alpha2-macroglobulin-plasmin complexes in plasma. Quantitation by an enzyme-linked differential antibody immunosorbent assay. J Clin Invest, 68(1):46-55.

205. Stephens RW, Tapiovaara H, Reisberg T, Bizik J, Vaheri A. (1991) Alpha 2-macroglobulin restricts plasminogen activation to the surface of RC2A leukemia cells. Cell Regul, 2(12):1057-65.

206. Borth W. (1992) Alpha 2-macroglobulin, a multifunctional binding protein with targeting characteristics. FASEB J, 6(15):3345-53.

207. McBane RD 2nd, Ford MA, Karnicki K, Stewart M, Owen WG. (2000) Fibrinogen, fibrin and crosslinking in aging arterial thrombi. Thromb Haemost, 84(1):83-7.

208. Kunitada S, FitzGerald GA, Fitzgerald DJ. (1992) Inhibition of clot lysis and decreased binding of tissue-type plasminogen activator as a consequence of clot retraction. Blood, 79(6):1420-7.

209. Komorowicz E, Kolev K, Léránt I, Machovich R. (1998) Flow rate-modulated dissolution of fibrin with clot-embedded and circulating proteases. Circ Res, 82(10):1102-8.

210. Wohner N. (2008) Role of cellular elements in thrombus formation and dissolution. Cardiovasc Hematol Agents Med Chem, 6(3):224-8.

211. Váradi B, Kolev K, Tenekedjiev K, Mészáros G, Kovalszky I, Longstaff C, Machovich R. (2004) Phospholipid barrier to fibrinolysis: role for the anionic polar head charge and the gel phase crystalline structure. J Biol Chem, 279(38):39863-71.

212. Monroe DM, Hoffman M, Roberts HR. (2002) Platelets and thrombin generation. Arterioscler Thromb Vasc Biol, 22(9):1381-9.

213. Tanaka K, Onji T, Okamoto K, Matsusaka T, Taniguchi H, Shibata N. (1984) Reorganization of contractile elements in the platelet during clot retraction. J Ultrastruct Res, 89(1):98-109.

214. Kolev K, Tenekedjiev K, Ajtai K, Kovalszky I, Gombas J, Váradi B, Machovich R. (2003) Myosin: a noncovalent stabilizer of fibrin in the process of clot dissolution. Blood, 101(11):4380-6.

215. Machovich R, Ajtai K, Kolev K, Owen WG. (1997) Myosin as cofactor and substrate in fibrinolysis. FEBS Lett, 407(1):93-6.

216. Carvalho FA, Connell S, Miltenberger-Miltenyi G, Pereira SV, Tavares A, Ariëns RA, Santos NC. (2010) Atomic force microscopy-based molecular recognition of a fibrinogen receptor on human erythrocytes. ACS Nano, 4:4609–4620.

217. Wohner N, Sótonyi P, Machovich R, Szabó L, Tenekedjiev K, Silva MM, Longstaff C, Kolev K. (2011) Lytic resistance of fibrin containing red blood cells. Arterioscler Thromb Vasc Biol, 31(10):2306-13.

218. Hawes MC, Curlango-Rivera G, Wen F, White GJ, Vanetten HD, Xiong Z. (2011) Extracellular DNA: the tip of root defenses? Plant Sci, 180(6):741-5.

219. Kaplan MJ, Radic M. (2012) Neutrophil extracellular traps: double-edged swords of innate immunity. J Immunol, 189(6):2689-95.

220. Medina E. (2009) Neutrophil extracellular traps: a strategic tactic to defeat pathogens with potential consequences for the host. J Innate Immun, 1(3):176-80.

221. Borissoff JI, ten Cate H. (2011) From neutrophil extracellular traps release to thrombosis: an overshooting host-defense mechanism? J Thromb Haemost, 9(9):1791-4.

222. Esmon CT. Basic mechanisms and pathogenesis of venous thrombosis. (2009) Blood Rev, 23(5):225-9.

223. Smeeth L, Cook C, Thomas S, Hall AJ, Hubbard R, Vallance P. (2006) Risk of deep vein thrombosis and pulmonary embolism after acute infection in a community setting. Lancet, 367(9516):1075-9.

224. Zawrotniak M, Rapala-Kozik M. (2013) Neutrophil extracellular traps (NETs) - formation and implications. Acta Biochim Pol, 60(3):277-84.

225. Goldmann O, Medina E. (2012) The expanding world of extracellular traps: not only neutrophils but much more. Front Immunol, 3:420.

226. Drescher B, Bai F. (2013) Neutrophil in viral infections, friend or foe? Virus Res, 171(1):1-7.

227. Itakura A, McCarty OJ. (2013) Pivotal role for the mTOR pathway in the formation of neutrophil extracellular traps via regulation of autophagy. Am J Physiol Cell Physiol, 305(3):C348-54.

228. Darrah E, Andrade F. (2012) NETs: the missing link between cell death and systemic autoimmune diseases? Front Immunol.3:428.

229. Brinkmann V, Zychlinsky A. (2012) Neutrophil extracellular traps: is immunity the second function of chromatin? J Cell Biol, 198(5):773-83.

230. Fuchs TA, Abed U, Goosmann C, Hurwitz R, Schulze I, Wahn V, Weinrauch Y, Brinkmann V, Zychlinsky A. (2007) Novel cell death program leads to neutrophil extracellular traps. J Cell Biol, 176(2):231-41.

231. Brinkmann V, Zychlinsky A. (2007) Beneficial suicide: why neutrophils die to make NETs. Nat Rev Microbiol, 5(8):577-82.

232. Yipp BG, Kubes P. (2013) NETosis: how vital is it? Blood, 122(16):2784-94.

233. Pilsczek FH, Salina D, Poon KK, Fahey C, Yipp BG, Sibley CD, Robbins SM, Green FH, Surette MG, Sugai M, Bowden MG, Hussain M, Zhang K, Kubes P. (2010) A novel mechanism of rapid nuclear neutrophil extracellular trap formation in response to Staphylococcus aureus. J Immunol, 185(12):7413-25.

234. Clark SR, Ma AC, Tavener SA, McDonald B, Goodarzi Z, Kelly MM, Patel KD, Chakrabarti S, McAvoy E, Sinclair GD, Keys EM, Allen-Vercoe E, Devinney R, Doig CJ, Green FH, Kubes P. (2007) Platelet TLR4 activates neutrophil extracellular traps to ensnare bacteria in septic blood. Nat Med, 13(4):463-9.

235. Yipp BG, Petri B, Salina D, Jenne CN, Scott BN, Zbytnuik LD, Pittman K, Asaduzzaman M, Wu K, Meijndert HC, Malawista SE, de Boisfleury Chevance A, Zhang K, Conly J, Kubes P. (2012) Infection-induced NETosis is a dynamic process involving neutrophil multitasking in vivo. Nat Med, 18(9):1386-93.

236. Palmer LJ, Cooper PR, Ling MR, Wright HJ, Huissoon A, Chapple IL. (2012) Hypochlorous acid regulates neutrophil extracellular trap release in humans. Clin Exp Immunol, 167(2):261-8.

237. Yousefi S, Gold JA, Andina N, Lee JJ, Kelly AM, Kozlowski E, Schmid I, Straumann A, Reichenbach J, Gleich GJ, Simon HU. (2008) Catapult-like release of mitochondrial DNA by eosinophils contributes to antibacterial defense. Nat Med, 14(9):949-53.

238. Yousefi S, Mihalache C, Kozlowski E, Schmid I, Simon HU. (2009) Viable neutrophils release mitochondrial DNA to form neutrophil extracellular traps. Cell Death Differ, 16(11):1438-44.

239. Krautgartner WD, Klappacher M, Hannig M, Obermayer A, Hartl D, Marcos V, Vitkov L. (2010) Fibrin mimics neutrophil extracellular traps in SEM. Ultrastruct Pathol, 34(4):226-31.

240. Cooper PR, Palmer LJ, Chapple IL. (2013) Neutrophil extracellular traps as a new paradigm in innate immunity: friend or foe? Periodontol 2000, 63(1):165-97.

241. Menegazzi R, Decleva E, Dri P. (2012) Killing by neutrophil extracellular traps: fact or folklore? Blood, 119(5):1214-6.

242. Urban CF, Ermert D, Schmid M, Abu-Abed U, Goosmann C, Nacken W, Brinkmann V, Jungblut PR, Zychlinsky A. (2009) Neutrophil extracellular traps contain calprotectin, a cytosolic protein complex involved in host defense against Candida albicans. PLoS Pathog, 5(10):e1000639.

243. Cho JH, Fraser IP, Fukase K, Kusumoto S, Fujimoto Y, Stahl GL, Ezekowitz RA. (2005) Human peptidoglycan recognition protein S is an effector of neutrophil-mediated innate immunity. Blood, 106(7):2551-8.

244. Wartha F, Beiter K, Normark S, Henriques-Normark B. (2007) Neutrophil extracellular traps: casting the NET over pathogenesis. Curr Opin Microbiol, 10(1):52-6.

245. Lögters T, Margraf S, Altrichter J, Cinatl J, Mitzner S, Windolf J, Scholz M. (2009)The clinical value of neutrophil extracellular traps. Med Microbiol Immunol, 198(4):211-9.

246. O'Donoghue AJ, Jin Y, Knudsen GM, Perera NC, Jenne DE, Murphy JE, Craik CS, Hermiston TW. (2013) Global substrate profiling of proteases in human neutrophil extracellular traps reveals consensus motif predominantly contributed by elastase. PLoS One, 8(9):e75141.

247. Cho JH, Sung BH, Kim SC. (2009) Buforins: histone H2A-derived antimicrobial peptides from toad stomach. Biochim Biophys Acta, 1788(8):1564-9.

248. Méndez-Samperio P. (2010) The human cathelicidin hCAP18/LL-37: a multifunctional peptide involved in mycobacterial infections. Peptides, 31(9):1791-8.

249. Bianchi M, Niemiec MJ, Siler U, Urban CF, Reichenbach J. (2011) Restoration of anti-Aspergillus defense by neutrophil extracellular traps in human chronic granulomatous disease after gene therapy is calprotectin-dependent. J Allergy Clin Immunol, 127(5):1243-52.e7.

250. Remijsen Q, Kuijpers TW, Wirawan E, Lippens S, Vandenabeele P, Vanden Berghe T. (2011) Dying for a cause: NETosis, mechanisms behind an antimicrobial cell death modality. Cell Death Differ, 18(4):581-8.

251. Way KJ, Chou E, King GL. (2000) Identification of PKC-isoform-specific biological actions using pharmacological approaches. Trends Pharmacol Sci, 21(5):181-7.

252. Balasubramanian N, Advani SH, Zingde SM. (2002) Protein kinase C isoforms in normal and leukemic neutrophils: altered levels in leukemic neutrophils and changes during myeloid maturation in chronic myeloid leukemia. Leuk Res, 26(1):67-81.

253. Gray RD, Lucas CD, Mackellar A, Li F, Hiersemenzel K, Haslett C, Davidson DJ, Rossi AG. (2013) Activation of conventional protein kinase C (PKC) is critical in the generation of human neutrophil extracellular traps. J Inflamm (Lond), 10(1):12.

254. Neeli I, Radic M. (2013) Opposition between PKC isoforms regulates histone deimination and neutrophil extracellular chromatin release. Front Immunol.4:38.

255. Hakkim A, Fuchs TA, Martinez NE, Hess S, Prinz H, Zychlinsky A, Waldmann H. (2011) Activation of the Raf-MEK-ERK pathway is required for neutrophil extracellular trap formation. Nat Chem Biol, 7(2):75-7.

256. Raad H, Paclet MH, Boussetta T, Kroviarski Y, Morel F, Quinn MT, Gougerot-Pocidalo MA, Dang PM, El-Benna J. (2009) Regulation of the phagocyte NADPH oxidase activity: phosphorylation of gp91phox/NOX2 by protein kinase C enhances

its diaphorase activity and binding to Rac2, p67phox, and p47phox. FASEB J, 23(4):1011-22.

257. El Benna J, Han J, Park JW, Schmid E, Ulevitch RJ, Babior BM. (1996) Activation of p38 in stimulated human neutrophils: phosphorylation of the oxidase component p47phox by p38 and ERK but not by JNK. Arch Biochem Biophys, 334(2):395-400.

258. Keshari RS, Verma A, Barthwal MK, Dikshit M. (2013) Reactive oxygen species-induced activation of ERK and p38 MAPK mediates PMA-induced NETs release from human neutrophils. J Cell Biochem, 114(3):532-40.

259. Lim MB, Kuiper JW, Katchky A, Goldberg H, Glogauer M. (2011) Rac2 is required for the formation of neutrophil extracellular traps. J Leukoc Biol, 90(4):771-6.

260. McInturff AM, Cody MJ, Elliott EA, Glenn JW, Rowley JW, Rondina MT, Yost CC. (2012) Mammalian target of rapamycin regulates neutrophil extracellular trap formation via induction of hypoxia-inducible factor 1 α. Blood, 120(15):3118-25.

261. Marcos V, Zhou Z, Yildirim AO, Bohla A, Hector A, Vitkov L, Wiedenbauer EM, Krautgartner WD, Stoiber W, Belohradsky BH, Rieber N, Kormann M, Koller B, Roscher A, Roos D, Griese M, Eickelberg O, Döring G, Mall MA, Hartl D. (2010) CXCR2 mediates NADPH oxidase-independent neutrophil extracellular trap formation in cystic fibrosis airway inflammation. Nat Med, 16(9):1018-23.

262. Neeli I, Dwivedi N, Khan S, Radic M. (2009) Regulation of extracellular chromatin release from neutrophils. J Innate Immun, 1(3):194-201.

263. Almyroudis NG, Grimm MJ, Davidson BA, Röhm M, Urban CF, Segal BH. (2013) NETosis and NADPH oxidase: at the intersection of host defense, inflammation, and injury. Front Immunol, 4:45.

264. Parker H, Winterbourn CC. (2012) Reactive oxidants and myeloperoxidase and their involvement in neutrophil extracellular traps. Front Immunol, 3:424.

265. Metzler KD, Fuchs TA, Nauseef WM, Reumaux D, Roesler J, Schulze I, Wahn V, Papayannopoulos V, Zychlinsky A. (2011) Myeloperoxidase is required for neutrophil extracellular trap formation: implications for innate immunity. Blood, 117(3):953-9.

266. Papayannopoulos V, Metzler KD, Hakkim A, Zychlinsky A. (2010) Neutrophil elastase and myeloperoxidase regulate the formation of neutrophil extracellular traps. J Cell Biol, 191(3):677-91.

267. Fadeel B, Ahlin A, Henter JI, Orrenius S, Hampton MB. (1998) Involvement of caspases in neutrophil apoptosis: regulation by reactive oxygen species. Blood, 92(12):4808-18.

268. Hampton MB, Stamenkovic I, Winterbourn CC. (2002) Interaction with substrate sensitises caspase-3 to inactivation by hydrogen peroxide. FEBS Lett, 517(1-3):229-32.

269. Wilkie RP, Vissers MC, Dragunow M, Hampton MB. (2007) A functional NADPH oxidase prevents caspase involvement in the clearance of phagocytic neutrophils. Infect Immun, 75(7):3256-63.

270. Sadikot RT, Zeng H, Yull FE, Li B, Cheng DS, Kernodle DS, Jansen ED, Contag CH, Segal BH, Holland SM, Blackwell TS, Christman JW. (2004) p47phox deficiency impairs NF-kappa B activation and host defense in Pseudomonas pneumonia. J Immunol, 172(3):1801-8.

271. Anzilotti C, Pratesi F, Tommasi C, Migliorini P. (2010) Peptidylarginine deiminase 4 and citrullination in health and disease. Autoimmun Rev, 9(3):158-60.

272. Li P, Li M, Lindberg MR, Kennett MJ, Xiong N, Wang Y. PAD4 is essential for antibacterial innate immunity mediated by neutrophil extracellular traps. J Exp Med. 2010;207(9):1853-62.

273. Leshner M, Wang S, Lewis C, Zheng H, Chen XA, Santy L, Wang Y. (2012) PAD4 mediated histone hypercitrullination induces heterochromatin decondensation and chromatin unfolding to form neutrophil extracellular trap-like structures. Front Immunol, 3:307.

274. Arita K, Hashimoto H, Shimizu T, Nakashima K, Yamada M, Sato M. (2004) Structural basis for Ca(2+)-induced activation of human PAD4. Nat Struct Mol Biol, 11(8):777-83.

275. Liu YL, Chiang YH, Liu GY, Hung HC. (2011) Functional role of dimerization of human peptidylarginine deiminase 4 (PAD4). PLoS One, 6(6):e21314.

276. Nakashima K, Hagiwara T, Yamada M. (2002) Nuclear localization of peptidylarginine deiminase V and histone deimination in granulocytes. J Biol Chem, 277(51):49562-8.

277. Vossenaar ER, Zendman AJ, van Venrooij WJ, Pruijn GJ. (2003) PAD, a growing family of citrullinating enzymes: genes, features and involvement in disease. Bioessays, 25(11):1106-18.

278. Zhang X, Bolt M, Guertin MJ, Chen W, Zhang S, Cherrington BD, Slade DJ, Dreyton CJ, Subramanian V, Bicker KL, Thompson PR, Mancini MA, Lis JT, Coonrod SA. (2012) Peptidylarginine deiminase 2-catalyzed histone H3 arginine 26 citrullination facilitates estrogen receptor α target gene activation. Proc Natl Acad Sci USA, 109(33):13331-6.

279. Rohrbach AS, Slade DJ, Thompson PR, Mowen KA. (2012) Activation of PAD4 in NET formation. Front Immunol, 3:360.

280. Andrade F, Darrah E, Gucek M, Cole RN, Rosen A, Zhu X. (2010) Autocitrullination of human peptidyl arginine deiminase type 4 regulates protein citrullination during cell activation. Arthritis Rheum, 62(6):1630-40.

281. Méchin MC, Coudane F, Adoue V, Arnaud J, Duplan H, Charveron M, Schmitt AM, Takahara H, Serre G, Simon M. (2010) Deimination is regulated at multiple levels including auto-deimination of peptidylarginine deiminases. Cell Mol Life Sci, 67(9):1491-503.

282. Wang Y, Li M, Stadler S, Correll S, Li P, Wang D, Hayama R, Leonelli L, Han H, Grigoryev SA, Allis CD, Coonrod SA. (2009) Histone hypercitrullination mediates chromatin decondensation and neutrophil extracellular trap formation. J Cell Biol, 184(2):205-13.

283. Neeli I, Khan SN, Radic M. (2008) Histone deimination as a response to inflammatory stimuli in neutrophils. J Immunol, 180(3):1895-902.

284. Wang Y, Wysocka J, Sayegh J, Lee YH, Perlin JR, Leonelli L, Sonbuchner LS, McDonald CH, Cook RG, Dou Y, Roeder RG, Clarke S, Stallcup MR, Allis CD, Coonrod SA. (2004) Human PAD4 regulates histone arginine methylation levels via demethylimination. Science, 306(5694):279-83.

285. Serafin WE, Katz HR, Austen KF, Stevens RL. (1986) Complexes of heparin proteoglycans, chondroitin sulfate E proteoglycans, and [3H]diisopropyl

fluorophosphate-binding proteins are exocytosed from activated mouse bone marrow-derived mast cells. J Biol Chem, 261(32):15017-21.

286. Kolset SO, Gallagher JT. (1990) Proteoglycans in haemopoietic cells. Biochim Biophys Acta, 1032(2-3):191-211.

287. Reeves EP, Lu H, Jacobs HL, Messina CG, Bolsover S, Gabella G, Potma EO, Warley A, Roes J, Segal AW. (2002) Killing activity of neutrophils is mediated through activation of proteases by K+ flux. Nature, 416(6878):291-7.

288. Farley K, Stolley JM, Zhao P, Cooley J, Remold-O'Donnell E. (2012) A serpinB1 regulatory mechanism is essential for restricting neutrophil extracellular trap generation. J Immunol, 189(9):4574-81.

289. Remijsen Q, Vanden Berghe T, Wirawan E, Asselbergh B, Parthoens E, De Rycke R, Noppen S, Delforge M, Willems J, Vandenabeele P. (2011) Neutrophil extracellular trap cell death requires both autophagy and superoxide generation. Cell Res, 21(2):290-304.

290. Fuchs TA, Brill A, Wagner DD. (2012) Neutrophil extracellular trap (NET) impact on deep vein thrombosis. Arterioscler Thromb Vasc Biol, 32(8):1777-83.

291. Darbousset R, Thomas GM, Mezouar S, Frère C, Bonier R, Mackman N, Renné T, Dignat-George F, Dubois C, Panicot-Dubois L. (2012) Tissue factor-positive neutrophils bind to injured endothelial wall and initiate thrombus formation. Blood, 120(10):2133-43.

292. Steinman CR. (1975) Free DNA in serum and plasma from normal adults. J Clin Invest, 56(2):512-5.

293. Leon SA, Shapiro B, Sklaroff DM, Yaros MJ. (1977) Free DNA in the serum of cancer patients and the effect of therapy. Cancer Res, 37(3):646-50.

294. Saha P, Humphries J, Modarai B, Mattock K, Waltham M, Evans CE, Ahmad A, Patel AS, Premaratne S, Lyons OT, Smith A. (2011) Leukocytes and the natural history of deep vein thrombosis: current concepts and future directions. Arterioscler Thromb Vasc Biol, 31(3):506-12.

295. Fuchs TA, Brill A, Duerschmied D, Schatzberg D, Monestier M, Myers DD Jr, Wrobleski SK, Wakefield TW, Hartwig JH, Wagner DD. (2010) Extracellular DNA traps promote thrombosis. Proc Natl Acad Sci USA, 107(36):15880-5.

296. Xu J, Zhang X, Pelayo R, Monestier M, Ammollo CT, Semeraro F, Taylor FB, Esmon NL, Lupu F, Esmon CT. (2009) Extracellular histones are major mediators of death in sepsis. Nat Med, 15(11):1318-21.

297. Gupta AK, Joshi MB, Philippova M, Erne P, Hasler P, Hahn S, Resink TJ. (2010) Activated endothelial cells induce neutrophil extracellular traps and are susceptible to NETosis-mediated cell death. FEBS Lett, 584(14):3193-7.

298. Saffarzadeh M, Juenemann C, Queisser MA, Lochnit G, Barreto G, Galuska SP, Lohmeyer J, Preissner KT. (2012) Neutrophil extracellular traps directly induce epithelial and endothelial cell death: a predominant role of histones. PLoS One, 7(2):e32366.

299. Villanueva E, Yalavarthi S, Berthier CC, Hodgin JB, Khandpur R, Lin AM, Rubin CJ, Zhao W, Olsen SH, Klinker M, Shealy D, Denny MF, Plumas J, Chaperot L, Kretzler M, Bruce AT, Kaplan MJ. (2011) Netting neutrophils induce endothelial damage, infiltrate tissues, and expose immunostimulatory molecules in systemic lupus erythematosus. J Immunol, 187(1):538-52.

300. Okrent DG, Lichtenstein AK, Ganz T. (1990) Direct cytotoxicity of polymorphonuclear leukocyte granule proteins to human lung-derived cells and endothelial cells. Am Rev Respir Dis, 141(1):179-85.

301. Pereira LF, Marco FM, Boimorto R, Caturla A, Bustos A, De la Concha EG, Subiza JL. (1994) Histones interact with anionic phospholipids with high avidity; its relevance for the binding of histone-antihistone immune complexes. Clin Exp Immunol, 97(2):175-80.

302. Kleine TJ, Gladfelter A, Lewis PN, Lewis SA. (1995) Histone-induced damage of a mammalian epithelium: the conductive effect. Am J Physiol, 268(5 Pt 1):C1114-25.

303. Brill A, Fuchs TA, Savchenko AS, Thomas GM, Martinod K, De Meyer SF, Bhandari AA, Wagner DD. (2012) Neutrophil extracellular traps promote deep vein thrombosis in mice. J Thromb Haemost, 10(1):136-44.

304. Wohner N, Keresztes Z, Sótonyi P, Szabó L, Komorowicz E, Machovich R, Kolev K. (2010) Neutrophil granulocyte-dependent proteolysis enhances platelet adhesion to the arterial wall under high-shear flow. J Thromb Haemost, 8(7):1624-31.

305. Drechsler M, Megens RT, van Zandvoort M, Weber C, Soehnlein O. (2010) Hyperlipidemia-triggered neutrophilia promotes early atherosclerosis. Circulation, 122(18):1837-45.

306. Megens RT, Vijayan S, Lievens D, Döring Y, van Zandvoort MA, Grommes J, Weber C, Soehnlein O. (2012) Presence of luminal neutrophil extracellular traps in atherosclerosis. Thromb Haemost, 107(3):597-8.

307. Fuchs TA, Bhandari AA, Wagner DD. (2011) Histones induce rapid and profound thrombocytopenia in mice. Blood, 118(13):3708-14.

308. Watson K, Gooderham NJ, Davies DS, Edwards RJ. (1999) Nucleosomes bind to cell surface proteoglycans. J Biol Chem, 274(31):21707-13.

309. Semeraro F, Ammollo CT, Morrissey JH, Dale GL, Friese P, Esmon NL, Esmon CT. (2011) Extracellular histones promote thrombin generation through platelet-dependent mechanisms: involvement of platelet TLR2 and TLR4. Blood, 118(7):1952-61.

310. Clejan L, Menahem H. (1977) Binding of deoxyribonucleic acid to the surface of human platelets. Acta Haematol, 58(2):84-8.

311. Dorsch CA. (1981) Binding of single-strand DNA to human platelets. Thromb Res, 24(1-2):119-29.

312. Ward CM, Tetaz TJ, Andrews RK, Berndt MC. (1997) Binding of the von Willebrand factor A1 domain to histone. Thromb Res, 86(6):469-77.

313. Kleine TJ, Lewis PN, Lewis SA. (1997) Histone-induced damage of a mammalian epithelium: the role of protein and membrane structure. Am J Physiol, 273(6 Pt 1):C1925-36.

314. Gamberucci A, Fulceri R, Marcolongo P, Pralong WF, Benedetti A. (1998) Histones and basic polypeptides activate Ca2+/cation influx in various cell types. Biochem J, 331 (Pt 2):623-30.

315. Crittenden JR, Bergmeier W, Zhang Y, Piffath CL, Liang Y, Wagner DD, Housman DE, Graybiel AM. (2004) CalDAG-GEFI integrates signaling for platelet aggregation and thrombus formation. Nat Med, 10(9):982-6.

316. Carestia A, Rivadeneyra L, Romaniuk MA, Fondevila C, Negrotto S, Schattner M. (2013) Functional responses and molecular mechanisms involved in histone-mediated platelet activation. Thromb Haemost, 110(5):1035-45.

317. Renesto P, Chignard M. (1993) Enhancement of cathepsin G-induced platelet activation by leukocyte elastase: consequence for the neutrophil-mediated platelet activation. Blood, 82(1):139-44.

318. Si-Tahar M, Pidard D, Balloy V, Moniatte M, Kieffer N, Van Dorsselaer A, Chignard M. (1997) Human neutrophil elastase proteolytically activates the platelet integrin alphaIIbbeta3 through cleavage of the carboxyl terminus of the alphaIIb subunit heavy chain. Involvement in the potentiation of platelet aggregation. J Biol Chem, 272(17):11636-47.

319. Wohner N, Kovács A, Machovich R, Kolev K. (2012) Modulation of the von Willebrand factor-dependent platelet adhesion through alternative proteolytic pathways. Thromb Res, 129(4):e41-6.

320. de Boer OJ, Li X, Teeling P, Mackaay C, Ploegmakers HJ, van der Loos CM, Daemen MJ, de Winter RJ, van der Wal AC. (2013) Neutrophils, neutrophil extracellular traps and interleukin-17 associate with the organisation of thrombi in acute myocardial infarction. Thromb Haemost, 109(2):290-7.

321. Duerschmied D, Suidan GL, Demers M, Herr N, Carbo C, Brill A, Cifuni SM, Mauler M, Cicko S, Bader M, Idzko M, Bode C, Wagner DD. (2013) Platelet serotonin promotes the recruitment of neutrophils to sites of acute inflammation in mice. Blood, 121(6):1008-15.

322. Marcus AJ, Silk ST, Safier LB, Ullman HL. (1977) Superoxide production and reducing activity in human platelets. J Clin Invest, 59(1):149-58.

323. Kraemer BF, Campbell RA, Schwertz H, Cody MJ, Franks Z, Tolley ND, Kahr WH, Lindemann S, Seizer P, Yost CC, Zimmerman GA, Weyrich AS. (2011) Novel anti-bacterial activities of β-defensin 1 in human platelets: suppression of pathogen growth and signaling of neutrophil extracellular trap formation. PLoS Pathog, 7(11):e1002355.

324. Nishinaka Y, Arai T, Adachi S, Takaori-Kondo A, Yamashita K. (2011) Singlet oxygen is essential for neutrophil extracellular trap formation. Biochem Biophys Res Commun, 413(1):75-9.

325. Massberg S, Grahl L, von Bruehl ML, Manukyan D, Pfeiler S, Goosmann C, Brinkmann V, Lorenz M, Bidzhekov K, Khandagale AB, Konrad I, Kennerknecht E, Reges K, Holdenrieder S, Braun S, Reinhardt C, Spannagl M, Preissner KT,

Engelmann B. (2010) Reciprocal coupling of coagulation and innate immunity via neutrophil serine proteases. Nat Med, 16(8):887-96.

326. Thomas GM, Carbo C, Curtis BR, Martinod K, Mazo IB, Schatzberg D, Cifuni SM, Fuchs TA, von Andrian UH, Hartwig JH, Aster RH, Wagner DD. (2012) Extracellular DNA traps are associated with the pathogenesis of TRALI in humans and mice. Blood, 119(26):6335-43.

327. Caudrillier A, Kessenbrock K, Gilliss BM, Nguyen JX, Marques MB, Monestier M, Toy P, Werb Z, Looney MR. (2012) Platelets induce neutrophil extracellular traps in transfusion-related acute lung injury. J Clin Invest, 122(7):2661-71.

328. Fuchs TA, Kremer Hovinga JA, Schatzberg D, Wagner DD, Lämmle B. (2012) Circulating DNA and myeloperoxidase indicate disease activity in patients with thrombotic microangiopathies. Blood, 120(6):1157-64.

329. Gardiner EE, Andrews RK. (2012) Neutrophil extracellular traps (NETs) and infection-related vascular dysfunction. Blood Rev, 26(6):255-9.

330. Andrews DA, Low PS. (1999) Role of red blood cells in thrombosis. Curr Opin Hematol, 6(2):76-82.

331. Laktionov PP, Tamkovich SN, Rykova EY, Bryzgunova OE, Starikov AV, Kuznetsova NP, Vlassov VV. (2004) Cell-surface-bound nucleic acids: Free and cell-surface-bound nucleic acids in blood of healthy donors and breast cancer patients. Ann N Y Acad Sci, 1022:221-7.

332. Goel MS, Diamond SL. (2002) Adhesion of normal erythrocytes at depressed venous shear rates to activated neutrophils, activated platelets, and fibrin polymerized from plasma. Blood, 100(10):3797-803.

333. von Brühl ML, Stark K, Steinhart A, Chandraratne S, Konrad I, Lorenz M, Khandoga A, Tirniceriu A, Coletti R, Köllnberger M, Byrne RA, Laitinen I, Walch A, Brill A, Pfeiler S, Manukyan D, Braun S, Lange P, Riegger J, Ware J, Eckart A, Haidari S, Rudelius M, Schulz C, Echtler K, Brinkmann V, Schwaiger M, Preissner KT, Wagner DD, Mackman N, Engelmann B, Massberg S. (2012) Monocytes, neutrophils, and platelets cooperate to initiate and propagate venous thrombosis in mice in vivo. J Exp Med, 209(4):819-35.

334. Higuchi DA, Wun TC, Likert KM, Broze GJ Jr. (1992) The effect of leukocyte elastase on tissue factor pathway inhibitor. Blood, 79(7):1712-9.

335. Kambas K, Mitroulis I, Apostolidou E, Girod A, Chrysanthopoulou A, Pneumatikos I, Skendros P, Kourtzelis I, Koffa M, Kotsianidis I, Ritis K. (2012) Autophagy mediates the delivery of thrombogenic tissue factor to neutrophil extracellular traps in human sepsis. PLoS One, 7(9):e45427.

336. Maugeri N, Brambilla M, Camera M, Carbone A, Tremoli E, Donati MB, de Gaetano G, Cerletti C. (2006) Human polymorphonuclear leukocytes produce and express functional tissue factor upon stimulation. J Thromb Haemost, 4(6):1323-30.

337. Müller I, Klocke A, Alex M, Kotzsch M, Luther T, Morgenstern E, Zieseniss S, Zahler S, Preissner K, Engelmann B. (2003) Intravascular tissue factor initiates coagulation via circulating microvesicles and platelets. FASEB J, 17(3):476-8.

338. Zillmann A, Luther T, Müller I, Kotzsch M, Spannagl M, Kauke T, Oelschlägel U, Zahler S, Engelmann B. (2001) Platelet-associated tissue factor contributes to the collagen-triggered activation of blood coagulation. Biochem Biophys Res Commun, 281(2):603-9.

339. Engelmann B, Massberg S. (2013) Thrombosis as an intravascular effector of innate immunity. Nat Rev Immunol, 13(1):34-45.

340. Kannemeier C, Shibamiya A, Nakazawa F, Trusheim H, Ruppert C, Markart P, Song Y, Tzima E, Kennerknecht E, Niepmann M, von Bruehl ML, Sedding D, Massberg S, Günther A, Engelmann B, Preissner KT. (2007) Extracellular RNA constitutes a natural procoagulant cofactor in blood coagulation. Proc Natl Acad Sci U S A, 104(15):6388-93.

341. Müller F, Mutch NJ, Schenk WA, Smith SA, Esterl L, Spronk HM, Schmidbauer S, Gahl WA, Morrissey JH, Renné T. (2009) Platelet polyphosphates are proinflammatory and procoagulant mediators in vivo. Cell, 139(6):1143-56.

342. Martinod K, Demers M, Fuchs TA, Wong SL, Brill A, Gallant M, Hu J, Wang Y, Wagner DD. (2013) Neutrophil histone modification by peptidylarginine deiminase 4 is critical for deep vein thrombosis in mice. Proc Natl Acad Sci USA, 110(21):8674-9.

343. Chang X, Yamada R, Sawada T, Suzuki A, Kochi Y, Yamamoto K. (2005) The inhibition of antithrombin by peptidylarginine deiminase 4 may contribute to pathogenesis of rheumatoid arthritis. Rheumatology (Oxford), 44(3):293-8.

344. Pemberton AD, Brown JK, Inglis NF. (2010) Proteomic identification of interactions between histones and plasma proteins: implications for cytoprotection. Proteomics, 10(7):1484-93.

345. Giannitsis DJ, St Pekker. (1974) Role of leukocyte nuclei in blood coagulation. Naturwissenschaften, 61(12):690.

346. Kheiri SA, Fasy TM, Billett HH. (1996) Effects of H1 histones and a monoclonal autoantibody to H1 histones on clot formation in vitro: possible implications in the antiphospholipid syndrome. Thromb Res, 82(1):43-50.

347. Ammollo CT, Semeraro F, Xu J, Esmon NL, Esmon CT. (2011) Extracellular histones increase plasma thrombin generation by impairing thrombomodulin-dependent protein C activation. J Thromb Haemost, 9(9):1795-803.

348. Takano S, Kimura S, Ohdama S, Aoki N. (1990) Plasma thrombomodulin in health and diseases. Blood, 76(10):2024-9.

349. Glaser CB, Morser J, Clarke JH, Blasko E, McLean K, Kuhn I, Chang RJ, Lin JH, Vilander L, Andrews WH, Light DR. (1992) Oxidation of a specific methionine inthrombomodulin by activated neutrophil products blocks cofactor activity. A potential rapid mechanism for modulation of coagulation. J Clin Invest, 90(6):2565-73.

350. Plow EF. (1980) The major fibrinolytic proteases of human leukocytes. Biochim Biophys Acta, 630(1):47-56.

351. Zeng B, Bruce D, Kril J, Ploplis V, Freedman B, Brieger D. (2002) Influence of plasminogen deficiency on the contribution of polymorphonuclear leucocytes to fibrin/ogenolysis: studies in plasminogen knock-out mice. Thromb Haemost, 88(5):805-10.

352. Kolev K, Machovich R. (2003) Molecular and cellular modulation of fibrinolysis. Thromb Haemost, 89(4):610-21.

353. Das R, Burke T, Plow EF. (2007) Histone H2B as a functionally important plasminogen receptor on macrophages. Blood, 110(10):3763-72.

354. Kolev K, Tenekedjiev K, Komorowicz E, Machovich R. (1997) Functional evaluation of the structural features of proteases and their substrate in fibrin surface degradation. J Biol Chem, 272(21):13666-75.

355. Machovich R, Owen WG. (1989) An elastase-dependent pathway of plasminogen activation. Biochemistry, 28(10):4517-22.

356. Masson-Bessière C, Sebbag M, Girbal-Neuhauser E, Nogueira L, Vincent C, Senshu T, Serre G. (2001) The major synovial targets of the rheumatoid arthritis-specific antifilaggrin autoantibodies are deiminated forms of the alpha- and beta-chains of fibrin. J Immunol, 166(6):4177-84.

357. Sanchez-Pernaute O, Filkova M, Gabucio A, Klein M, Maciejewska-Rodrigues H, Ospelt C, Brentano F, Michel BA, Gay RE, Herrero-Beaumont G, Gay S, Neidhart M, Juengel A. (2013) Citrullination enhances the pro-inflammatory response to fibrin inrheumatoid arthritis synovial fibroblasts. Ann Rheum Dis, 72(8):1400-6.

358. Lacks SA. (1981) Deoxyribonuclease I in mammalian tissues. Specificity of inhibition by actin. J Biol Chem, 256(6):2644-8.

359. Napirei M, Ricken A, Eulitz D, Knoop H, Mannherz HG. (2004) Expression pattern of the deoxyribonuclease 1 gene: lessons from the Dnase1 knockout mouse. Biochem J, 380(Pt 3):929-37.

360. Takeshita H, Yasuda T, Nakajima T, Hosomi O, Nakashima Y, Kishi K. (1997) Mouse deoxyribonuclease I (DNase I): biochemical and immunological characterization, cDNA structure and tissue distribution. Biochem Mol Biol Int, 42(1):65-75.

361. Shiokawa D, Tanuma S. (2001) Characterization of human DNase I family endonucleases and activation of DNase gamma during apoptosis. Biochemistry, 40(1):143-52.

362. Napirei M, Ludwig S, Mezrhab J, Klöckl T, Mannherz HG. (2009) Murine serum nucleases--contrasting effects of plasmin and heparin on the activities of DNase1 and DNase1-like 3 (DNase1l3). FEBS J, 276(4):1059-73.

363. Farrera C, Fadeel B. (2013) Macrophage clearance of neutrophil extracellular traps is a silent process. J Immunol, 191(5):2647-56.

364. Napirei M, Wulf S, Mannherz HG. (2004) Chromatin breakdown during necrosis by serum Dnase1 and the plasminogen system. Arthritis Rheum, 50(6):1873-83.

365. Harvima RJ, Yabe K, Fräki JE, Fukuyama K, Epstein WL. (1988) Hydrolysis of histones by proteinases. Biochem J, 250(3):859-64.

366. Esmon CT. (2013) Molecular circuits in thrombosis and inflammation. Thromb Haemost, 109(3):416-20.

367. Papayannopoulos V, Zychlinsky A. (2009) NETs: a new strategy for using old weapons. Trends Immunol, 30(11):513-21.

368. Lundblad RL, Kingdon HS, Mann KG. (1976) Thrombin. Meth Enzymol, 45: 156–76.

369. Deutsch D, Mertz E. (1970) Plasminogen: purification from human plasma by affinity chromatography. Science, 170(3962):1095–6

370. Chase T, Shaw E. (1970) Titration of trypsin, plasmin, and thrombin with p-nitrophenyl p′-guanidinobenzoate HCl. Methods Enzymol, 19,20-27

371. Komorowicz E, Kolev K, Machovich R. (1998) Fibrinolysis with des-kringle derivatives of plasmin and its modulation by plasma protease inhibitors. Biochemistry, 37(25):9112-8.

372. Rácz Z, Baróti C. (1993) Technical aspects of buffy coat removal from whole blood and those of platelet production from single buffy coat units. Biomed Tech (Berl), 38(11):266-9.

373. Thelwell C, Longstaff C. (2007) The regulation by fibrinogen and fibrin of tissue plasminogen activator kinetics and inhibition by plasminogen activator inhibitor 1. J Thromb Haemost, 5: 804–11.

374. Longstaff C, Thelwell C, Williams S, Silva MMCG, Szabó L, Kolev K. (2011) The interplay between tissue plasminogen activator domains and fibrin structures in the regulation of fibrinolysis: kinetic and microscopic studies. Blood, 117: 661–8.

375. Gonzales RC, Woods RE, Eddins SL. (2009) Digital Image Processing with Matlab, 2nd edn. Gatesmark Publishing, http://www.gatesmark.com 535–96.

376. Rånby M. (1982) Studies on the kinetics of plasminogen activation by tissue plasminogen activator. Biochim Biophys Acta, 704(3):461-9

377. Tanka-Salamon A, Tenekedjiev K, Machovich R, Kolev K. (2008) Suppressed catalytic efficiency of plasmin in the presence of long-chain fatty acids: Identification of kinetic parameters from continuous enzymatic assay with Monte Carlo simulation. FEBS J, 275(6):1274–82.

378. Longstaff C, Whitton CM. (2004) A proposed reference method for plasminogen activators that enables calculation of enzyme activities in SI units. J Thromb Haemost, 2(8):1416–21.

379. Kolev K, Léránt I, Tenekedjiev K, Machovich R. (1994) Regulation of fibrinolytic activity of neutrophil leukocyte elastase, plasmin, and miniplasmin by plasmaprotease inhibitors. J Biol Chem, 269: 17030–4.

380. Nikolova ND, Toneva DS, Tenekedjieva AMK. (2009) Statistical procedures for finding distribution fits over datasets with applications in biochemistry. Bioautomation, 13:27-44.

381. Ferry JD, Morrison PR. (1947) Preparation and properties of serum and plasma proteins; the conversion of human fibrinogen to fibrin under various conditions. J Am Chem Soc, 69(2):388-400.

382. Lord ST. (2011) Molecular Mechanisms Affecting Fibrin Structure and Stability. Arterioscler Thromb Vasc Biol, 31(3):494-9.

383. Whittaker P, Przyklenk K. (2009) Fibrin architecture in clots: a quantitative polarized light microscopy analysis. Blood Cells Mol Dis, 42:51-6.

384. Collet JP, Moen JL, Veklich YI, Gorkun OV, Lord ST, Montalescot G, Weisel JW. (2005) The alphaC domains of fibrinogen affect the structure of the fibrin clot, its physical properties, and its susceptibility to fibrinolysis. Blood, 106: 3824–30.

385. Sakharov DV, Rijken DC. (2000) The effect of flow on lysis of plasma clots in a plasma environment. Thromb Haemost, 83: 469–74.

386. Gersh KC, Edmondson KE, Weisel JW. (2010) Flow rate and fibrin fiber alignment. J Thromb Haemost, 8: 2826–8.

387. Campbell RA, Aleman M, Gray LD, Falvo MR, Wolberg AS. (2010) Flow profoundly influences fibrin network structure: implications for fibrin formation and clot stability in haemostasis. Thromb Haemost, 104: 1281–4.

388. Sabovic M, Lijnen HR, Keber D, Collen D. (1989) Effect of retraction on the lysis of human clots with fibrin specific and non-fibrin specific plasminogen activators. Thromb Haemost, 62: 1083–7.

389. Braaten JV, Jerome WG, Hantgan RR. (1994) Uncoupling fibrin from integrin receptors hastens fibrinolysis at the platelet-fibrin interface. Blood, 83: 982–93.

390. Rábai G, Szilágyi N, Sótonyi P, Kovalszky I, Szabó L, Machovich R, Kolev K. (2010) Contribution of neutrophil elastase to the lysis of obliterative thrombi in the context of their platelet and fibrin content. Thromb Res, 126(2):e94-101.

391. Esmon CT, Xu J, Lupu F. (2011) Innate immunity and coagulation. J Thromb Haemost, 9 Suppl 1:182-8.

392. Yeromonahos, C., Polack, B., and Caton, F. (2010) Nanostructure of the fibrin clot. Biophys. J, 99, 2018–2027.

393. Weisel, JW. (1986) The electron microscope band pattern of human fibrin: various stains, lateral order, and carbohydrate localization. J. Ultrastruct. Mol. Struct. Res, 96, 176–188.

394. Yang, Z., Mochalkin, I., and Doolittle, R. F. (2000) A model of fibrin formation based on crystal structures of fibrinogen and fibrin fragments complexed with synthetic peptides. Proc. Natl. Acad. Sci. USA, 97,14156–14161.

395. Ryan, E. A., Mockros, L. F., Weisel, J. W., and Lorand, L. (1999) Structural origins of fibrin clot rheology. Biophys. J, 77, 2813–2826.

396. Scrutton, M. C., Ross-Murphy, S. B., Bennett, G. M., Stirling, Y., and Meade, T. W. (1994) Changes in clot deformability—a possible explanation for the epidemiological association between plasma fibrinogen concentration and myocardial infarction. Blood Coagul. Fibrinolysis, 5,719–723.

397. Gomides LF, Duarte ID, Ferreira RG, Perez AC, Francischi JN, Klein A. (2012) Proteinase-activated receptor-4 plays a major role in the recruitment of neutrophils induced by trypsin or carrageenan during pleurisy in mice. Pharmacology, 89(5-6):275-82.

398. Rocha, V. Z., and Libby, P. (2009) Obesity, inflammation, and atherosclerosis. Nat. Rev. Cardiol, 6, 399–409.

LIST OF PUBLICATIONS

[1] **Varjú I**, Sótonyi P, Machovich R, Szabó L, Tenekedjiev K, Silva MM, Longstaff C, Kolev K. (2011) Hindered dissolution of fibrin formed under mechanical stress. J Thromb Haemost, 9: 979-986. doi: 10.1111/j.1538-7836.2011.04203.x.

Impact factor: 5.731

[2] Longstaff C, **Varjú I**, Sótonyi P, Szabó L, Krumrey M, Hoell A, Bóta A, Varga Z, Komorowicz E, Kolev K. (2013) Mechanical stability and fibrinolytic resistance of clots containing fibrin, DNA, and histones. J Biol Chem, 288: 6946-6956. doi: 10.1074/jbc.M112.404301.

Impact factor: 4.600

[3] **Varjú I**, Kolev K. Fibrinolysis at the Interface of Thrombosis and Inflammation — The Role of Neutrophil Extracellular Traps. In: Kolev K (Ed.), Fibrinolysis and Thrombolysis. InTech, Rijeka, 2014: pp. 31-59. doi: 10.5772/57259.

Impact factor: -

DOI:10.14753/SE.2015.1738

ACKNOWLEDGEMENTS

Every single piece of the work presented here results from a strong cooperation of a number of people whom I was lucky to work with throughout the past few years.

First and foremost, I would like to give my gratitude to my former biochemistry laboratory teacher who later became my tutor and supervisor, **Dr. Krasimir Kolev**. His immensely precise and accurate approach to science started to draw me onto this path as a second year medical student. Later, working under his supervision first as an undergraduate researcher, then as a PhD student, I could always count on his support and guidance, for which I am very grateful.

I am thankful towards the two subsequent heads of our institute, **Prof. Veronika Ádám-Vizi** and **Prof. László Tretter** for making research possible for me in the Department of Medical Biochemistry at Semmelweis University.

I would like to thank the members of the **Haemostasis Research Division** for the welcoming environment that they represented through all these years. In case of any technical difficulties, the broad methodological knowledge and excellent assistance of **Györgyi Oravecz** was always there to help me. Discussions with **Prof. Raymund Machovich** were particularly helpful and shed light on further interesting aspects and directions of our research. I would also like to acknowledge **Dr. Erzsébet Komorowicz** for indispensable help with rheometer experiments. **Dr. Anna Tanka-Salamon, Dr. András Kovács** and **Dr. Nikolett Wohner** also provided me with solutions for the problems and ideas for the progress of our work. I would also like to thank **Dr. Katalin Bartha**, **Dr. István Lérant**, **Krisztina Magyarné Holti,** and –as an honorary member of our group- **Dr. Beáta Törőcsik** for useful help.

Our scanning electron microscopic studies would have been impossible without the fruitful cooperation with **Dr. László Szabó**. I would also like to acknowledge **Prof. Kiril Tenekedjiev** for establishing a mathematical background for our studies. I highly appreciate the help of **Dr. Craig Thelwell** and **Dr. Colin Longstaff,** who provided us with materials and valuable advice, and **Dr. Péter Sótonyi**, who made it possible for us to examine thrombi from patients.

I would also like to acknowledge **OTKA** (Országos Tudományos Kutatási Alapprogram) for providing the financial background of the work presented here (OTKA 83023).

DOI:10.14753/SE.2015.1738

At last, but not least, I am very grateful towards our two undergraduate researchers **Veronika Judit Varga-Szabó** and **Ádám Zoltán Farkas**, whom I was lucky to be the secondary supervisor of, and who both participated in the research presented in this thesis.